Theses and Dissertations--Biosystems and Agricultural Engineering

Biosystems and Agricultural Engineering

2012

COMPUTATIONAL TOOLS FOR IMPROVING ROUTE PLANNING IN AGRICULTURAL FIELD OPERATIONS

Rodrigo S. Zandonadi
University of Kentucky, zandonadi.rodrigo@gmail.com

Click here to let us know how access to this document benefits you.

Recommended Citation

COMPUTATIONAL TOOLS FOR IMPROVING ROUTE PLANNING IN
AGRICULTURAL FIELD OPERATIONS

_____

DISSERTATION
_____

A dissertation submitted in partial fulfillment of the
requirements for the degree of Doctor of Philosophy in the
College of Engineering
at the University of Kentucky

By
Rodrigo Sinaidi Zandonadi

Lexington, Kentucky

Director: Dr. Timothy S. Stombaugh, Associate Professor of Biosystems
and Agricultural Engineering

Lexington, Kentucky

2012

ABSTRACT OF DISSERTATION

COMPUTATIONAL TOOLS FOR IMPROVING ROUTE PLANNING IN
AGRICULTURAL FIELD OPERATIONS

In a farming operation, machinery represents a major cost; therefore, good fleet management can have a great impact on the producer's profit, especially considering the increasing costs of fuel and production inputs in recent years. One task that could improve fleet management is planning an optimum route that the machine should take to cover the field while working.

Researchers around the world have proposed methods that approach specific aspects related to route planning, the majority addressing machine field efficiency per-se, which a function of effective working time relative to total time spent in the field. However, wasted inputs due to off-target application areas in the maneuvering regions, especially in oddly shaped agricultural fields, might be as important as field efficiency when it comes down to the total operation cost. Thus, the main purpose of this research was to develop a routing algorithm that accounts for not only machinery field efficiency, but also the supply inputs.

This research was accomplished in a threefold approach where in the first step an algorithm for computing off-target application area was developed, implemented and validated resulting in a computational tool that can be used to evaluate potential savings when using automatic section control on agricultural fields of complex field boundary. This tool was used to investigate the effects of field size and shape as well as machine width on off-target application areas resulting in an empirical method for such estimations based on object shape descriptors. Finally, a routing algorithm was developed and evaluated that took into consideration, costs associated with machine field efficiency as well as off-target application areas.

Rodrigo Sinaidi Zandonadi

October 23, 2012

COMPUTATIONAL TOOLS FOR IMPROVING ROUTE PLANNING IN
AGRICULTURAL FIELD OPERATIONS

By

Rodrigo Sinaidi Zandonadi

Timothy S. Stombaugh
Director of Dissertation

Dwayne Edwards
Director of Graduate Studies:

October 23, 2012

This work is dedicated to the memory of my father Mateus, who always tutored and instigated me and my sisters to pursue the best possible academic education, but has been sharing our achievements in another life. I wonder if he ever thought that his desire for a college education of his children would lead us to come this far. I'm sure you are proud of our achievements.

ACKNOWLEDGMENTS

I would like to start my acknowledgments by thanking God in first place, for blessing my way with a lot of good people that somehow, came across to contribute to the accomplishment of this work. However, some special thanks are deserved in completion of this thesis and I first direct it to my advisor Dr. Timothy Stombaugh who, spent a considerably extra amount of time fixing my English throughout this dissertation. I thank my committee members; Dr. Scott Shearer and Daniel Marçal de Queiroz for the effort of making personal presence in the final exam, traveling from different state and different country during a very busy time of the semester. I appreciate. I also would like to thank Dr. Dillon, that completed the committee and offered his time and economic expertise towards the completion of this work. I want to extend my thanks to Dr. Thomas Barnes for serving as the outside examiner.

My sincere appreciation also goes to my colleagues, Joe Luck, Michael Sama, and Santosh Pitla, that were such good help for this and many other projects I had the honor to be part throughout the years I spent at the BAE department. I hope that I get a chance to work with those guys again sometime in the future.

I would like to say a very special thanks to a Karen and Joe Dan Luck that welcomed me many times in their home on weekends making me feel like on a retreat, especially during dove hunting season. I need to keep in mind the labor day holiday for a quick trip to western KY in the future.

I cannot forget to thanks the family that initiated me in the USA long time ago and that without the wonderful experience and lessons I had back then, I probably would not have come back to USA for my graduate degrees. Thanks Dosdall family for all the support and affection I have received from you along this years.

I would like to extend my appreciation to Freire Pecegueiro do Amaral family, specially Marcio Pecegueiro, that although life might have taken us to different routes, I do appreciate the support I've had in certain portion of the process.

I surely want to express my appreciation to the closest ones; my mom Lourdes (that kept sending with me the goods she makes every time I went home); sisters Alessandra and Heloisa; and nephew Matheus that although far away, were very supportive in the pursuit of this degree.

LIST OF CONTENTS

LIST OF TABLES

LIST OF FIGURES

CHAPTER 1:INTRODUCTION

Good fleet management can have a great impact on the producer's profit, especially considering the increasing costs of fuel and production inputs in recent years. Moreover, the increasing capacity and technological resources of agricultural machinery demand a higher capital investment, arising from the greater interest in field efficiency and precision placement of inputs.

Improving field efficiency might take place by making use of technologies such as light-bars and automatic guidance (this will also improve input placement by reducing the overlapped areas in adjacent areas). Improving the precision of input metering and placement might also take place by using variable-rate systems (planting, fertilizing, spraying), and improving the resolution of the implement toolbar (automatic section control for sprayers, planters, and suitable fertilizer applicators). However, because of the high cost and complexity of such systems, the producer decision-making process is often complicated by the range of technologies and pricing structures available. It often demands great management effort to fully explore the potential of such tools.

Field efficiency and operating costs of farm machinery, including the use of high end technology, is driven by the planning of field operation. Field operation planning has become more important not only because of cost reduction, but also because of the increasing adoption of semi-autonomous farm machines. The advent of farm machinery automation based on geo-position systems for guidance allows accomplishment of challenging tasks that are beyond the capabilities of the human operator, thus creating the necessity of improving the field task planning process.

The planning of a field task, or mission planning, is rather complex and some researchers have proposed a hierarchy decomposition of the system into simpler problems with fewer variables to be solved independently and efficiently (Bochtis et al., 2007). One of the individual problems to be solved according to the authors was the coverage path planning for individual vehicles. Reid (2004) stated that path planning is one of the key tasks in the mission planning process.

Coverage path planning determines a path that guarantees that an agent will pass over every point in a given environment (Choset and Pignon, 1997). The subject has been extensively studied in the realm of mobile robotics, but most of the developed approaches cannot be directly applied to agricultural operations (Huang, 2001). One of the reasons which make planning an optimal path for agricultural machinery a difficult task is the fact that, different from the majority of mobile robots, agricultural machinery are nonholonomic, which means they cannot make a turn without moving their pivot point (Oksanen, 2007).

In the role of path planning for agricultural applications, field operation costs and environment preservation are the main targets taken into consideration. Hence, minimizing distance traversed to cover a field, maneuvering time, overlapped areas, skipped areas, and down time due to loading/unloading process are relevant variables to be considered in the cost function for path planning process. However, addressing all these variables at once is rather difficult, especially considering that some of them might present competitive behavior in the objective function. For instance, the coverage path of a planting operation with the shortest distance travelled in the field might not result in the coverage path with the least double-coverage area because of point rows in the headland region. In this case the trade-off is driven by the actual cost of the machinery operation and the cost of seed, fertilizer, and chemicals applied during the operation. Also, working with complex boundary geometry (oddly shaped fields typically found in some regions), compounded by the three dimensional space of the farming terrain, makes path planning for agricultural fields even more challenging.

Nevertheless, approaches for field operation path planning reported in the literature focused on different aspects of the problem, often times relying on over-simplification of the problem to make the algorithms work. However, the majority of studies address the number of turns and how complicated the maneuver is, and also how to decompose a complex field boundary into sub-fields for better planning. The issue of off-target application attributed to point rows in the headland region has not received much attention in the reported studies, although its importance is recognized by the majority of researchers in the area.

CHAPTER 2: LITERATURE REVIEW

Researchers and producers are aware, for the most part, of the issues related to the path planning for agricultural machinery. However, these problems are fairly difficult to describe mathematically given the characteristics of various agricultural field operation scenarios. Thus, methods have been reported with no complete solution, but yet addressing specific issues mostly related to the field efficiency of farming equipment.

Field efficiency is defined by the ratio of the actual area covered by a machine to the theoretical area that could be covered. Field efficiency accounts for a failure to use the theoretical working width of a machine, operator habits, turning time, and field characteristics (ASABE, 2011). According to Grisso et al. (2001), factors that affect field efficiency are: machine maneuverability, field/traffic pattern, field shape and size, crop yield (harvesting operation), and system capabilities (e.g. unloading combine on-the-go).

Machine maneuverability affects the field/traffic pattern since the decision as to which pattern to use is mainly dependent on what types and number of maneuver/turns that are going to be made. The turns to be made depend on the type of operation, implement type, implement width, and the space constraints (headland area and field boundary complexity). When a field boundary deviates from a rectangular shape and/or presents an obstacle that needs to be avoided by the machine, the approach utilized is to divided the field in sub-parcels and execute the planning at sub-parcels level to cope with a general solution. Field size will affect field efficiency in such a way that the producer might have to use large equipment for a small irregular field. System capabilities encompass the logistics of the support/servicing operation (e.g. refilling a planter or sprayer, unloading a harvesting on the go).

As mentioned before, the off-target application area is an important factor to consider in the optimization process. The majority of the work in the literature addresses the issue indirectly by means of minimizing the number of turns and/or complexity of turns. A few studies are found in the matter of optimizing off-target application area directly. Bruin et al. (2009) addressed the issue with the purpose of optimizing the spatial configuration of cropped swaths in agricultural fields while creating space for field margins taking into consideration the cost of inputs and field margin subsidy available in

the Netherlands. On the other hand, the subject of off-target application area has gained attention because of the recent adaption of automatic section control systems in agricultural machinery. Economic analyses carried out on idealized fields have proven that the benefits of automatic boom section control increase with an increase in farm size, especially in areas with waterways, drainage ditches, and similar obstructions (Batte and Ehsani, 2006). Furthermore, researchers have also presented potential savings on off-target application area using data collected from automatic section control systems (Dillon et al., 2007; Luck et al., 2010a; Luck et al., 2010b). Therefore a method for computing off-target application area based on the characteristics of the field boundary and application equipment would be of a great value for not only improving economic analysis but, also to assist producers in their decision making process regarding equipment adoption.

Sisk (2005) and Luck et al. (2010a) reported that perimeter-to-area ratios (P/A) might present a relationship with off-target application areas. In a later study, Luck et al. (2010b) confirmed the trend between off-target application area and P/A ratios by presenting a coefficient of determination of 0.5 for the 21 fields included in the report. This indicates that off-target application area may be indirectly estimated by correlating it with some sort of shape descriptor (P/A ratio in the cited study). However, Luck et al. (2010b) collected the data during a spraying operation, thus the off-target area was from a particular working direction. Considering that off-target area is a function of point row and headland patterns that will change considerably according to the working direction, it is difficult to determine if the cases analyzed were close to the optimal working direction. The coefficient of determination would probably increase if the relationship was developed between the average off-target area (among a certain range of possible working directions) and applicable shape descriptors.

2.1   Machine Maneuverability Regarding Path Planning

Oksanen and Visala (2004) proposed an optimal control approach to model vehicle-implement turning in the headland. Because of the nonlinearity of the model, numerical methods were used for solving the system of equations. The authors reported

that the requisite computational effort was high and that the solved path could be approximated with Bezier curves.

Jin and Tang (2006) mentioned that the cost for each turn is made up of three parts; the wasted area in the headland (off-target application area), the total distance traveled within the off-target area, and the distance traveled while making the actual turn. The authors cited a method to compute the off-target area in the headland (Hunt, 2001) but an actual cost factor for the off-target area was not incorporated in the final cost function.

In a later work Jin and Tang (2010), defined the time cost of five cases of turns based on swath width (w), headland width (W_h), minimum turning radius of the implement and vehicle (r), and the angle between swath and field edge as follows: 1) "flat" turn when the vehicle and implement turning radius (r) is smaller than half of the swath width (w); 2) "U" turn when r was equal to $w/2$; 3) "Bulb" turn when r was greater than $w/2$; and 4) the Asymmetric "Bulb" turn ("Hook" turn), which is a variation of the "Bulb turn." The last case was the headland turn with limited headland width (the "fishtail" turn or switchback turn). This cost function was left for future work. Kise et al. (2002) modeled the forward and switchback turns for cases where the tractor intersects the headland area at a right-angle.

Noguchi et al. (2001) developed a turning function for a tractor robot based on a third order spline function. The feasible pathway for the vehicle was created off-line (a priori) according to the non-holonomic constraints of the vehicle as well as the response of the steering actuator.

Taïx et al. (2006) used a cost criterion depending on the path length, working duration, number of "U" turns and jumps from one pass to pass other than the next pass to optimize the coverage path.

Bochtis and Vougioukas (2008) analyzed a scenario in which the field was covered with a headland pattern where the cost of going to different adjacent passes was minimized. The authors modeled the system as Travelling Salesman Problem (TSP) and represented the possible routes on an undirected weighted graph. The cost criterion

utilized by the authors was based on the non-working distance traversed during turning considering that the vehicle crossed the field boundary at a right angle.

2.2   Handling Complex Field Boundary Regarding Path Planning

Dividing a complex field boundary into simpler shapes might improve the optimization process. The trapezoidal decomposition is a popular technique for subdividing a field. In the decomposition process, the trapezoids/triangles, also called cells, are formed by drawing lines through each polygon vertex. The lines (sweep lines) must be created using a predetermined direction and parallel to each other. Then, the coverage of each cell can be achieved with simple back and forth motions (boustrophedon paths) (Choset and Pignon, 1997), and coverage of the entire field is achieved by visiting each cell in the adjacency graph at least once (the traveling salesman problem). On an adjacency graph, each cell can be represented as a node, where adjacent cells have an edge connecting their corresponding nodes.

According to Choset (2000) and Choset and Pignon (1997), the trapezoidal decomposition approach requires too many redundant back and forth motions to guarantee complete coverage. The authors proposed a modified form of cellular decomposition called the boustrophedon decomposition. In their approach, cells are merged upon certain criteria reducing the number of redundant motion. Oksanen and Visala (2007) also used the trapezoidal decomposition for field subdivision and presented different criteria for merging neighboring cells. In both studies the authors did not address the issue of choosing the direction of the trapezoidal decomposition lines for purposes of minimizing the coverage cost.

Stoll (2003) proposed that the main working direction should be determined by the longest segment of the polygon by which the coverage process begins. When the next path is laid out, a new polygon is formed adjacent to the headland. The rest of the polygon encloses the remaining area which is still left to be covered. This process is repeated until the number of vertices of the polygon with remaining area changes indicating that shape has changed. Then, the new longest segment is determined for working direction purposes. The authors presented the algorithm performance on one

fairly simple field shape. They suggest that the method should be evaluated with different field shapes, machine types, and optimization criteria.

Jin and Tang (2010) developed an algorithm that searches for the optimal field decomposition and working direction for each sub-field. The algorithm decomposes the field in multiple regions which are evaluated individually for the best path direction. Then, a topological undirected graph was constructed as the tool for the searching task. A solution for fields with no more than 20 vertices was found within 60 seconds. The authors stated the best sequence of sub-regions to be covered could be approached similarly to a traveling salesman problem, but it was not addressed in the report. Huang (2001) demonstrated that in order to improve decomposition of convex polygons, a sweep line that is parallel to an edge of the boundary should be used.

With the algorithm proposed by Hofstee et al. (2009), concave shaped fields were recursively split until only convex fields were left. Within the convex area, the direction parallel to the longest segment of the polygon was chosen as the working direction. The issue of sub-region coverage sequence was not addressed in this study.

Oksanen (2007) conducted a study of a field database in an attempt to classify the field complexity based on a field shape index or shape descriptors for purposes of path planning algorithm validation/verification. The descriptors used in the research were convexity, compactness, rectangularity, triangularity, ellipticity, and ratio of the principal moments. The authors reported that only 25% of the field plots were classified into some clear class.

2.3   Yield and System Capability/Machine Servicing

Oksanen and Visala (2009) developed an algorithm to handle the servicing time (refilling or emptying) assuming that service always occurs at the end of the segment. Spekken (2010) developed an algorithm based on the Clarke and Wright method (Clarke and Wright, 1964) for truck scheduling. The Clarke and Wright method optimizes for the shortest route and to ensure the delivering truck returns to the depot as empty as practical.

2.4   Off-Target Application Area in the Headland

Hunt (2001) analyzed and described the driving pattern for rectangular fields. The author presented a method to compute the wasted travel distance and area (off-target

application area) in the headland based on implement width and the angle between vehicle trajectory segment and the headland segment. This method is approached in other studies (Jin and Tang, 2006, 2010; Spekken, 2010). However, in odd shaped fields, the headland edge segments are often shorter than the actual implement width. Thus, especially on occasions where the implement boom width is large, this method sacrifices accuracy in computing the wasted distance travelled as well as the off-target area in the headland.

Bruin et al. (2009) developed a GIS model that, based on straight non-overlapping swaths, attempted to relocate areas of inefficient machine maneuvering to boundary strips by minimizing the costs of area loss and additional swaths minus any subsidy received for field boundaries in The Netherlands. The authors used fields with relatively simple geometry in their study.

2.5   Field Shape Descriptors

Shape representation and description techniques have been widely used in the realm of the image processing and GIS with for the purpose of object identification. Zhang and Lu (2004) divided the description techniques in two classes of methods: contour-based and region-based methods, depending if the shape features are extracted from the contour only, or from the whole shape region. Some descriptors are simple to calculate and do not require significant computational power while others (usually region based) are computationally complex.

There are several different types of field shape descriptors reported in the literature. Peura and Iivarinen (1997) evaluated the efficiency of five simple shape descriptors for object identification as follows: convexity, principal axes, compactness, circular variance, and elliptic variance.

Brinkhoff et al. (1995) developed a set of quantitative parameters to characterize the complexity of a polygonal object. These parameters were combined resulting in the Complexity Index (CI) which was used to classify field polygons from a spatial dataset. The same concept was utilized by Souza and Guliato (2008) for breast cancer tumor classification.

Gonzalez et al. (2004) used shape description techniques for land consolidation in Spain. The authors addressed the issue of field size and shape regarding field efficiency with the purposes of grouping small and irregular fields to improve efficiency. The Combined Size and Shape Index (*CSSI*) was based on the tillage time per hectare of useful surface area (*RT*) that was computed for 36 simplified field shapes considered the standard. For each of the 36 shapes, the *RT* was computed over an area range of 50 m^2 to 5 ha at 50 m^2 increments yielding 1000 plots of each shape. Then, the *RT* of a given field shape was adjusted using size and shape-based correction factors (a and b, respectively) based on the standard plots.

2.6   Summary

This literature review introduces the concept of path planning for agricultural machines addressing the many related issues and solutions proposed by researchers around the world, the majority addressing machine field efficiency. However, field operation costs can be minimized not only by maximizing machine field efficiency, but also minimizing inputs, especially in the headland areas where maneuvering takes place. Such issues may not be critical in operations where the field boundaries are close to the ideal rectangular shapes, but it certainly makes a difference in regions with odd shaped fields such as some areas in the state of central Kentucky. The complex field boundary imposes a challenge in the field geometric decomposition techniques, computation of the wasted distance travelled in the headland, and off-target areas in the headlands. The methods for computing off-target area in the headland regions found in the literature are not well suited to complex field boundaries. Further, the development empirical methods will only be possible if a suitable tool for off-target application area computation exists.

CHAPTER 3: PROJECT OBJECTIVES

The goal of this research was to develop a routing algorithm method that accounts for not only machinery field efficiency, but also the cost of inputs. The project goal was achieved by addressing the following objectives:

1. Develop and validate a robust method for off-target application area computation capable of handling complex field boundaries;
2. Develop a simplified approach for estimating the off-target application areas in agricultural fields, based on shape descriptors, considering the combined effects of field shape, field size, and implement width.
3. Develop a routing algorithm based on off-target application area and machinery efficiency.

Chapters 4, 5, and 6 address each of these objectives individually and are intended to be stand-alone publishable units. Chapters 7 and 8 provide overall project summary, conclusions, and recommendations for future work.

CHAPTER 4: A COMPUTATIONAL TOOL FOR ESTIMATING OFF-TARGET APPLICATION AREAS IN AGRICUTURAL FIELDS

4.1   Introduction

As production agriculture operations have grown in size and competitiveness, the agricultural equipment industry has followed the trend by providing larger and faster machines to satisfy producer demand. At the same time, Global Position System (GPS) based technologies for field task improvement have been developed allowing more precise crop input management and more efficient field operations. Many of these technologies can be quite expensive and relatively complicated to use. Because of the high cost and complexity, a producer's decision of whether to adopt these technologies has become more difficult.

An example of these recent innovations in precision agriculture is automatic section control for application equipment. An automatic section control system continuously records areas that have been covered during a field operation based on GPS positions and then automatically turns on and off sections of the machine to prevent off-target application of inputs. Off-target application could be manifest as either double coverage on a previously treated area such as a headland or application in areas outside of the field boundary. Luck et al. (2010a) conducted an analysis on three irregular fields in the central Kentucky area that had been sprayed using an automatic section control system. The treated area was computed based on the data recorded by the application system and compared with the area that would have been treated if the sprayer had not been utilizing automatic section control. The reductions of the treated area in the three fields were 17.5 %, 16.2 %, and 15.2 %. Reductions in off-target application in these fields were largely due to the irregular shape of the fields; less reduction would be observed in rectangular fields. Another study conducted on a wider variety of field shapes and sizes indicated that substantial reductions in off-target application could be seen with the implementation of automatic boom section control using only seven independently controlled sections (Luck et al., 2010b).

Economic analyses have proven that benefits of automatic boom section control increase with an increase in farm size, especially in areas with waterways, drainage ditches, and similar obstructions (Batte and Ehsani, 2006). However, the scenarios in that

study were hypothetically created in order to compute off-target application area and distance traveled. Dillon et al. (2007) concluded that the savings on input expenses justified the adoption of the automatic section control technology based on data collected in three irregular fields in the state of Kentucky. Thus, considering the effect of the field shape and size on the performance of the automatic section control system, a method or computational tool for estimating the off-target application area based characteristics of the field boundary and application equipment would be of a great value for improving economic analysis. Producers could use such a tool to evaluate the potential impacts of the technology based on their particular field conditions and application equipment. Currently there are no simple tools available to provide producers with these quantitative analyses.

4.2 Objectives

The goal of this study was to develop a tool to provide quantitative measures of off-target application in agricultural fields that could be used to assist producers in automatic section control purchase decisions and to assist researchers and equipment manufacturers in technology development. This goal was accomplished by:

- Developing a computational method for quantifying off-target application areas in agricultural fields;
- Implementing the unique algorithm in software with a graphical user interface; and
- Comparing the output from software runs with field data from a previous study.

4.3 Materials and Methods

The intention of the authors was to develop a software program that could accept field boundary information from a common Geographic Information System (GIS) file format (namely a shape file), allow the user to select the machine parameters, then produce results showing anticipated off-target application areas for a straight parallel swath approach to field coverage. The program focused only on the overlap caused by wide swaths intersecting headlands at non-right angles, which implicitly assumed that there was no overlap or skips between adjacent headland or parallel swaths. The field

topography was not considered in the proposed method since according to findings by Stombaugh et al. (2010) topography will not have a significant impact on machine overlap. The software tool, which is called the Field Coverage Analysis Tool (*FieldCAT*), was developed in MatLab® (MathWorks, 2009) using customized functions and routines from the MatLab® Mapping Toolbox.

The first task in developing the software was to develop the analysis algorithm. Once this algorithm was completed, it was apparent that several preprocessing steps there were required on the field boundaries to make the program work more efficiently. Some preprocessing steps could be automated and some required user input. Given these requirements, data input and editing modules were then designed to facilitate input of field boundaries to the algorithm. Consequently, the overall program could be divided into three different modules: Data Import, Data Preparation or Editing, and Coverage Analysis (Figure 4.1). The modules were integrated with a graphical user interface (GUI) to facilitate *FieldCAT* usage and are discussed in more detail below.

Two analyses were performed to evaluate the performance of the *FieldCAT* software. The first analysis was designed to demonstrate the off-target calculation capabilities of the programs including analyses of section control resolution and path orientation. It involved detailed evaluation of nine different field boundaries. The second analysis was intended to provide validation of the program output by comparing the *FieldCAT* simulation output with actual field performance data from 25 different fields.

4.3.1 Program Module Development


```
┌──────────────┐        ┌─────────────────────────────┐
│              │────────│ •  Local cartesian coordinate│
│  Data Import │        │    transformation            │
│              │        │ •  Organize exterior and     │
└──────┬───────┘        │    interior boundaries       │
       │                │    (clockwise and            │
       │                │    counter-clockwise         │
       │                │    direction respectively)   │
       │                │ •  Data structure generation │
       ▼                └─────────────────────────────┘
┌──────────────┐        ┌─────────────────────────────┐
│  Data        │────────│ •  Identification of         │
│  preparation │        │    navigable and             │
│              │        │    non-navigable regions     │
└──────┬───────┘        │ •  Polygon filtering         │
       │                └─────────────────────────────┘
       ▼
┌──────────────┐        ┌─────────────────────────────┐
│  Coverage    │────────│ •  Parameter definition      │
│  analyses    │        │ •  Headland definition       │
│              │        │ •  Coverage generation       │
└──────────────┘        └─────────────────────────────┘
```

Figure 4.1: Summary of the basic functionality of each of the three *FieldCAT* modules.

4.3.1.1 Data Import

Shape files are loaded into *FieldCAT* using the built-in Matlab "shaperead" function. The field boundary coordinates are converted to a local Cartesian coordinate system with a reference at the southwestern limits of the field boundary to make all easting and northing coordinates positive and relatively small. The coordinates of the exterior field polygon boundaries are ordered in a clockwise traverse of the boundary, and the coordinates of isolated polygons within field boundaries are ordered counter-clockwise. At this point a data structure is created to manage the information throughout the process. The data structure allows multiple "callback" routines triggered from the GUI to access and share data without creating global variables. Some of the data contained in the data structure include the complete set of boundary coordinates, navigable and non-navigable boundary coordinates, filtered boundary coordinates, headland width, and swath width.

4.3.1.2 Data Preparation

After field boundary data are imported into the program, there are two primary tasks that are completed in the edit mode of the program. The first task involves

identification of portions of the boundary as navigable or non-navigable, and the second involves filtering boundary data to reduce the number of vertices used to describe the boundaries.

4.3.1.2.1 Identification of Navigable Areas

In the program's "edit mode" the user is able to select portions of the field boundaries using the GUI and define them as navigable or non-navigable. This distinction is critical for accurate assessment of off-target application, particularly in fields with internal waterways or other obstructions. Exterior field boundaries are normally considered non-navigable, meaning that machines physically cannot cross the boundary. If, for example, a waterway boundary is navigable, meaning that the machinery can traverse through the obstruction, the operator will not need to make a headland pass around the obstruction boundary. On the other hand, if the obstruction is non-navigable, such as a deep ditch or tree, then the machine operator would normally need to make a headland pass along the boundary of the obstruction. This extra headland coverage will have a significant impact on the off-target application area computation. Once the regions are selected and individually saved, the final boundary is updated in the data structure.

4.3.1.2.2 Filtering polygon vertices

In agricultural settings, field boundary coordinates are usually collected with a GPS receiver connected to a data logger. Typically, position data along the boundary are recorded at a constant frequency as the logging equipment traverses the boundary, which can produce a high density of data points along the boundary depending on logging frequency and vehicle speed. Large numbers of points might be necessary to define a sharp curve in the field boundary, but considerably fewer points may adequately define straight edges of the boundary. Furthermore, the number of iterations of the analysis algorithm is directly dependent on the number of field polygon vertices. Consequently, a filtering algorithm to reduce the number of boundary points was implemented using Matlab's "reducem.m" function, which is based on the Douglas-Peucker line simplification algorithm (MathWorks, 2009). The Doublas-Peucker method recursively subdivides a polygon until a window of points can be replaced by a straight line segment,

where no point in that window can deviate from the straight line by more than a defined distance tolerance. A tolerance in terms of the percentage of the polygon area is more intuitive for this application; therefore, the *FieldCAT* user inputs the maximum area error tolerance, and the length tolerance is computed automatically. The area error is computed by comparing the initial area and the area of the reduced polygon. If the area error is greater than the desired tolerance, the length tolerance is recursively decreased until the area tolerance is less than the desired error. A filtering procedure to check for self-intersecting segments of the polygon is also implemented to compensate for changes in vehicle direction while GPS field boundaries were being logged. A message box reporting the percentage area error for the navigable and non-navigable regions and a graphical presentation of the filtered boundary allow the user to visually judge if the filtering process produces satisfactory results.

4.3.1.3 Coverage analysis

4.3.1.3.1 Parameter definition

Once the field editing is completed, *FieldCAT* will enter the "Coverage mode". At this point, the controlled section and headland widths are defined along with the path orientation. The user is able to either select a single fixed path direction for field coverage or multiple directions thereby allowing the program to rotate the path direction by a user-selectable angle increment.

4.3.1.3.2 Headland generation

The headland areas are created prior to the coverage generation. The coordinates of the headland are computed by buffering the clockwise non-navigable boundaries towards the interior of the polygon and buffering the counter-clockwise non-navigable obstruction boundaries towards the outside the polygon. If there is a portion of the outside field boundary selected as navigable, that region is clipped by the headland polygon. The program then resolves issues with overlapping headland areas and navigable waterways by clipping or combining regions as appropriate.

4.3.1.3.3 Coverage generation

The coverage analysis algorithm (Figure 4.2) implemented in *FieldCAT*, as stated earlier, focuses only on the overlap caused by swaths intersecting headlands at non-right

17

angles. It overlays a series of straight parallel swaths onto the field boundary and then computes the encroachment of those swaths into the headland areas of the field or extension outside the field boundary. It does this by first constructing a series of parallel lines separated by the machine or section width and oriented at the defined angle onto the boundary. Two adjacent lines would define the edges of a swath. For each swath, all vertices of the headland boundary polygon that fall within the swath are identified. Then lines orthogonal to the swath lines passing through each vertex within the swath region are constructed (Figure 4.3). The orthogonal lines are sorted based on Northing offset. The intersection of two consecutive orthogonal lines with the swath boundary lines forms a rectangle, which are either totally in the field area or, partially in the field area and partially in the headland or outside the field boundary. Using the polygon Boolean operation function, the portions of the rectangle that fall inside and outside the headland or field boundaries are computed (Figure 4.4). For instance, if the portion of a rectangle area that does not intersect the headland polygon is the same as the area of the original rectangle, the rectangle is considered totally included in the field area and, consequently, it would receive only a single coverage. If the rectangle is partially included in the headland area, the intersecting region is separated from the original rectangle and that portion of the area is classified as "double coverage" area while the rest of the rectangle is classified as single coverage. The algorithm also accounts for machine travel into areas outside of navigable boundaries (e.g., waterways). With a similar Boolean approach, the portions of rectangles extending across navigable boundaries into the exterior of the field boundary are classified as "wasted application." If a rectangle is completely outside the field boundary area in a navigable boundary region, this area is classified as "no application" since the machine should be shut off by the operator even without the use of automatic section control, and its area does not affect off-target area calculation. This entire classification process is repeated for every rectangle bounded by two adjacent orthogonal lines along each swath of the field. The number of algorithm iterations is dependent on the number of vertices of the headland polygon; thus, the polygon filtering operation is an important step to reduce algorithm execution time.

The areas of each region and their respective coordinates are stored in the data structure. The total off-target area reported is the sum of the double coverage and wasted application areas.

```
┌─────────┐      ╱──────────────────────╱     ┌──────────────────┐
│  Start  │─────▶╱  • Field data structure ╱───▶│ Compute parallel │
└─────────┘     ╱──────────────────────╱     │  swath lines     │
                                              └──────────────────┘
```

Figure 4.2: Structure of **FieldCAT** coverage simulation algorithm.

19

The areas of each region and their respective coordinates are stored in the data structure. The total off-target area reported is the sum of the double coverage and wasted application areas.

Figure 4.2: Structure of **FieldCAT** coverage simulation algorithm.

19
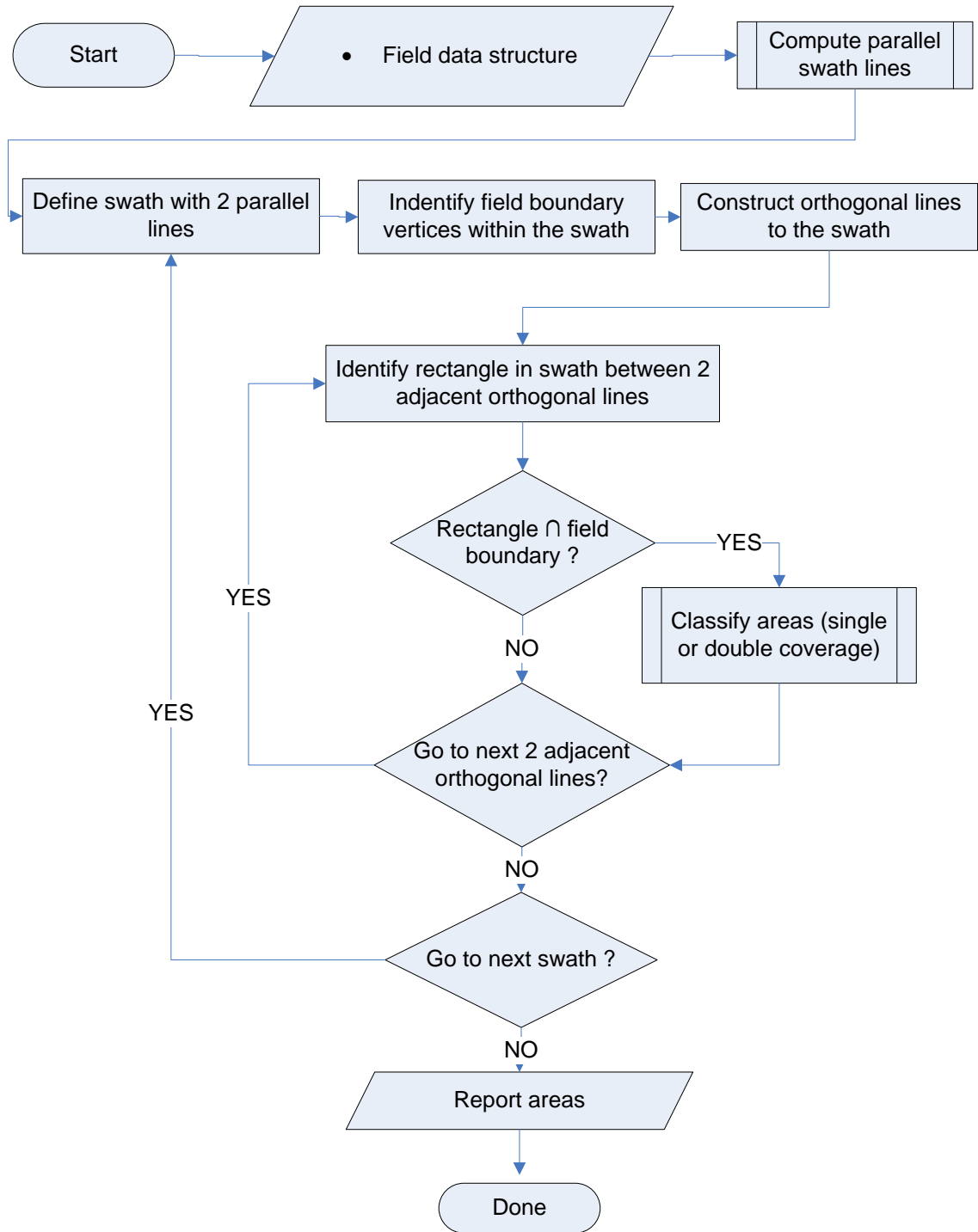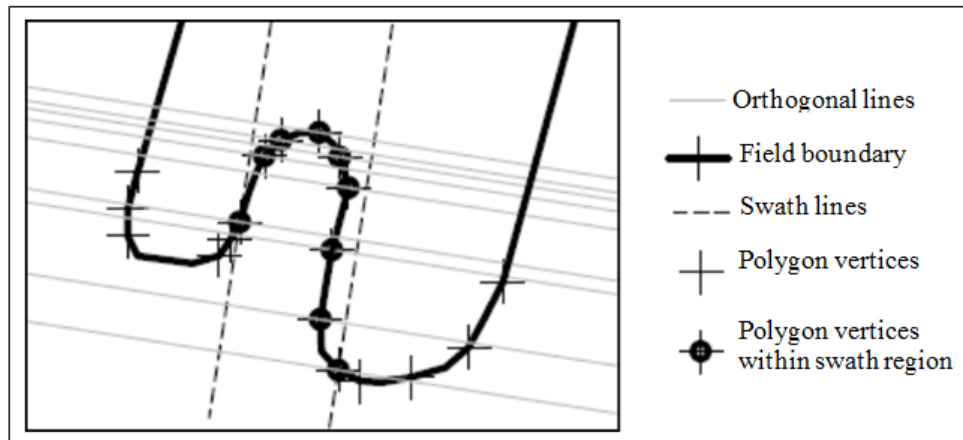
Figure 4.3: Identification of boundary vertices within a swath and construction of orthogonal lines through each of those vertices.
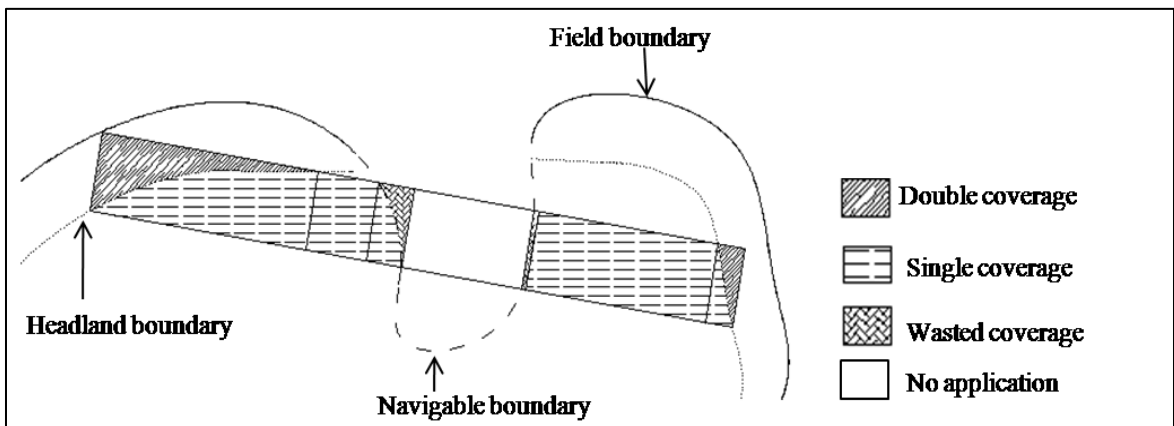
Figure 4.4: Example of identification and classification of areas in a swath through a navigable boundary that would receive single, double, wasted, or no coverage. The total off-target application area was the sum of the double and wasted coverage areas.

The program output is generated based on the field data structure information stored during the computations. A summary containing the simulation parameters as well as the area information is displayed at the end of the process (Figure 4.5). The summary is also saved in a comma delimited text file and the field data structure is saved in a .mat file.
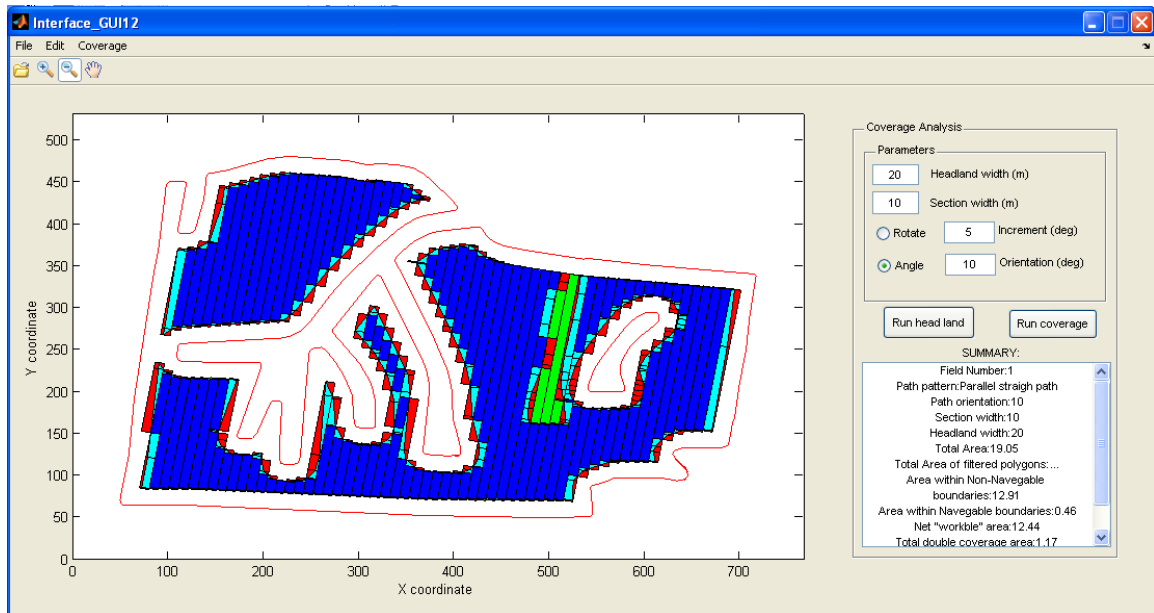
Figure 4.5: Screen capture of the data out displayed after a simulation. Red color represents overlap and wasted application (Off-target application areas). Cyan and dark blue represents the single coverage area, and green represents the no application areas.

4.3.2 Experimental Procedure

4.3.2.1 Program test

Nine irregular field boundaries representing farms in central and western Kentucky (Figure 4.6) were used as examples to test and demonstrate the algorithm. The *boundary filtering* technique performance was reported for the nine fields as well as results from evaluation of *section control resolution* and *path rotation effects* on off-target application area. A 27 m wide implement was used with the smallest controllable section width of 0.5 m. To evaluate the effects of automatic section control, the boom was divided into 2, 3, 6, 9, 18, 27, and 54 sections, which corresponded to controlled section widths of 13.5, 9, 4.5, 3, 1.5, 1 and 0.5 m, respectively. The angle at which the parallel paths were generated was varied from 0 to 175 degrees in 5 degree increments to evaluate the influence of the path orientation on off-target application area. Since there were eight different section widths evaluated and each path pattern was rotated from 0 to 175 degrees, there were 288 different coverage patterns evaluated for each field.

21
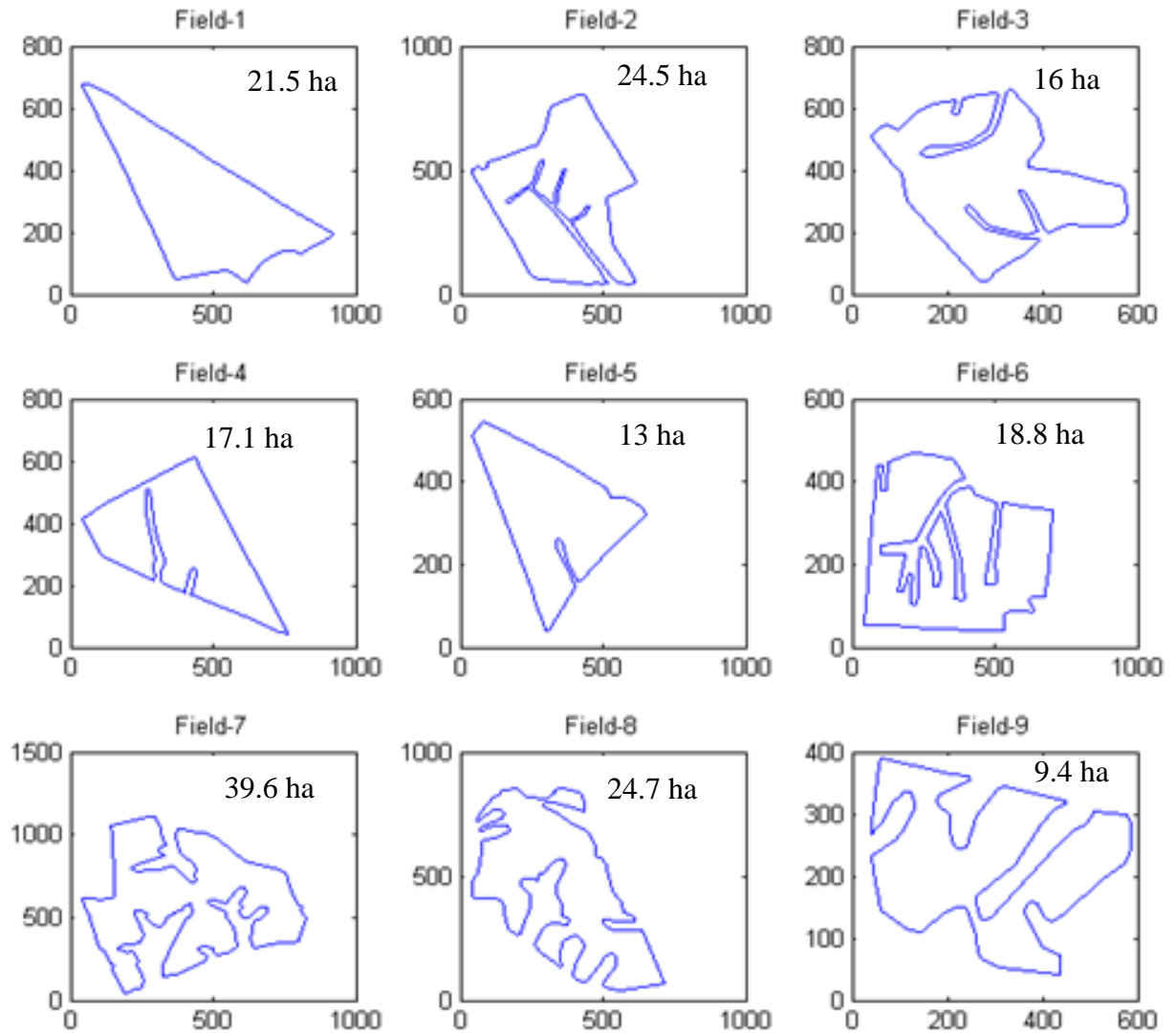
Figure 4.6: Boundaries of the nine example fields typical of Kentucky farms that were used to test the *FieldCAT* algorithm.

4.3.2.2   Field Data Comparison

For field data comparison, simulation results from *FieldCAT* were compared to field performance data reported by Luck et al. (2010b). Twenty one fields ranging in size from 3.1 ha to 101.0 ha were evaluated. Some of the fields contained grassed waterways and non-navigable obstacles within a unique field boundary, which is very typical of agricultural fields in Kentucky. Fields that were comprised of multiple non-connecting polygons were separated into multiple individual fields for coverage simulation purposes resulting in a total of 25 fields.

22

The field data were collected with a 24.8 m sprayer, which was equipped with an automatic boom section control system and an autosteer system utilizing a sub-meter accuracy GPS receiver. The autosteer system was configured to maintain a pass-to-pass overlap of 15 cm. The boom of the sprayer was divided into 7 sections. The middle section of the boom was 648 cm wide, the next sections out on both sides were 609 cm wide, and the outside two sections on either end of the boom were 152.5 cm wide. In order to perform an equitable comparison, *FieldCAT* parameters were adjusted to simulate the same boom configuration and swath spacing used by the sprayer.

4.4 Results and Discussion

4.4.1 Program Test Results

4.4.1.1 Boundary Filtering Algorithm

The field boundary filtering algorithm proved to be robust and efficient. In the nine example fields evaluated, polygon vertices were reduced by as much as 92% with an area error less than 0.1% (Table 4.1). Even in the most complicated field boundaries, the algorithm was able to reduce the number of vertices by more than 50% without a drastic change to the area (Figure 4.7).
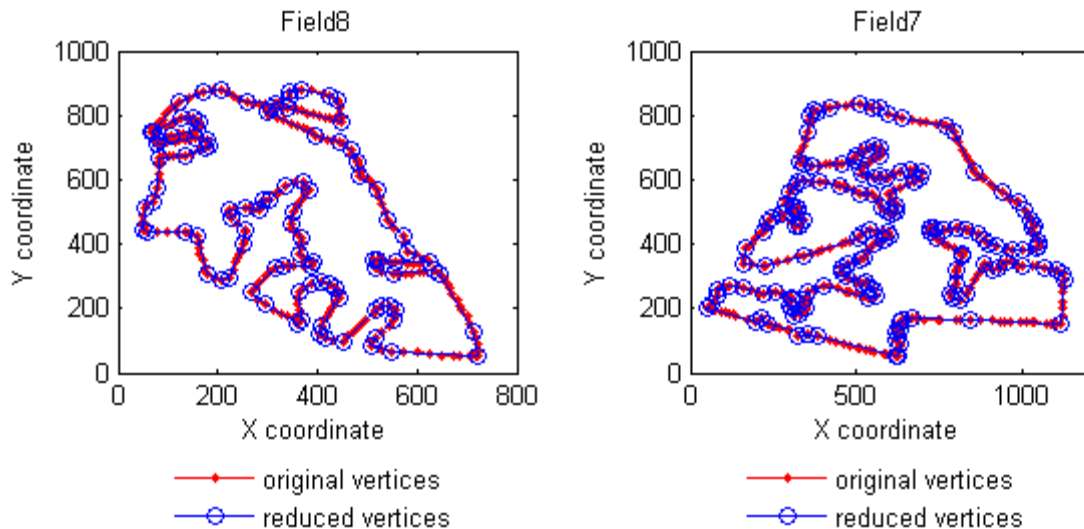
Figure 4.7: Results of the polygon filtering operation for two example fields.

Table 4.1: Results of the polygon filtering operation for the nine fields analyzed.

Field	Total points on non-navigable boundary	Points removed (%)	Area error (%)
1	442	91.6	0.07
2	498	82.7	0.07
3	348	64.4	0.07
4	379	88.1	0.09
5	173	71.1	0.09
6	1038	77.7	0.03
7	378	58.7	0.06
8	307	67.4	0.04
9	220	59.5	0.06

4.4.1.2   Section Control Width

Because of the number of computation permutations that the software can perform on each field, there are a number of analyses that could be performed using the program output. For example, researchers might be interested in using the data to explore field efficiency and path optimization studies. Producers are particularly interested in the value of automatic section control. The results obtained with *FieldCAT* by varying the section control width clearly showed the advantages of controlling smaller sections as evidenced by reduced off-target application area.

For fields 1, 2, 4 and 5, it was possible to determine the predominant orientation of the travel paths in current practice by interpreting the GPS coordinates collected during field operations. For the other fields, approximations of row orientations were determined by inspection of aerial photography (KDGI, 2006). *FieldCAT* was used to determine the potential impact of different resolutions of automatic section control applied to machinery operated at the current practice orientation (Figure 4.8, Table 4.2). These data could be used by a producer, for example, to compare the savings that would result from different numbers of controlled sections on the machine to the cost of implementing the automatic control at those resolutions to determine the best equipment complement for a particular field or set of fields.

The results revealed that even for less complex field boundaries (e.g. Fields 4 and 5), reduction of the double coverage area was notable. Reductions of this magnitude when applied to multiple field operations (e.g. spraying, planting, or nitrogen application) executed throughout the season could yield substantial cost reductions.

Table 4.2: Percentage off-target application resulting from four different section widths in the nine test fields.

Field	Area (ha)	Controlled sections width			
		27 m	13.5 m	1 m	0.5 m
1	21.5	9.1	6	0.5	0.2
2	24.5	13.7	7.2	0.6	0.3
3	16	15.5	9	0.7	0.3
4	17.1	15.4	8.1	0.6	0.3
5	13	12.5	7.2	0.5	0.3
6	18.8	17.3	9.7	0.7	0.4
7	39.6	16.8	8.1	0.6	0.3
8	24.7	16.5	8.4	0.6	0.3
9	9.4	27	13.1	1	0.5
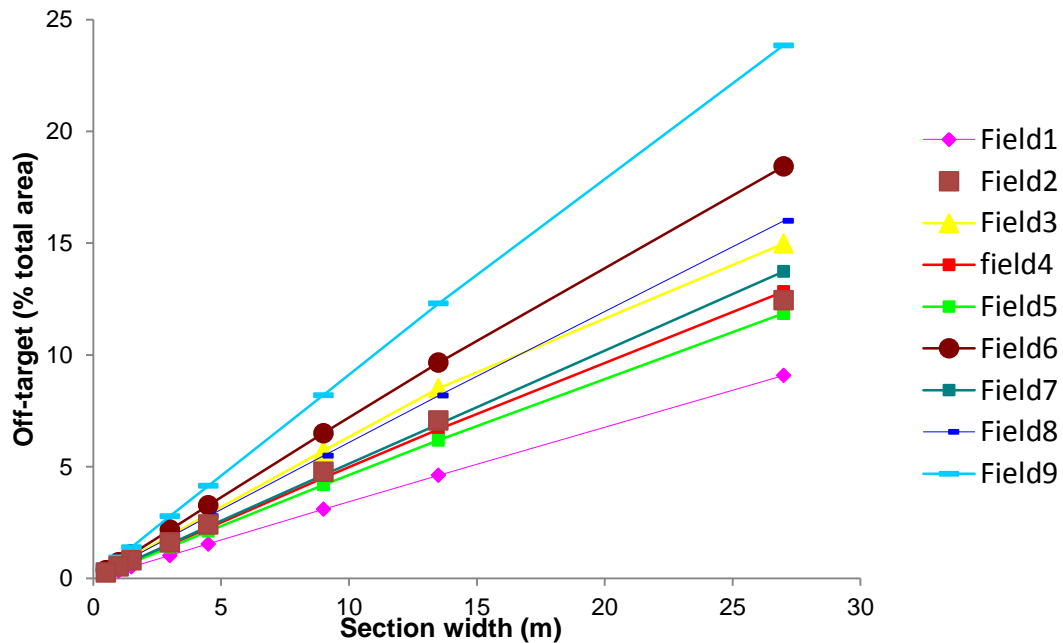
Figure 4.8: Percent of the field area classified as off-target application area at different section control widths for the nine test fields at a path orientation typically used in each field.

4.4.1.3 Path Rotation

Off-target application coverage analyses were performed on each of the nine fields at different path orientations and different section widths. At first glance, the results showed that the software tool could be useful for producers to determine the best

25

path orientation for their equipment set because, as expected, the results clearly showed that path orientation has an effect on the percentage of the field that receives off-target coverage (Table 4.3, Figure 4.9). For less complex boundaries such as Fields 1, 4 and 5, path orientations that resulted in minimum and maximum off-target application tended to be similar across the different section control widths, whereas for more complicated shapes, the path orientation varied to a greater extent depending on the section control width.
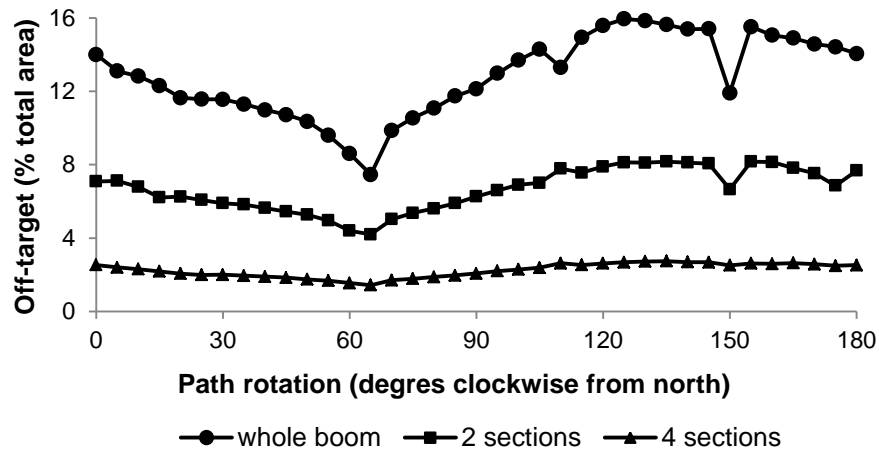
Figure 4.9: Percent of the field area that would receive off-target application at different path orientations in field 4 as a function of quantity of sections controlled. This field is typically managed at a path orientation of 150°.

Table 4.3: Maximum and minimum off-target coverage for 27 m and 0.5 m section widths presented along with the path orientation at which each occurred in the nine test fields.

| field | area (ha) | @ 27 m | | @ 0.5 m | |
		maximum %, deg.	minimum %, deg.	maximum %, deg.	minimum %, deg.
1	21.5	12.5, 125	5.0, 30	0.2, 115	0.1, 30
2	24.5	15.4, 175	7.9, 60	0.5, 135	0.2, 60
3	16.0	17.0, 150	12.6, 75	0.4, 135	0.3, 70
4	17.1	15.9, 125	7.5, 65	0.3, 135	0.2, 65
5	13.0	15.4, 150	7.3, 55	0.4, 135	0.2, 55
6	18.8	20.6, 40	14.7, 90	0.4, 35	0.3, 95
7	39.6	17.3, 10	9.7, 85	0.3, 0	0.2, 85
8	24.7	17.3, 140	13.2, 90	0.9, 135	0.3, 90
9	9.4	29.8, 50	17.8, 180	1.0, 135	0.4, 145

An interesting finding regarding the simpler field boundaries was that the minimum double coverage path orientation did not always coincide with the most intuitive path orientation that would often be chosen to cover the field. This was particularly noticeable in fields 1 and 4 where the minimum double coverage path orientation was not the typical orientation (Figure 4.10). An important point to note is that the number of turn maneuvers required for the minimum off-target path orientation was much higher than the maximum off-target path orientation. For instance, 25 swaths were needed to cover Field 1 with the 30° orientation whereas 17 swaths were sufficient with the 125° pattern (Figure 4.10). This issue results in an optimization problem to evaluate the tradeoff between machine field efficiency and application error.

Figure 4.10: Path orientations causing minimum (A) and maximum (B) double coverage for Field 1 and minimum (C) and maximum (D) double coverage for Field 4.
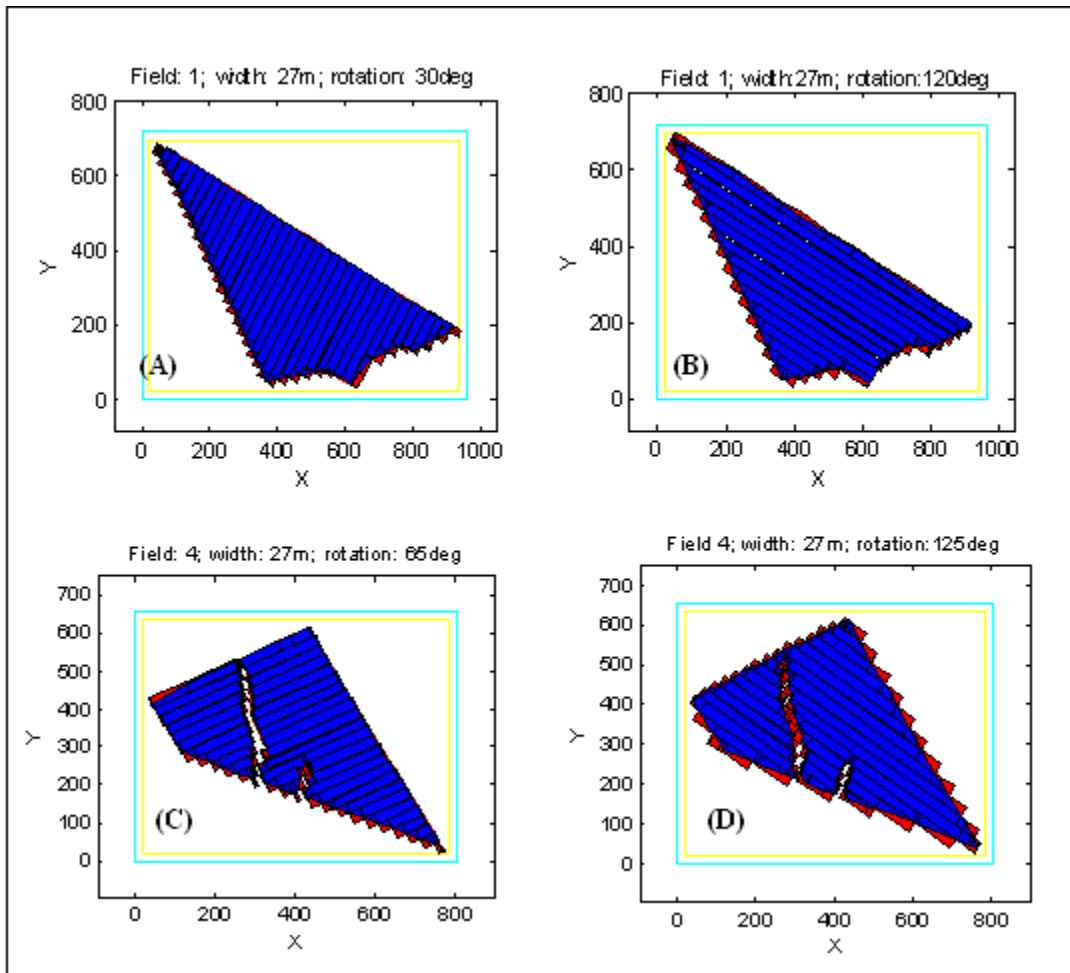
4.4.2   Field Data Comparison Results

Actual field performance data from an automatic section control system (Luck et al., 2010b) were compared to simulation results obtained using *FieldCAT* (Figure 4.11). Note that the simulated off-target application area was always less than the actual off-target area observed from the field dataset. Though at least part of this discrepancy may be attributed to less than ideal performance from the automatic section control system, the automatic steering system employed on the sprayer was also a major contributing factor, especially considering that it relied on sub-meter accuracy GPS rather than a more precise RTK-GPS. Luck et al., (2010a) discussed DGPS contribution to overlap errors. Position accuracy would not significantly affect the off-target computation since the section control is based on the perceived position of the vehicle as indicated by the GPS data. Similarly, the automatic steering system performance is based on perceived position; however, increased noise in position data would make it more difficult for the steering control to follow the desired path thus decreasing the perceived steering accuracy along the paths. In addition, there was some deviation from desired path, on headlands, through curves, and near the ends of swaths as the machine steering was converging to the desired path. The off-target application estimates reported by Luck et al. (2010b) included this lateral deviation as well as the headland encroachment overlap. FieldCAT assumes perfect guidance and thus no lateral overlaps or skips between adjacent passes. Unexpected maneuvers in the middle of the field were also observed in the field datasets, which caused additional overlapped areas that were not replicated by the simulation algorithm.
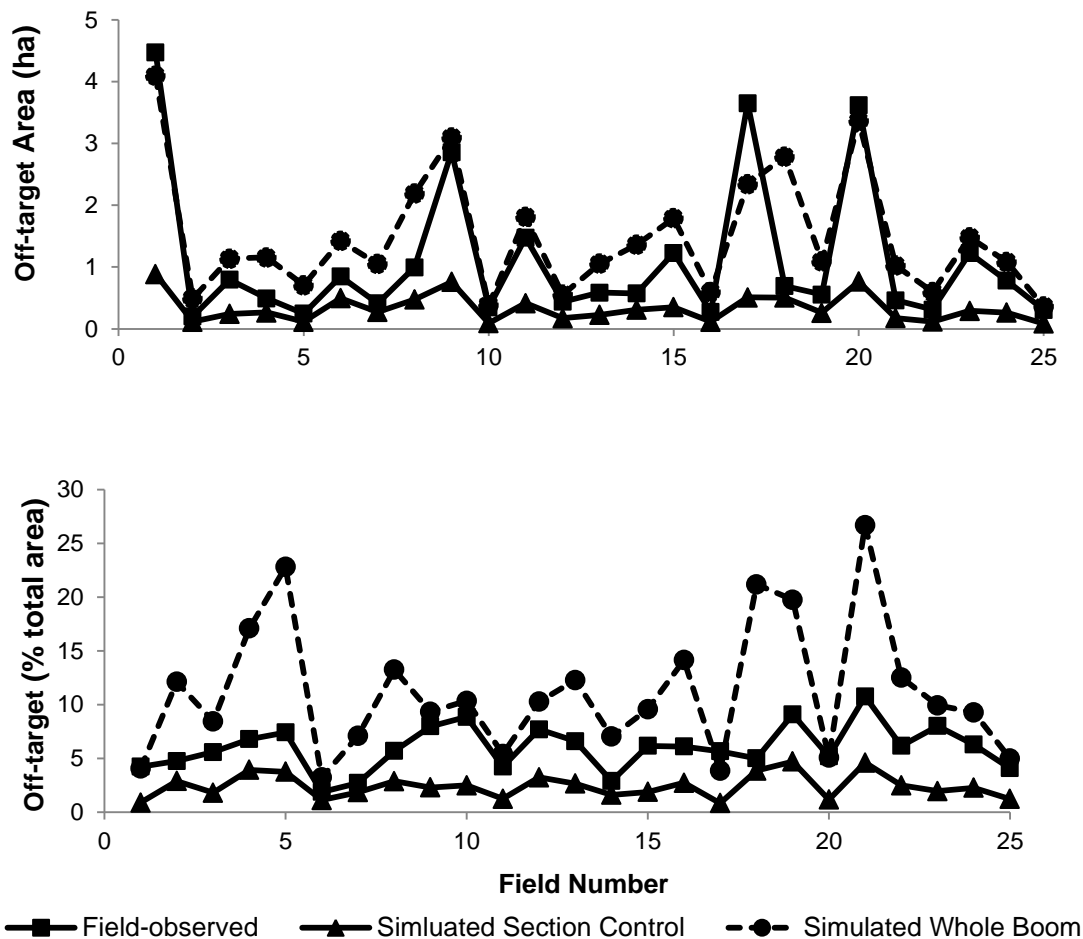
Figure 4.11: Off-target application computed from field-observed section control data and from the simulation tool for each of the 25 fields analyzed.

On initial inspection, the larger fields as well as fields with greater numbers of internal obstacles appeared to have more off-target application area and more discrepancy between the simulated and the field-observed off-target areas. Fields 1, 17, and 20, were the largest fields of the dataset. As expected, they exhibited the largest overall off-target application area, but they also exhibited the largest difference between the simulated and field-observed data. Field 9, though slightly smaller, also exhibited a large discrepancy that was probably due to the high number of non-navigable obstacles encountered in that field that required irregular maneuvering by the operator.

Although the simulated data underestimated the off-target area, it presented a strong relationship (coefficient of determination of 0.77 and coefficient of correlation of

29

0.87) with the field observed data (Figure 4.12 (A)), indicating the validity of the method. A simple compensation factor could be applied to the model if the error was systematic or constant; however, the errors were proportional to the field size as previously explained. The difference between the simulated and observed off-target areas was found to be a factor 0.04 times the field area (Figure 4.12 (B)). Thus, this data could be used, for example, to quantify the effectiveness of a guidance system combined with the operator skill in maneuvering on headlands passes and in headland turns. To further validate the model results, a 4% area proportional factor was applied to program output, and the resulting simulated data were very close to the field-observed data (Figure 4.13).
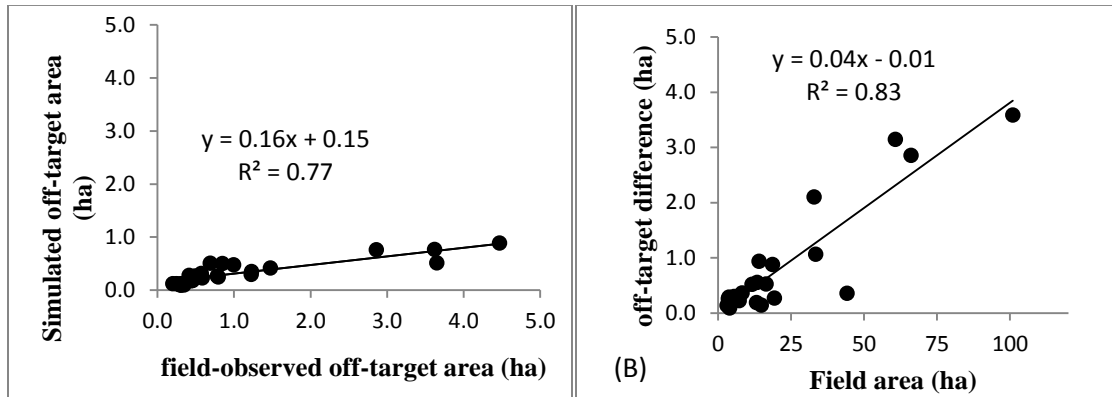
Figure 4.12: Simulated off-target application versus observed off-target application (A); Difference between the off-target application areas measured from field performance and the simulation program, versus field area (B).
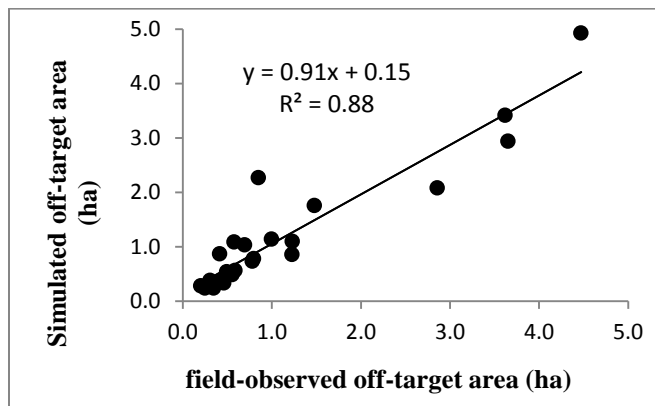
Figure 4.13: Simulated off-target application considering 4.0% off-target due to pass-to-pass overlap versus observed off-target application (A).

4.5   Conclusions

A software tool (*FieldCAT*) developed and described herein was able to provide a quantitative estimate of off-target application of inputs that would occur because of limited resolution of machine section control width and path orientation for different field shapes. Results clearly showed potential savings that could be achieved with the implementation of automatic section control technology. *FieldCAT* was also used to illustrate that path orientation can have a significant impact on input errors due to point rows and headland encroachment. Additionally, use of the tool elucidated the conflict between the optimum path orientation for minimizing application errors and the optimum path for maximizing machine field efficiency.

The comparison of *FieldCAT* output with the field data confirmed the validity of using the tool to evaluate off-target application area. The field data comparison also indicated that a complete analysis of off-target coverage during application of field inputs must consider guidance errors.

CHAPTER 5: EVALUATING FIELD SHAPE DESCRIPTORS FOR ESTIMATING OFF-TARGET APPLICATION AREA IN AGRICULTURAL FIELDS

5.1   Introduction

Decision aid tools to help evaluate the potential impacts of new technology are in great demand in agriculture. One of these newer technologies receiving much attention is automatic section control. Producers are very interested in this technology because of its potential to reduce the amount of off-target input application errors caused by larger machinery operating in non-rectangular fields. These off-target areas could be either double coverage in previously treated headland and point row areas or application outside the crop boundary.

There has been some research activity recently on the economic impact of automatic section control (Batte and Ehsani, 2006; Dillon et al., 2007; Shockley et al., 2012) as well as its performance (Mickelaker and Svensson, 2009; Molin et al., 2009). Batte and Ehsani (2006), by analyzing hypothetical farm fields, showed that the benefits of automatic section control increased with the increase of farm size, especially in areas with presence of waterways, drainage ditches and similar obstructions. Dillon et al. (2007) conducted a profitability analysis on three irregular fields that were sprayed using an automatic section control system and concluded that input expense savings alone would justify the adoption of the technology in many cases.

Luck et al. (2010a, 2010b) conducted several studies on the effectiveness of automatic section control. They reported a reduction of 15.2 % -17.5 % in the sprayed area of a field when using a 30-channel automatic section control system on a 25 m boom sprayer as compared to no section control. They also compared the results of a manually controlled 5-section spray boom with an automatically controlled 7-section spray boom operated over 21 fields. The over application areas reported were 12.4 % and 6.2 % for the manually and automatically controlled systems, respectively, indicating significant improvement with automatic over manual section control (Luck et al., 2010b).

One of the limitations inherent in much of the previous work is the fact that results are often based on hypothetical fields and/or a very limited equipment set and field conditions. With the goal of providing a much more universal tool for aiding the

decision-making process of adopting automatic section control on agricultural machinery,(Zandonadi et al., 2011; Zandonadi et al., 2009) developed a software tool called *FieldCAT* (Field Coverage Analysis Tool) for estimating off-target application areas based on the field boundaries and machine controlled section width. Although the comprehensive approach was functional and presented good performance when compared to field data, it was computationally intensive and required great effort and knowledge by the user to configure all input parameters. Therefore, a more simplified approach for estimating the effectiveness of automatic section control in particular fields would be desirable.

One possible method for predicting the performance of automatic section control in a particular field would be to find a simple way to characterize the shape of the field that would be predictive of off-target application. Shape representation and description techniques have been widely used in the realm of image processing and GIS (Geographical Information System) for the purpose of object identification. Zhang and Lu (2004) divide the shape description techniques into two classes of methods: contour-based and region-based methods, which are distinguished by whether the shape features are extracted from the boundary only (contour-based) or boundary plus interior content (region-based) of the object. Some descriptors are simple to calculate and do not require excessive computational power while others (usually the region based methods) can be fairly complex and computationally extensive.

There are several different types of field shape descriptors reported in the literature. Peura and Iivarinen (1997) evaluated the efficiency of five simple shape descriptors for object identification: convexity, principal axes, compactness, circular variance, and elliptic variance. Brinkhoff et al. (1995) also developed a set of quantitative parameters to characterize the complexity of a polygonal object. Theses parameters were combined resulting in what they defined as a Complexity Index (CI), which was used to classify polygons from a spatial dataset. The same concept was utilized by Souza and Guliato (2008) for purposes of breast cancer tumor classification.

Gonzalez et al. (2004) used the concept of shape description techniques for land consolidation in Spain. The authors addressed the issue of field size and shape regarding field efficiency with the purposes of grouping small and irregular fields in order to

improve efficiency. The Combined Size and Shape Index (CSSI) was based on the tillage time per hectare of useful surface area (RT), which was computed for 36 simplified field shapes considered the standard. For each of the 36 standard shapes, the RT was computed over an area range of 50 m^2 to 5 ha at 50 m^2 increments yielding 1000 plots of each shape. Then the RT of a given field shape was compensated by the size-based and shape-based correction factors a and b, respectively, which were based on the standard plots.

Regarding the effects of shape description techniques on off-target application areas, Sisk (2005) suggested that perimeter-to-area (P/A) ratio may affect the off-target application areas. Luck et al. (2011) confirmed the trend by presenting a coefficient of determination of 0.5 for the 21 fields included in their reported study. Like other works addressing off-target application, both of these studies were limited somewhat by the number of fields used and equipment parameters. For instance, machine width, which is a known factor that affects off-target application areas, was not considered in either study.

While factors such as field shape and size, as well as machine width and/or control resolution are known to affect the off-target application areas, the individual as well as the interactive effects of these factors on the off-target application areas are not defined. The major reason for this is that collecting a complete set of field data for such analyses would not feasible. Thus, the use of a computational tool such as *FieldCAT* (Zandonadi et al., 2011) would allow the generation of data for such a study. These analyses would then lead to a simplified method based on shape description techniques for estimating the off-target application areas considering the combined effects of the field shape and size, as well as the implement width.

5.2   Objectives

The goal of this study was to develop a simplified approach for estimating off-target application areas in agricultural fields considering the combined effects of field shape, field size, and implement width. This goal was achieved by accomplishing the following specific tasks:

- Quantify the effects of implement width on off-target application;
- Evaluate the combined effects of field shape, field size, and implement width on off-target application;

- Quantify the effects of field size and shape on off-target application using shape descriptor techniques; and

- Fit and validate a simple model, based on shape descriptors, for estimating off-target application areas in agricultural fields.

5.3   Materials and Methods

5.3.1   Shape Descriptors

Considering that the characteristics of the field polygon that affect off-target application area are its size and shape, contour-base shape descriptions techniques were evaluated. There were 12 contour-based descriptors evaluated:

(1) Convexity

(2) Principal axis ratio

(3) Compactness

(4) Circular variance

(5) Elliptic variance

(6) Rectangularity

(7) Frequency of the concave regions

(8) Deviation of the concave regions

(9) Complexity index (CI)

(10) Mean centroid distance

(11) Perimeter-to-area ratio

(12) Headland area-to-field area ratio

Convexity   Principal axis ratio   Compactness   Circular variance   Elliptic variance
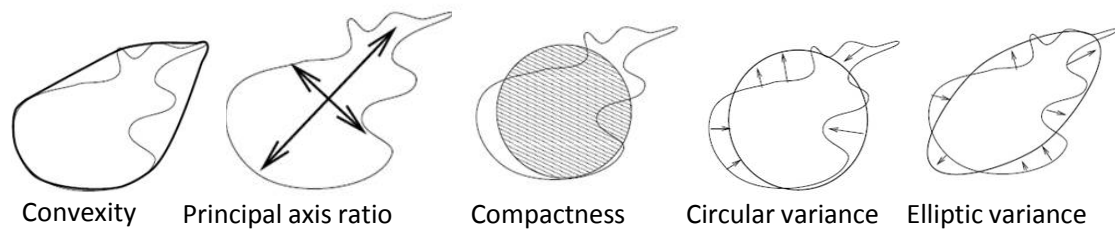
Figure 5.1: Simple shape descriptors (Peura and Iivarinen, 1997).

The first five descriptors (Figure 5.1) were defined according to Peura and Iivarinen (1997). Convexity can be defined as the ratio of perimeter of the convex hull of the contour (the envelope with no concavity that contains all the polygon vertices) and the original polygon (Equation 5.1)

$$conv = \frac{P_{convex\ hull}}{P}$$ Equation 5.1

Principal axes of an object can be uniquely defined as segments of lines crossing each other orthogonally in the centroid. The lengths of the two principal axes are given by the eigenvalues of the contour vertices covariance matrix. Peura and Iivarinen (1997), however, stated that it can be calculated directly according to Equation 5.2 where c_{ij} are relative to the covariance between the coordinates x and y of the polygon vertices.

$$prax = \frac{c_{yy} + c_{xx} - \sqrt{(c_{yy} + c_{xx})^2 - 4(c_{yy}c_{yy} - c_{xy}^2)}}{c_{yy} + c_{xx} + \sqrt{(c_{yy} + c_{xx})^2 - 4(c_{yy}c_{yy} - c_{xy}^2)}}$$ Equation 5.2

Compactness is often defined as the ratio of the squared perimeter to the area of an object. It reaches the minimum in a circular object. For this study, the compactness (Equation 5.3) value was divided by 4π such that a circular polygon would present a value of 1.

$$comp = \frac{P^2/A}{4\pi}$$ Equation 5.3

The circular variance (*Cvar;* Equation 5.4) is a method of comparing the shape of a polygon to a circle of the same area. It is calculated by the proportional mean-squared deviation of all vertices on the polygon from the circle. Thus, **Cvar** is zero for a perfect circle and it increases with the shape complexity and elongation. The elliptic variance (**Evar**; Equation 5.5), is based on the same principal as the circular variance except that the polygon is compared to an ellipse created based on the principal axes. The parameters used in the computation of **Cvar** and **Evar** were defined according to Peura and Iivarinen (1997).

$$Cvar = \frac{1}{N\mu_r^2} \sum_i (\|p_i - \mu\| - \mu_r)^2 \qquad \text{Equation 5.4}$$

$$Evar = \frac{1}{N\mu_{rc}} \sum_i \left(\sqrt{(p_i - \mu)^T C^{-1} (p_i - \mu)} - \mu_{rc} \right)^2$$

$$\mu_{rc} = \frac{1}{N} \sum_i \sqrt{(p_i - \mu)^T C^{-1} (p_i - \mu)} \qquad \text{Equation 5.5}$$

- $p_i = \begin{bmatrix} Xi \\ Yi \end{bmatrix}$ contour point
- $\mu = \frac{1}{N} \Sigma_i p_i$ centroid
- $\mu_r = \frac{1}{N} \Sigma_i \|p_i - \mu\|$ mean radius
- $C = \frac{1}{N} \Sigma_i (p_i - \mu)(p_i - \mu)^T$ covariance matrix

Rectangularity (Equation 5.6) can be defined by the area of the polygon divided by the area of the smallest rectangle that encompasses the original contour. The rectangle is also called the bounding box.

$$rec = \frac{A_{polygon}}{A_{bounding\ box}} \qquad \text{Equation 5.6}$$

The Complexity Index (**CI**; Equation 5.11), developed by Brinkhoff et al. (1995), was based on the combination of three other descriptors: frequency of concave regions (**Feq**; Equation 5.7); deviation of the polygon from its convex hull (**Dev**; Equation 5.9); and amplitude of the concave regions (**Amp;** Equation 5.10). The authors' approach of shape complexity (**CI**) of a polygon was based on what they called the shape global complexity and the shape local complexity, represented by the local vibration of its boundary. The local vibration was represented by **Feq** and **Amp**, whereas the global shape was represented by **Dev** where **N**_*norm* (Equation 5.8) was the normalized number of concave regions (**N**; Figure 5.2) in a polygon of *(V)* number of vertices.
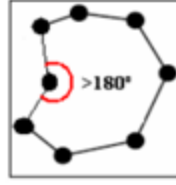
Figure 5.2: Polygon with **V** equal 8 and **N** equal 1

$$Feq = 16(N_{norm} - 0.5)^4 - 8(N_{norm} - 0.5)^2 + 1$$

Equation 5.7

$$N_{norm} = \frac{N}{V - 3}$$

Equation 5.8

$$Dev = \frac{A - A_{convex\ hull}}{A}$$

Equation 5.9

$$Amp = \frac{P - P_{convex\ hull}}{P}$$

Equation 5.10

$$CI = 0.8 Feq \cdot Amp + 0.2 Dev$$

Equation 5.11

The authors experimentally defined the weights given in Equation 5.11 and stated that **Dev** allowed users to distinguish the complexity of polygons with similar values of **Feq·Amp**. **CI** presents an interval of 0 to 1; values close to 0 indicate a simple convex polygon whereas values larger than 0.4 indicate very complex polygons.

The last two descriptors studied were the field perimeter divided by field area (**P/A**) and field headland area divided by field area (**H/A**).

5.3.2 Experimental Procedures

Agricultural field boundaries from different agricultural regions of the state of Kentucky were either digitized from an aerial imagery data base (KDGI, 2006) or surveyed using RTK solution GPS. The western region (Fulton County) presented more regular field shapes whereas the central region (Shelby County) presented more oddly shaped fields with the presence of grassed water-ways and other interior obstructions. A total of 121 field boundaries (Figure 5.3) were gathered with areas ranging from 1.3 to

82.5 ha. The field boundaries were processed in **FieldCAT** to compute the off-target application areas for different scenarios.
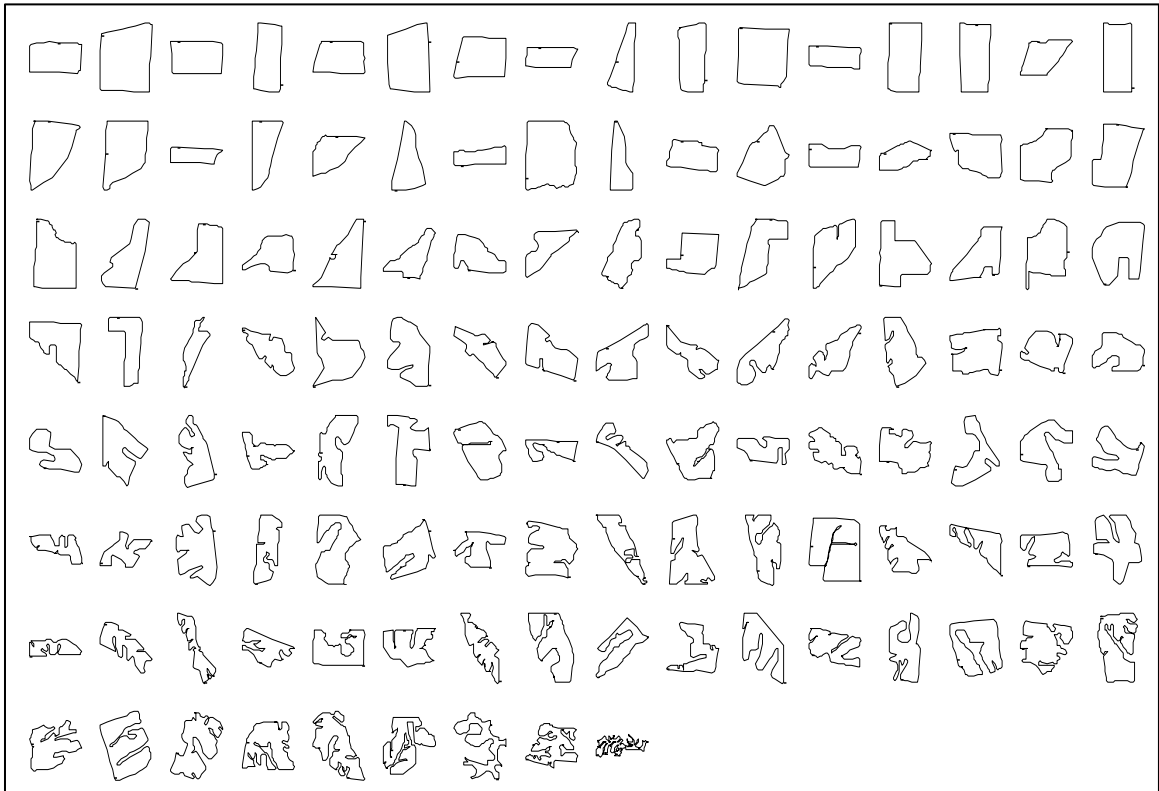

Figure 5.3: The set of 121 field boundaries used in the experiment. Boundaries are not to scale and are sorted according to the Complexity Index.

There are many parameters that can affect the off-target application errors including field size and shape, machinery operator's skills or guidance accuracy, driving pattern and orientation, implement total width, and in the case of automatic section control, the control resolution. **FieldCAT** assumes perfect parallel straight swaths (no pass to pass overlap or skips), so the calculated off-target areas result only from the swath's intersecting headland or boundary areas at non-right angles. Because path orientation affects the off-target application areas, the approach used in this study was to compute the average off-target areas of several path orientations. More specifically, the path orientation was rotated from 0 (relative to northing) to 178 degrees in 2-degree increments and the average was computed over the resulting 90 data points for each field. Regarding the headland areas, **FieldCAT** was configured to create a buffer twice the implement width inside the field boundary, which was called the headland area. The

practice of making one or two machine passes around the entire field before starting the parallel swaths is very common especially in odd-shaped fields.

5.3.3   Field Size Effects

For the evaluation of field size effects, two fields of distinct geometry complexity were chosen based on the complexity index and scaled to a single reference area of approximately 46.5 ha. Those fields were then scaled from approximately 1:10 up to 2:1 of that original reference area in increments of 1:20 of the original reference area. The off-target areas were computed for each field size using a fixed implement width of 15.2 m.

5.3.4   Implement Width Effects

To evaluate implement width effects, the off-target areas were computed for the same fields as above at the reference area of 46.5 ha while varying the implement width from 1.5 to 73.2 m. Although the largest common implement width in today's agricultural machines is about 36.6 m, the 73.2 m width was used for illustration purposes.

5.3.5   Field Shape and Area Effects

The field shape effects were evaluated by scaling all 121 fields to a common reference area, computing the off-target application area with the same implement width (15.2 m) for every field, and then evaluating the effect of each shape descriptor.

Once the relationships to the descriptors and field shape alone were determined, the field size and shape were combined for further evaluation. Here, the percent off-target application and off-target application area were computed with the same implement width (15.2 m) for every field at its original size.

5.3.6   Field Shape, Field Area, and Boom Width Effects

Finally, the off target application was evaluated considering field shape, field size, and implement width all together. This step was accomplished by computing the average

off-target areas for each field at its original size while varying the boom width over five widths (3.8, 7.6, 15.2, 22.9, and 30.5 m) and then plotting them according to the field shape descriptors.

5.3.7 Model Fitting and Validation

After identifying the best descriptor response to off-target application when all the variables were considered, the data were divided into two sub-datasets (one for model fitting and the other for model validation). The model validation was performed by regressing the observed percent off-target against the estimated percent off-target for the validation sub-dataset, and the t-test for regression slope (β) equal to one (H_0: β =1 VS H_0: $\beta \neq 1$) and regression intercept (α) equal to zero (H_0: α =0 VS H_0: $\alpha \neq 0$) was applied.

5.4 Results and Discussion

5.4.1 Field Size Effects

The two fields that were chosen to evaluate the field size effects on off-target application were the first and next-to-last field shown in Figure 5.3. This decision was based on their Complexity Indices, which were 0.0013 and 0.51 for the simple and the complex fields, respectively. The results obtained from the analysis, which considered a 15.2 m wide implement, revealed that off-target application area increased more rapidly for the complex field as the field area increased as expected (Figure 5.4). The percent off-target application was determined by dividing the off-target area by the total field area. For very small field areas, the off-target application in the complex field was smaller than the off-target area of the simple field, which at first seems contradictory; however, in small fields, the majority of the complex field was covered by the headland area.

Notice in Figure 5.4 (B) that the percent off-target application follows an exponential relationship for the simple field and that approximately 50 % of its area is covered by the headland in the worst case. On the other hand, the complex field presented a more linear trend for the headland covering less than approximately 80 % of the total area. The off-target area trend was linearized by applying a natural logarithmic transformation to both axes considering the off-target areas for the H/A ratio less than 0.8

41

(Figure 5.5). The slopes of the transformed data were similar for both fields considering the 95 % confidence intervals (Table 5.1). The off-target area increased at the same rate for both fields when considering the transformed data such that one could fit a line into the transformed data and use the slope of the fitted line to explain the off-target application area response to the field area. The intersect, however, is related to the complexity of the field and one could adjust it according to the complexity index.

(A)

(B)
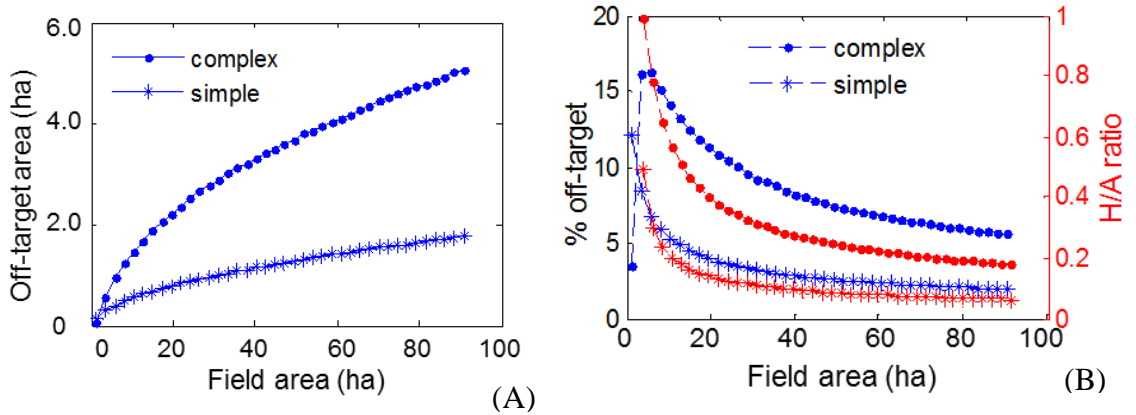
Figure 5.4: Off-target application area (A) and percent off-target application (B) for simple and complex field boundaries of different sizes.
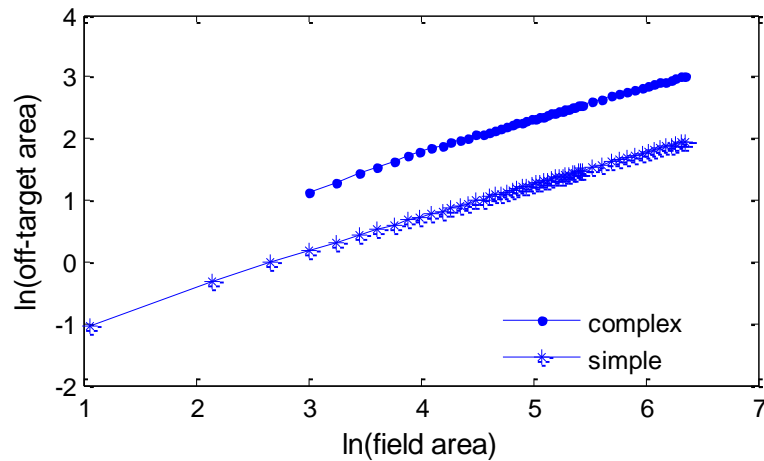

Figure 5.5: Logarithmic transformation of off-target application area versus field area for the simple and complex field boundaries.

Table 5.1: Regression parameters of the transformed off-target area data.

| | slope | 95 % interval | | Intercept | 95% interval | |
		lower	upper		lower	upper
complex	0.545	0.538	0.553	-0.422	-0.461	-0.383
simple	0.545	0.538	0.552	-1.477	-1.510	-1.444

5.4.2   Implement Width Effects

Results obtained from the implement width effects study revealed a linear trend in off-target application up to a width of approximately 30.5 m (Figure 5.6 (A)). For large implements, the off-target area for the complex field deviates from the linear trend (Figure 5.6 (B)). This transition occurs at an H/A ratio of approximately 0.6. Note that even for the largest boom, the H/A ratio for the simple field was below 0.4 maintaining the linear trend across the range of widths tested. The errors illustrated by the one standard deviation bars in Figure 5.6 (B) are based on the variation at different path orientations. As expected, the standard deviation increases with boom width since the difference between minimum and maximum value of off-target area at different path orientations should increase.
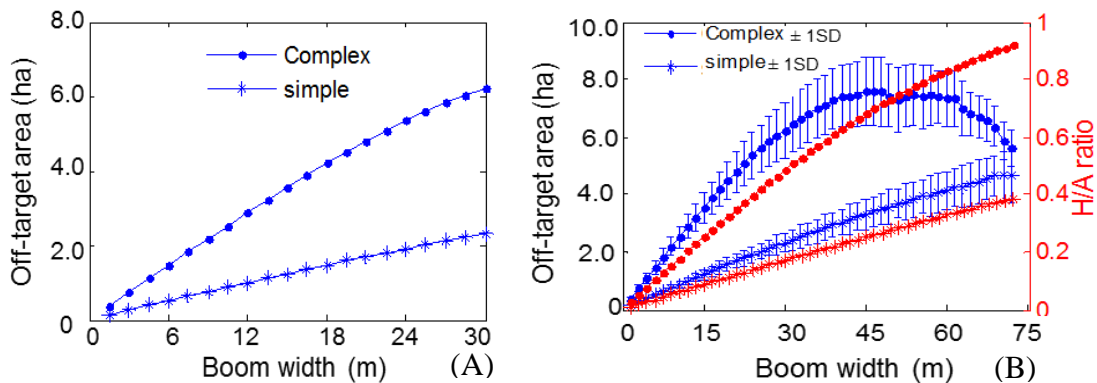

Figure 5.6: Linear trend between off-target area and boom width (A); and non-linear response for high H/A ratio (B).

5.4.3   Field Shape and Area Effects

Results obtained from the field shape effects study on the off-target application area are presented in Figure 5.7. Recall that the all fields were scaled to a similar reference area (46.5 ha), and that the implement width was fixed at 15.2 m. Considering that the area was constant for all the fields, the off-target application areas were presented as a percentage of the total field area.
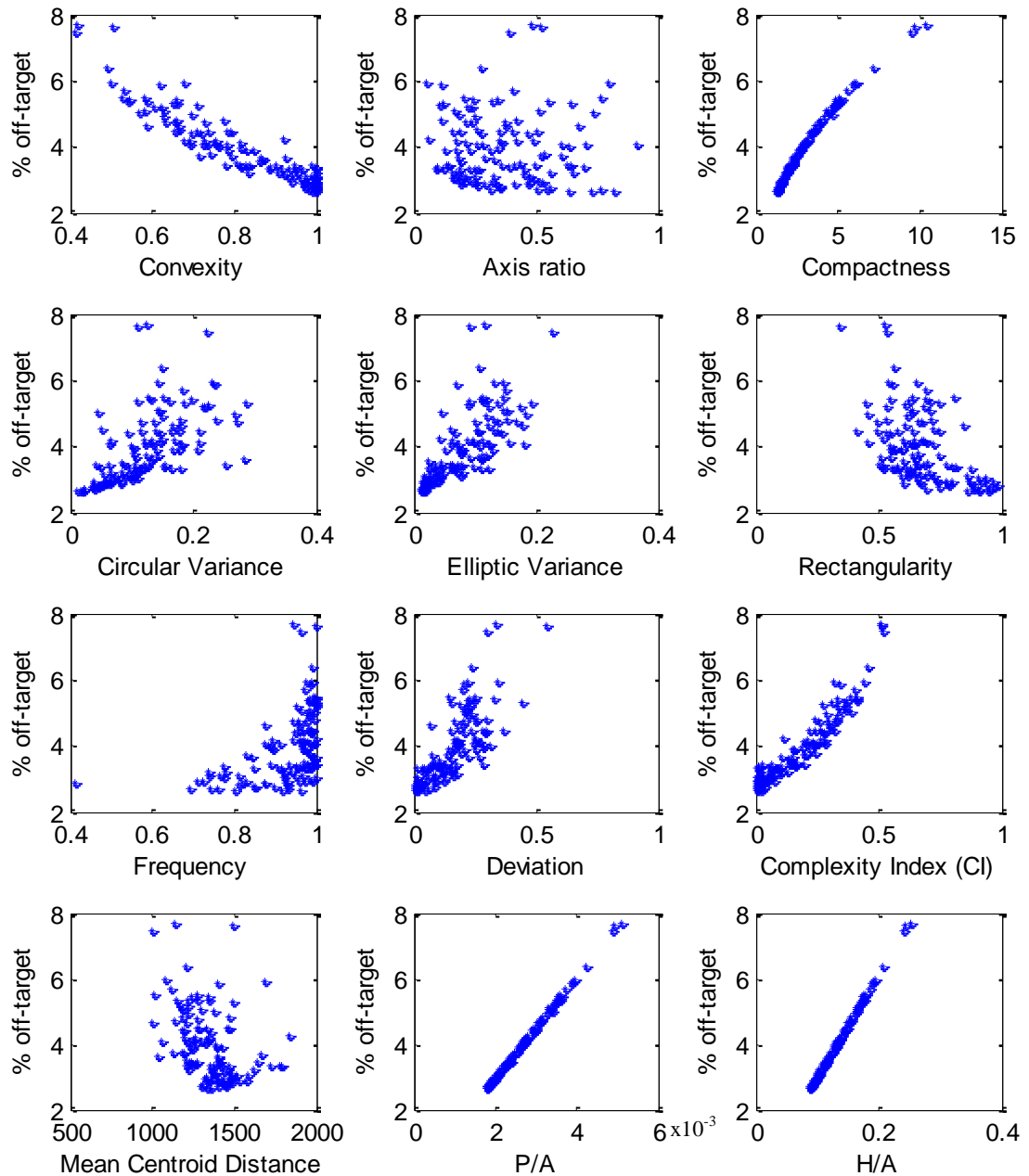
Figure 5.7: Percent off-target application according to field shape descriptors for all the fields scaled to an area of approximately 46.5 ha. Off-target application was computed based on a 15.2 m wide implement.

Percent off-target application due to field shape exhibited a strong linear response to the P/A and H/A descriptors. Compactness, complexity index and convexity also presented a fairly good predictive ability; however, the relationships were not linear.

To show the combined effects of field size and shape, off-target area and percent off-target were computed for a 15.2-m implement in all fields at their original size (Figure 5.8). Notice that there were no trends defined for the first nine descriptors for either off-target area or percent off-target area. The last three descriptors showed a more defined trend, especially for the percent off-target. This is due to the fact that the first nine descriptors do not carry any information about the total field area whereas mean centroid distance carries some information about total area, and obviously P/A and H/A are directly affected by field area. Thus, all the descriptors except P/A and H/A, were normalized by the field area, which improved the trends considerably (Figure 5.9). The off-target area tended to present a form of a reciprocal function, so a reciprocal transformation was applied to all area calculations (Figure 5.9).

The area normalization improved the overall trend for every descriptor; however, P/A and H/A are still the best predictors for percent off-target application. Regarding the off-target area, the reciprocal transformation linearized the trends for the most part; however, mean centroid distance, rectangularity and convexity seem to have a stronger relationship to the transformed off-target area.

It is clear that H/A or P/A could be used to estimate percent off-target application, or, if the off-target area is necessary, mean centroid distance/A or rectangularity/A would be good predictors.
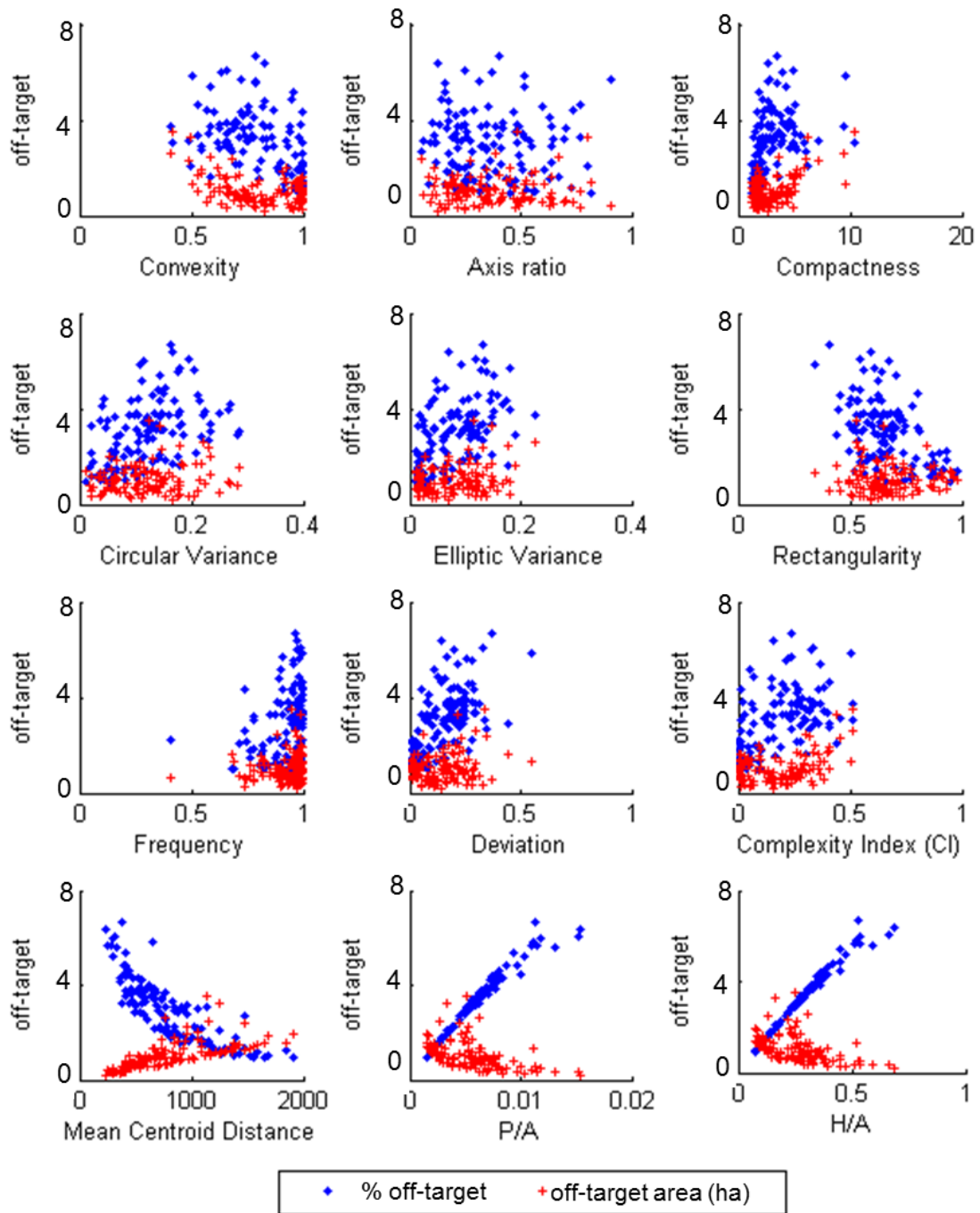
Figure 5.8: Off-target area and percentage off-target according to field shape descriptors based on a 15.2 m wide boom.
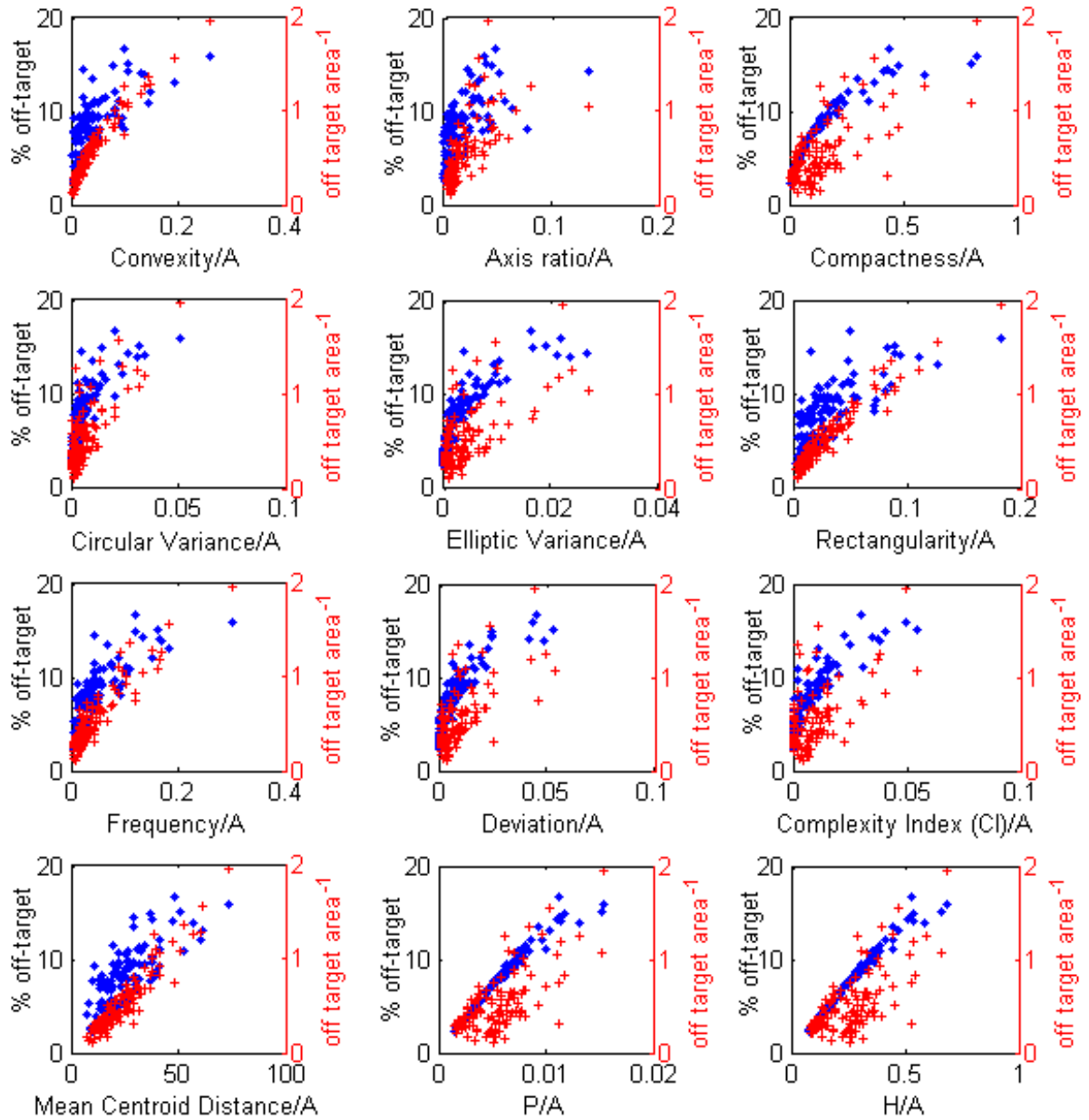
Figure 5.9: Percent off-target application according to area normalized shape descriptors for a 15.2 m wide implement.

5.4.4   Field Shape, Field Area, and Boom Width Effects

Finally, the implement width was allowed to vary in each field (Figure 5.10 and Figure 5.11). Given that the H/A descriptor was not practical on very small fields (recall Figure 5.4 (B) and Figure 5.6 (B)), a threshold value of 0.6 for H/A was used for the analysis. The varying implement width shifted the trends in percent off-target application

for all the descriptors except the H/A, which is reasonable since the H/A is the only descriptor that carries information about the implement width. Observe that the trends for the off-target area shifts even for the H/A ratio.

Considering that the off-target application percentage and area varied linearly with the boom width (Figure 5.6 (A)), an attempt of normalization by implement width was made. The shifting in the trends were considerably reduced for both off-target percent and area; however, the relationship between H/A and percent off-target is still the strongest. This is very promising since headland area can be estimated fairly well by multiplying the field perimeter, which is simple to compute, by the implement width. Besides the simplicity of computation, it is the only descriptor that takes into account the size of the machine with respect to field size.
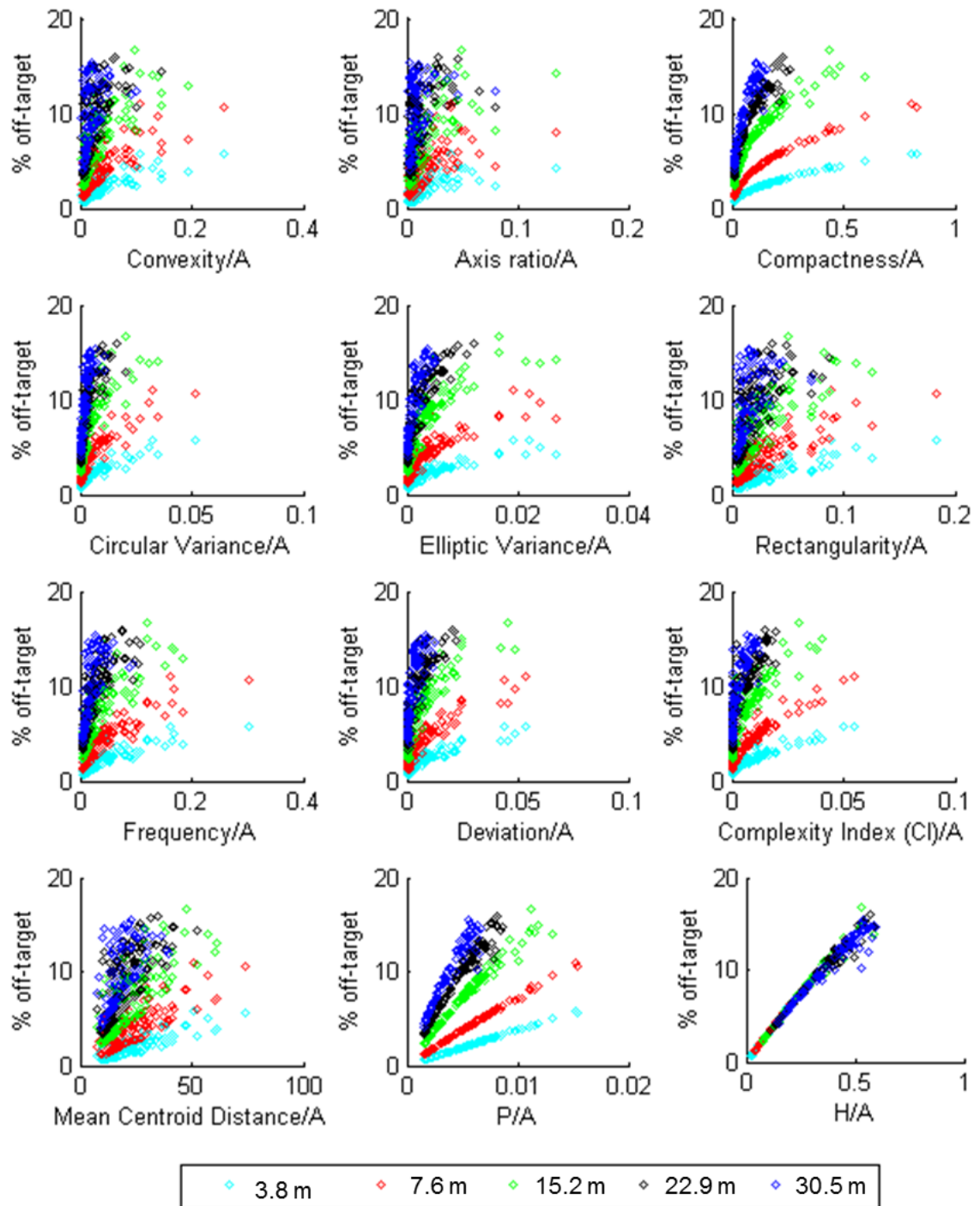
Figure 5.10: Percent off-target application according to area normalized shape descriptors for 3.8, 7.6, 15.2, 22.9, and 30.5 m implement widths.
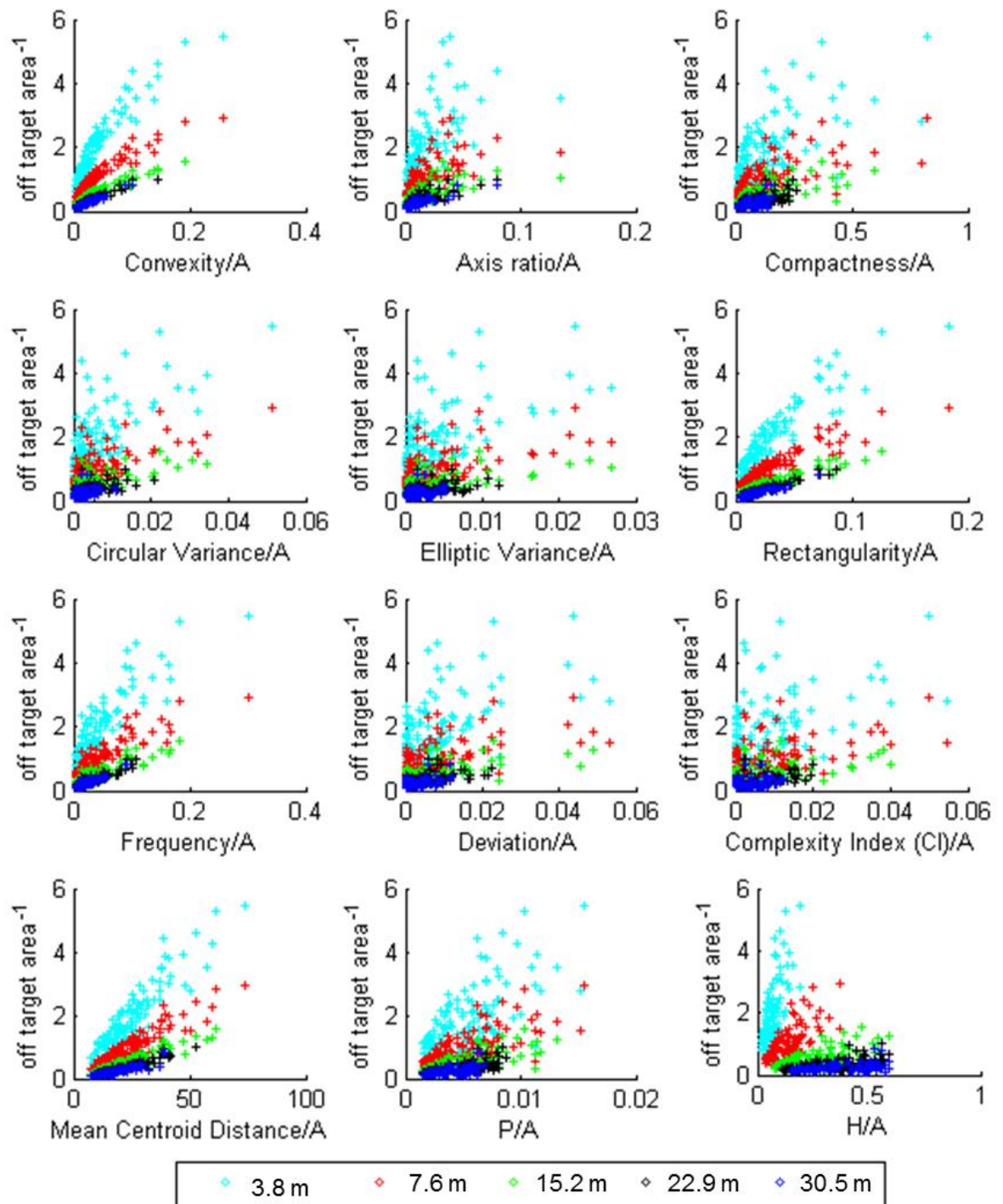
Figure 5.11: Transformed off-target application area according to area normalized shape descriptors for 3.8, 7.6, 15.2, 22.9, and 30.5 m boom width.

5.4.5 Modeling Fitting and Validation

Finally, for the model fitting and validation step, the data were divided in two sub-datasets. The number of field coverage data points considering the five implement widths over the 121 fields evaluated was 605. However, as presented in the previous sections, the most promising descriptor (H/A) was not practical for very small fields. Thus, the sub-datasets were reduced by eliminating scenarios with H/A lower than 0.6, which resulted in 258 data points in each sub-dataset. The results of the model fitting calculations revealed that not only did the percent off-target application increase with H/A, but the variance also increased (Figure 5.12). Thus, a variance-stabilizing transformation was applied to better fit the model (Figure 5.12 (B)). The fitted model (Equation 5.12) was then used to estimate the average percent off-target for the validation dataset. The results from the t-test applied to the validation dataset are presented in Figure 5.13 and Table 5.2. The P-value supported the hypothesis for a slope of one with a strong probability; the intercept had significance at 2%.
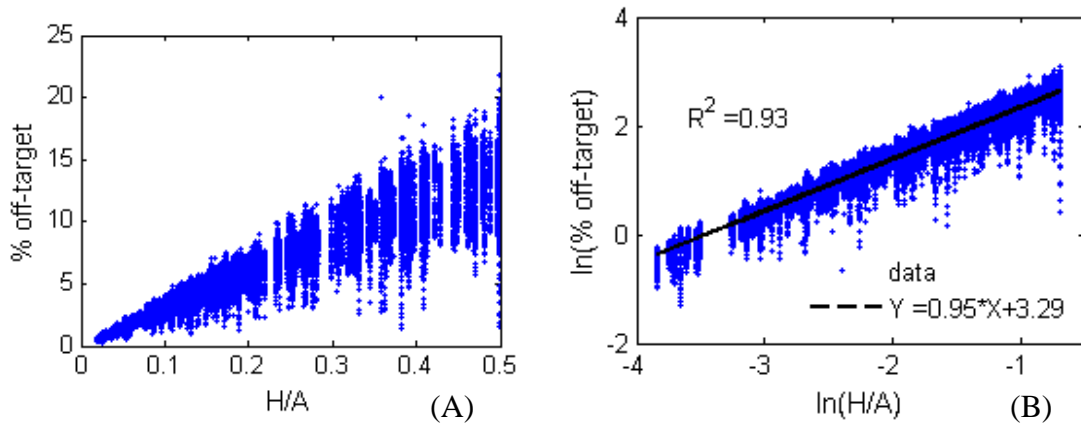

Figure 5.12: Percent off-target for every path orientation in each field from the fitting dataset (A); and variance-stabilizing transformation of the same data (B).

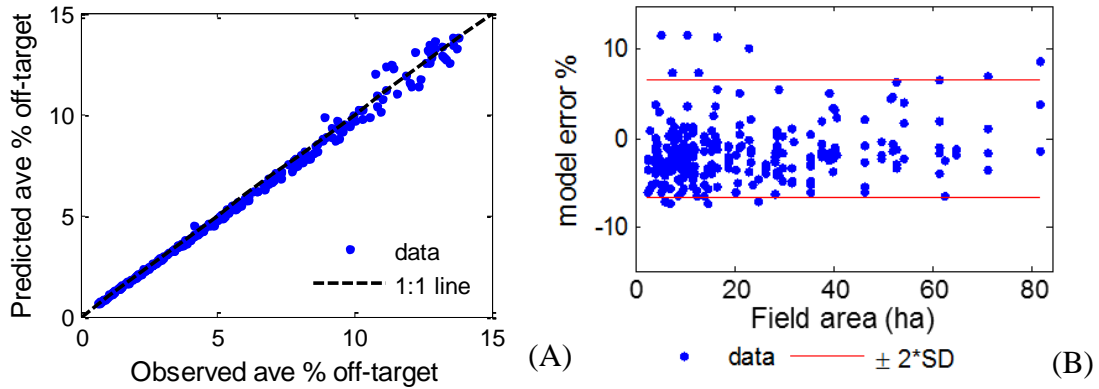$$ave\ \%\ Offtarget = e^{\ln\left(\frac{H}{A}\right)0.95+3.28}$$

Equation 5.12

51

Figure 5.13: Validation results of predicted versus observed percent off-target application (A) and model error according to the field area (B).

Table 5.2: T-test results for the model validation evaluation

| | Coefficient | 95 % Confidence interval | | T stat | P value |
		Lower	Upper		
slope	0.994	0.985	1.004	-1.158	0.124
Intercept	-0.067	-0.13	-0.002	-2.047	0.021

The observed errors (Figure 5.13 (B)), can give an insight about the model performance. Although errors up to 11.6 % were found, 95 % of the errors were within ±6.7 % (2 standard deviations). While ±6.7 % error in estimated average percent off-target application may be considered acceptable, caution must be exercised with this method. Recall that the percent off-target application exhibited a large variation within the same field depending on the orientation of the coverage path (Figure 5.13 (A)) and that the variation increased as the H/A increased. For the purpose of average estimation, a transformation was applied to minimize the error variance to fit the model.

5.5 Conclusions

This study revealed encouraging results toward simplified techniques for estimation of off-target application areas in agricultural fields caused by field shape and size as well as implement width. The following specific conclusions were drawn from the study:

- The relationship between field area and off-target application area for fields of same complexity can be linearized by applying a natural logarithmic

52

transformation on both axes. The slopes of the linearized curves for fields of different complexity were the same and the intercepts were a function of the field complexity. This trend was found for situations where the H/A ratio was lower than 0.8.

- Implement width effects on off-target application areas for fields of same size were linear as long as the ratio H/A was less than 0.6. As expected, complex field shapes increased the off-target area more rapidly according to the implement width when compared to the simple fields.

- Percent off-target application exhibited some correlation to several different shape descriptors when fields were all scaled to a common reference area; however, when field size was taken into account, only P/A and H/A exhibited reasonable trends. Area normalization improved the trends for the most part, but P/A and H/A still exhibit the strongest relationships for a variety of scenarios.

- The P/A descriptor, while well correlated to off-target application, was sensitive to implement width. The H/A descriptor was more stable across varying implement widths and was therefore found to be the best indicator of off-target application and used in the model.

- The linear model that included a natural logarithmic transformation was found to be able to predict average percent off-target application within ±6.7 % at 2 standard deviations.

Field area and perimeter can be easily computed using an electronic spreadsheet; therefore, the proposed method can be used as a quick alternative for estimating average percent off-target application for a particular field and machine widths up to 30.5 m. However, coverage simulation is still needed if detailed information about the path coverage orientation that yields the absolute minimum off-target application area is desired.

CHAPTER 6: ROUTING ALGORITHM BASED ON MACHINE FIELD EFFICIENCY AND OFF-TARGET-APPLICATION AREAS

6.1 Introduction

In an agricultural production system, machinery operation costs represent a significant portion of the total production cost (Edwards, 2009); therefore, good fleet management could have a considerable impact in the producer's net income. Moreover, increases in capacity as well as technologic resources available in modern machines demand a higher investment of capital, which heightens interest in optimizing machine efficiency as well as improving the accuracy of the input placement.

Field efficiency, as well as the operational cost of agricultural machines, is directly impacted by the planning of the task. Semi-autonomous machines guided by Global Navigation Satellite Systems (GNSS) permit the accomplishment of tasks sometimes beyond the capacity of the operators, thus requiring an adequate planning of the task to be conducted in the field.

The planning of a field operation, or mission planning, is rather difficult. Bochtis et al. (2007) discussed the complexity of a field task planning using a harvesting operation as an example including the dynamic aspects of the system. The authors proposed a hierarchy decomposition of the system in simpler problems with fewer variables to be solved independently and efficiently. One of the individual problems to be solved was the coverage path planning for individual vehicles. Reid (2004) stated that path planning is one of the key tasks in the mission planning process.

In most agricultural field operations, coverage path planning determines a path that guarantees an agent will pass over every point in a given environment (Choset and Pignon, 1997). The subject has been extensively studied in the realm of mobile robotics, but most of the developed approaches cannot be directly applied to agricultural operations (Huang, 2001). One of the reasons which make planning an optimal path for agricultural machinery a difficult task is the fact that agricultural machinery are nonholonomic, which means that they cannot make a turn without moving their pivot point (Oksanen, 2007). In the role of path planning for agricultural applications, field operation costs and environment preservation are the main targets taken into consideration. Hence, minimizing distance traversed to cover a field, maneuvering time,

overlapped areas, skipped areas, and down time due to loading/unloading process are desired variables used in the cost function for the path planning process. However, addressing all these variables at once is rather difficult, especially considering that some of them might present competitive behavior in the objective function. For instance, the coverage path of a planting operation with the shortest distance travelled in the field my not result in the coverage path with the least off-target application because of point rows in the headland region. In this case the trade-off is driven by the actual cost of the machinery operation and the cost of seed, fertilizer and chemicals applied during the operation. Also, working with complex boundary geometry of oddly shaped fields typically found in some regions compounded by the three dimensional space of the farming terrain makes path planning for agricultural fields even more challenging.

Researchers have developed methods for coverage path planning applied to agricultural fields (Choset, 2000; Choset and Pignon, 1997; Dillon et al., 2003; Stoll, 2003) focused on different aspects of the problem, often relying on over-simplification of the problem to make the algorithms work. However, the majority of these studies address the number of turns, how complicated the maneuver is, and how to decompose a complex field boundary into sub-fields for better planning. The issue of off-target application attributed to point rows in the headland region has not received much attention in the reported studies, although its importance is recognized by the majority of researchers in the area. Hunt (2001) presented a method to compute the wasted travel distance and off-target application area in the headland based on implement width and the angle between vehicle trajectory segment and the headland segment. This method is used in other studies (Jin and Tang, 2006, 2010; Spekken, 2010). However, in odd shaped fields, the headland edge segments are often shorter than the actual implement width. Thus, especially on occasions where the implement boom width is large, this method sacrifices accuracy in computing the wasted travel distance as well as the off-target area in the headland.

Zandonadi et al. (2011) developed a software tool called *FieldCAT* (Field Coverage Analysis Tool) for estimating off-target application areas based on the field boundaries and machine controlled section width, which overcomes the limitation of the simplified method, but requires more computing power. The authors also pointed out that

the number of turns required to achieve the minimum off-target application coverage pattern was not the same as the coverage pattern that presented minimum number of turns indicating a tradeoff between machine field efficiency and application error.

6.2   Objectives

The goal of this study was to develop a routing algorithm capable of determining the optimum coverage pattern that considers both the time required to complete the task and the amount of off-target application due to headland encroachment at point rows. Thus, the overall goal of this work was achieved by means of development of two different routing algorithms and a comparison among the results obtained as is enumerated in the following objectives.

- Develop a routing algorithm that can be applied to a whole field polygon and can be used for the route simulation process;
- Develop a field decomposition technique to decompose a non-convex polygon into a set of convex polygons for route simulation; and
- Compare the results of simulation analyses that result in minimized operating costs and minimized input costs to determine the best economic route.

6.3   Materials and Methods

The algorithms were developed in a MATLAB platform (MathWorks, 2009) taking advantage of the functions and routines available with the Mapping Toolbox whenever possible. The majority of the routines were developed as needed for solving specific tasks of the problem.

Some simplifying assumptions were made to facilitate reasonable implementation of the routing algorithms:

- Only straight parallel swaths were used to simulate field coverage. Also, the parallelism between swaths was assumed perfect resulting in no skipped or overlapped regions between passes. Thus, the off-target application areas of a given route were a result of the swaths intersecting the headland or boundary areas at non-right angles.

56

- The maneuvering model used in the simulation was the U-turn type. The headland area was assumed to be twice the effective working width of the implement as if the machine had made two passes along the field boundary.

- The machine servicing time such as for refilling/unloading was not considered in the simulated scenarios.

- Machine transport from one part of the field to another was accomplished only over the headland areas.

- The field polygon geometry considered in this study contained no more than one non-convex vertex.

- All polygons were considered two-dimensional not taking into consideration the topography of the terrain.

Since route orientation affects off-target application areas as well as machine efficiency, the optimum route was accomplished by an exhaustive search among a given set of different route directions. For instance, the route orientations were simulated from 0 to 179 degrees in steps of one degree for every polygon analyzed.

As mentioned before, two routing methods were considered. In the first, the routing was accomplished in a field as a whole. In the second, a field decomposition technique was used to divide the polygon into sub-polygons with simpler geometry for further analyses.

The following are definitions of key terms used in the study:

Non-convex polygon: Is a polygon that presents at least one concave border area (Figure 6.1).
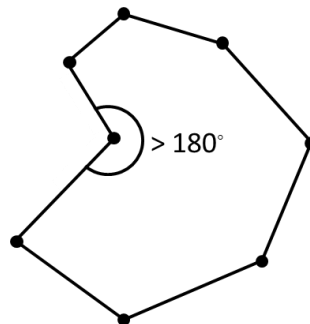
Figure 6.1: Illustration of a non-convex polygon.

Doubly connected list (dcl): Method of representing polygon vertices by including information about adjacent vertices. For instance, node **2** of the polygon shown

below (Figure 6.2) would carry information about its x, y coordinate, as well as information about the two adjacent segments or edges (**1** to **2**, and **2** to **3**) that forms the vertex 2. The polygon data structure was represented in *dcl* to allow vertex manipulation during the field decomposition process.
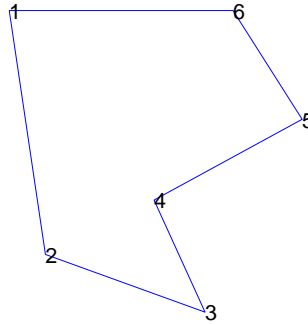

Figure 6.2: Nodes of dcl representing the polygon vertices**.**

Headland region: Region created by offsetting polygon boundaries inwards forming the region were maneuvering would take place. The headland was created considering to be twice the implement working width (Figure 6.3).
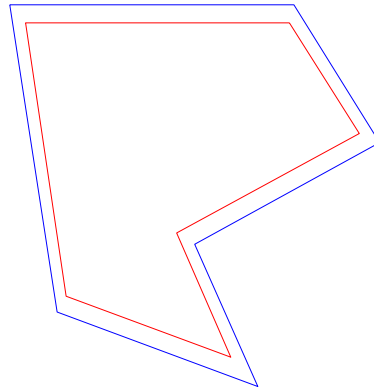
Figure 6.3: Representation of the headland boundary.

Frame rotation: To simplify calculation and make the algorithmic solution more intuitive, the polygon coordinate frame was rotated such that base line was always coincident with the y (vertical) axis (Figure 6.4). The rotation matrix was defined by Equation 6.1 and the rotated polygon coordinates were defined by Equation 6.2. All computations were carried out using the rotated coordinates and then transformed back to the original reference frame once the calculation was complete.
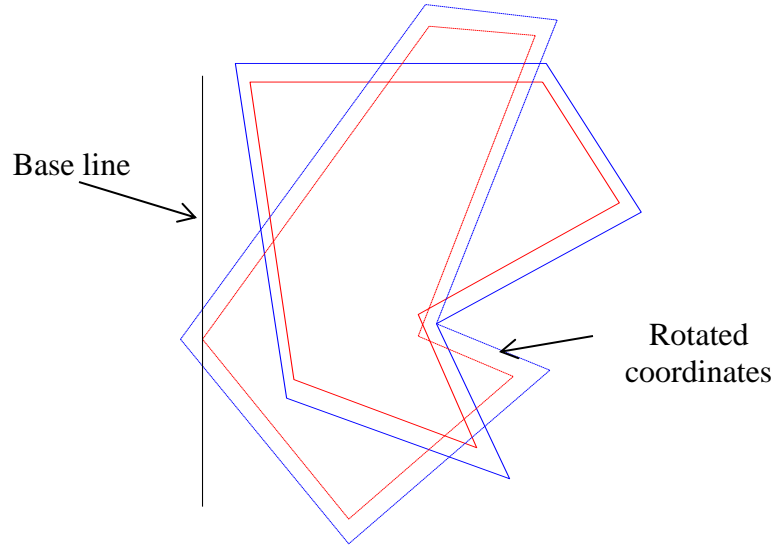
Figure 6.4: Rotation of field polygon with respect to the base line.

$$R = \begin{bmatrix} cos\theta & sin\theta \\ -sin\theta & cos\theta \end{bmatrix}$$

Equation 6.1

$$xy_{i_{rot}} = xy_i \cdot [R]$$

Equation 6.2

Where :

$xy_{i_{rot}}$: the ith vertex coordinate in the transformed coordinated system

xy_i : the ith vertex in original coordinate system

Headland turns: (Jin and Tang, 2010) considered headland turns would take place on a straight segment of the headland (Figure 6.5). On an irregular field boundary, this ideal situation does not occur very often especially with larger machines. Most likely there will be headland boundary vertices within the machine width (

Figure 6.6) that could affect the distance traveled during the maneuvering operation and also the off-target application area in the headland. Therefore, the approach in this study was to extract the necessary information from the actual geometric model (

Figure 6.6.)

The traveled distance for the actual turning portion (point ***A*** to point ***B***) of the headland maneuver was computed according to the ***"U"*** turn maneuver (

Figure 6.6). Thus, the turning radius (R) of the machine/implement was assumed to be half of the machine width (W).
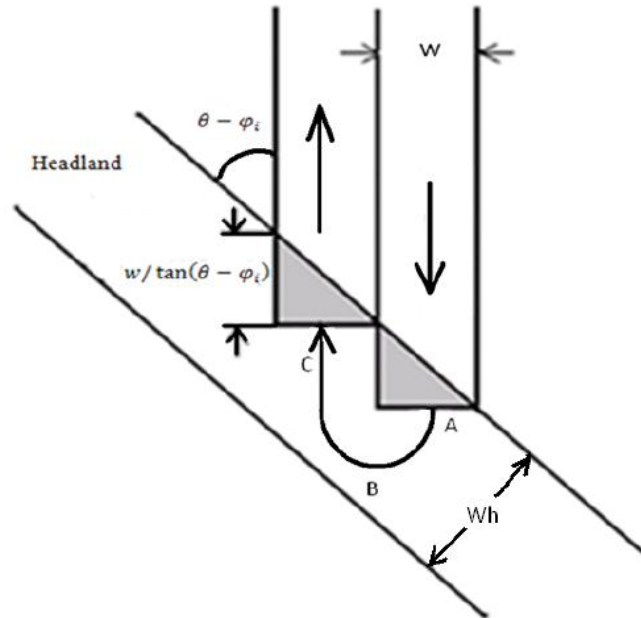
Figure 6.5: Headland parameters according to Hunt (2001) used by (Jin and Tang, 2010).
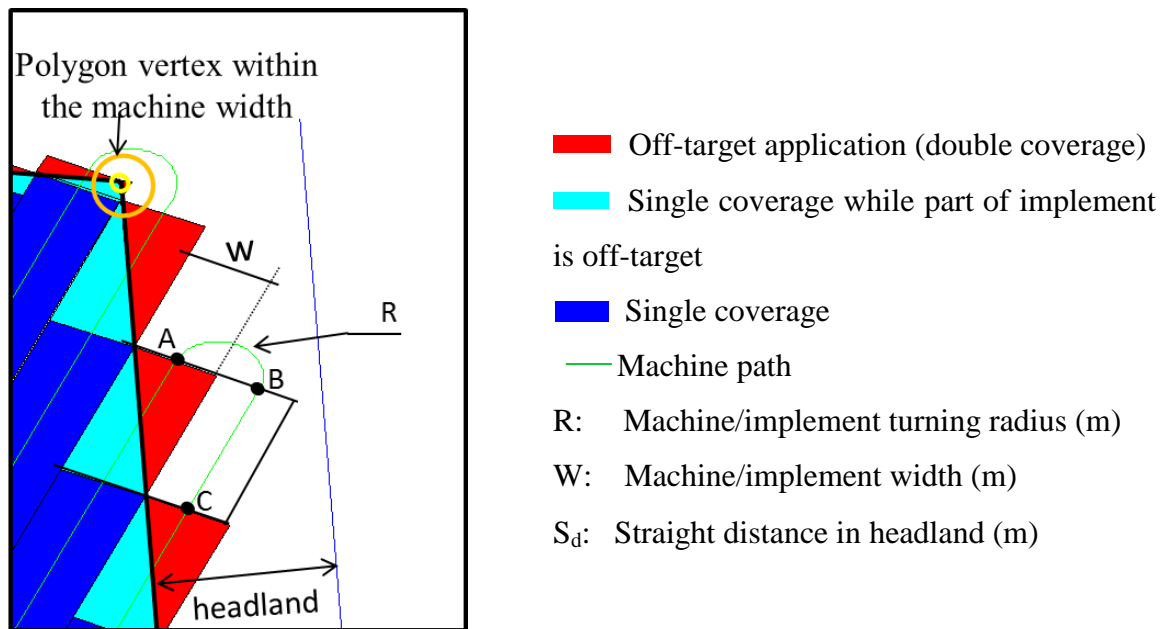
Figure 6.6: Headland turning model and off-target application area.

Computed parameters: Two fundamental pieces of information needed to be computed for each defined route to compose the objective function: ***total area covered (A_c)*** area and ***time required (T_m)*** to accomplish the task. A_c was the sum of the single coverage area and the off-target application areas, and T_m was estimated based on the computed distances traversed by the machinery in order to accomplish the field task. Here, different speeds were used depending on whether the machine was maneuvering, effectively working, going along straight distances in the headland or navigating to different spots within the field.

Objective function: The objective function (Equation 6.3) used in the optimization process was composed of two distinct costs: a cost portion related to machinery operation, and a cost portion related to inputs. The machinery related costs were defined in terms of cost per hour (***$/h***) whereas the input supply cost was defined in terms of cost per area (***$/ha***).

$$f_o = T_m \, C_m + A_c \cdot C_i$$

Equation 6.3

Where:

T_m: The time required to accomplish the field task (hours)

C_m: Hourly cost of the machinery ($/h)

A_c: Coverage area where inputs were applied (ha)

C_i : Input cost ($/ha)

6.3.1 Single field routing algorithm development

In this approach, the optimum route was achieved by simulating coverage patterns for different swath orientations within the polygon as a whole. No decomposition into simpler sub-polygons was performed.

Consider the non-convex polygon presented in Figure 6.7 (A) with a base line for the route orientation parallel to the *y* axis. One option for covering the field would be to begin at the upper left corner traveling south and keep on going back and forth in consecutive parallel passes until the machine reaches one of the decision points. The decision points occur when the next path of the vehicle cannot be completed contiguously without interruption by the field boundary or another obstruction. At that point a decision

would have to be made about how to proceed with the operation. One option would be to continue treating the lower right portion of the field, then traverse to the lower left corner of the remaining portion of the field to finish coverage. Another option would be to complete the upper right portion of the field before the lower right portion.

To algorithmically solve this problem, a routine (Figure 6.9) was written to divide the field into a block structure (Figure 6.7 (B)). Then, when the decision point of a working block was achieved, a search for the next closest block was accomplished. Each block had the starting point restricted to its four corners, thus yielding eight possible routes that could be taken to the next block (Figure 6.8 (A)). This way, the block structure was iterated in the process until no more blocks were available for evaluation (Figure 6.8 (B)).
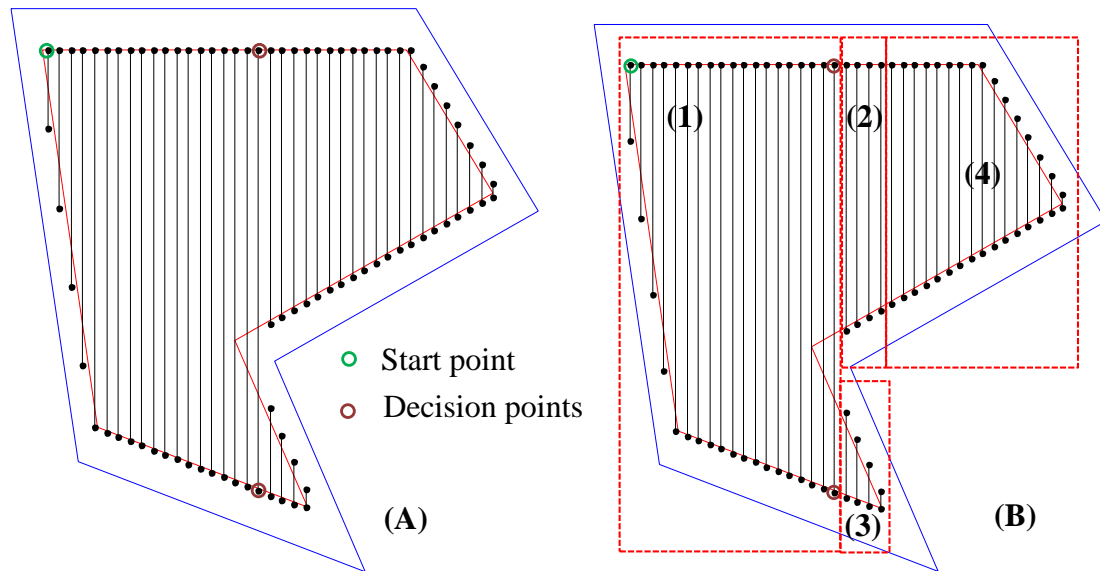
Figure 6.7: Representation of the start and decision points (A); and the field divided into block structure (B).
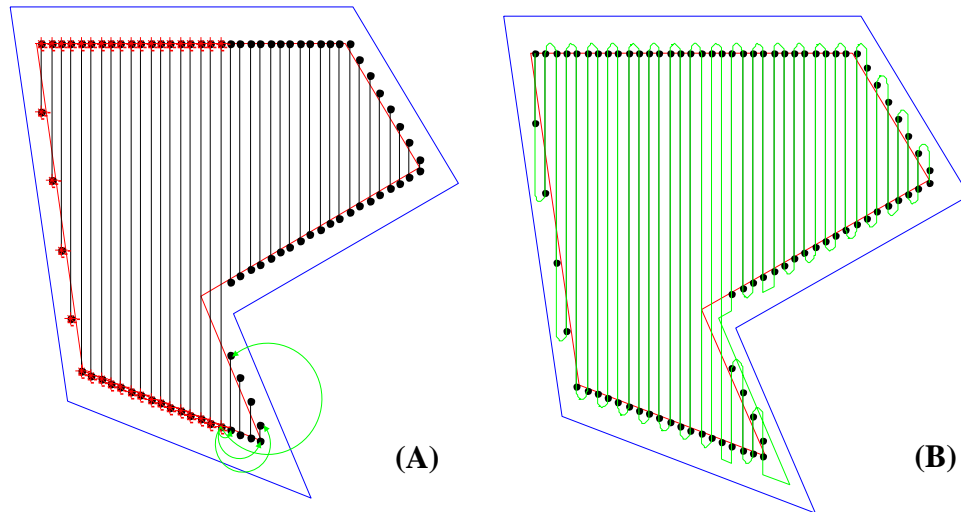
Figure 6.8: Representation of possible routes to the next block (A); final route (B).
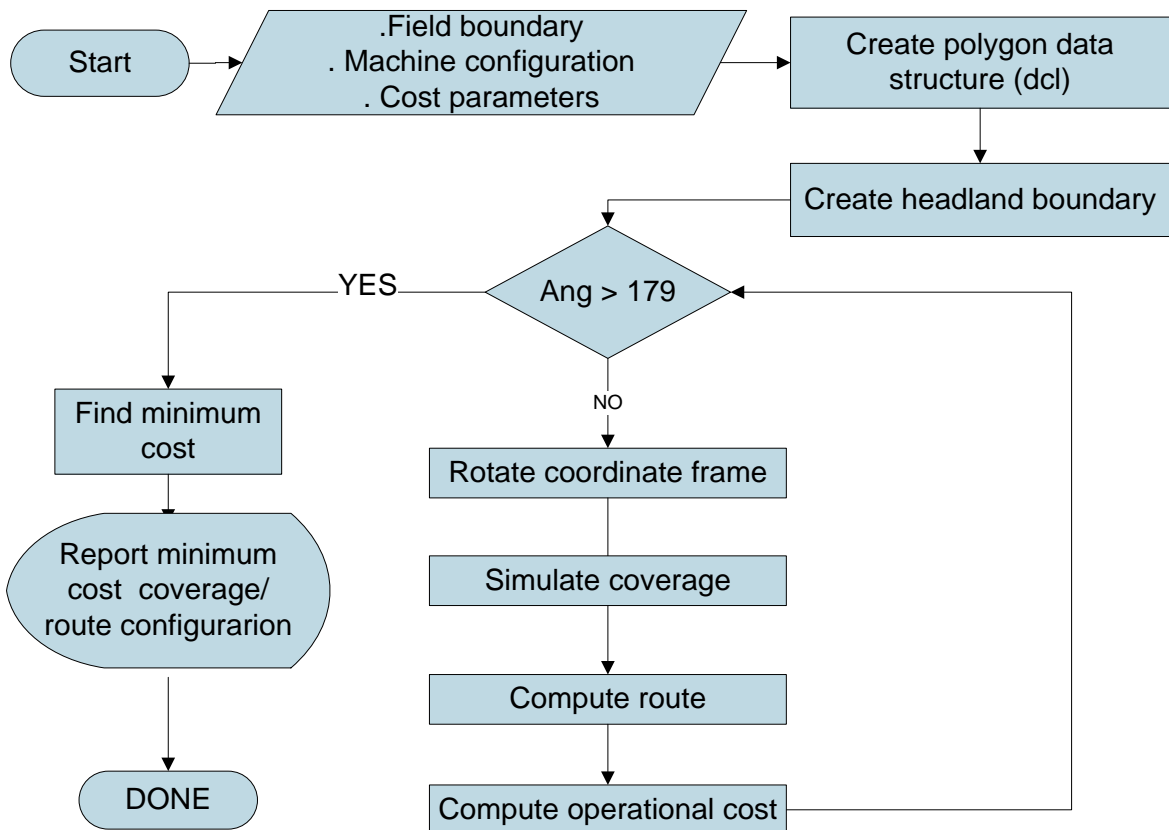
Figure 6.9: Simplified flow chart of the single field routing algorithm.

6.3.2   Field decomposition routing algorithm development

In the field decomposition routing algorithm, before the coverage and route were simulated, the non-convex polygon was subdivided into simpler sub-polygons to search for the optimum cost working pattern. Consider the polygon presented in Figure 6.10 (A), which contains five convex vertices and one non-convex vertex (vertex 4) connecting six non-parallel segments. The concept for dividing the polygon into sub-polygons was to let one polygon boundary segment at a time be shifted parallel to itself until it intersects vertex 4. The shifted segment was then elongated until it reached the polygon limits where the intersecting points were added to the original polygon data structure forming a set of convex sub-polygons. A set of three sub-polygons with their respective headland limits formed as result of the splitting line *a'* are presented in Figure 6.10 (B).

The coverage and route simulation was then evaluated by searching for the optimum on each one of those sub-polygons. Note that for the six-vertex polygon shown, there would be six different sets of sub-polygons and the optimum route was the one that yielded minimum cost among the set of sub-polygons. In the case of parallel segments, only one of the segments would be used as a splitting line eliminating redundant processing. Depending on the size and shape of the sub-polygon, the generation of the headland boundary could be hampered. Sub-polygon sets falling into this category were not used in the routing simulation.

A simplified flow chart of the field decomposition method is presented in Figure 6.11 and a simplified flow chart of the field decomposition routing algorithm is presented in Figure 6.12.
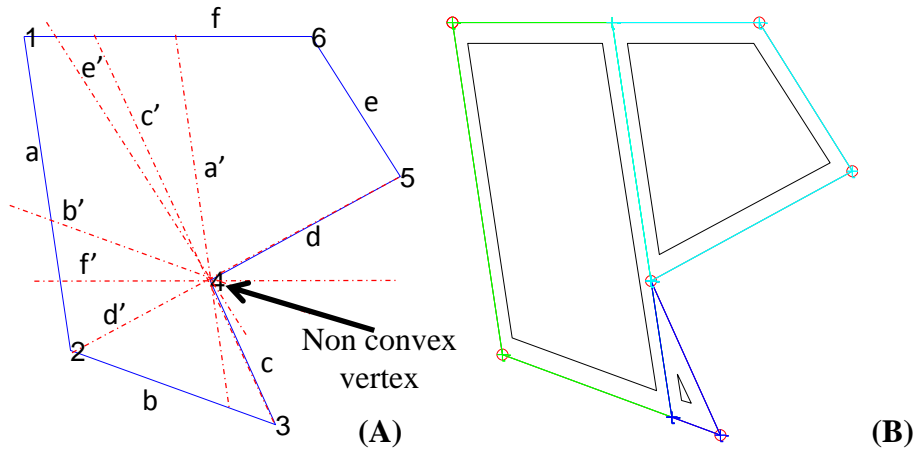
Figure 6.10: Illustration of the field decomposition method with possible splitting lines (A); and a decomposition resulting from splitting line *a'* (B).
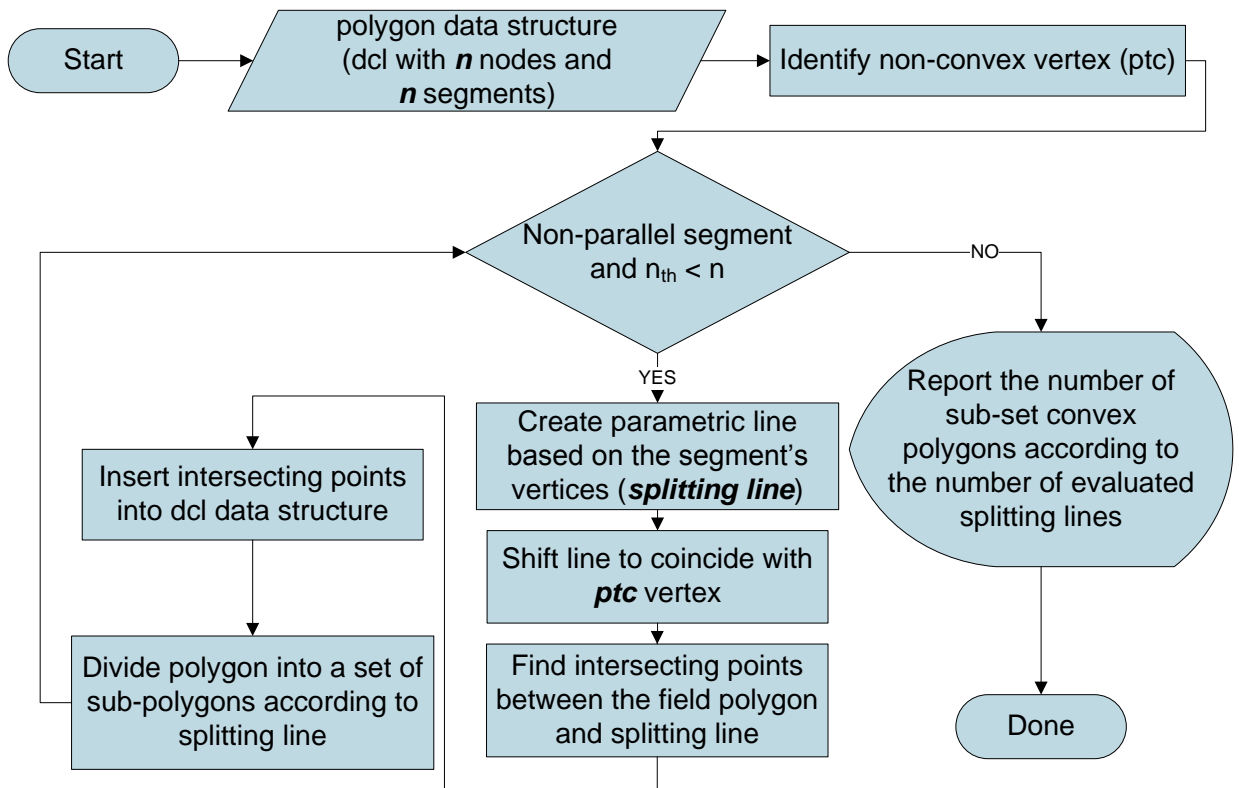

Figure 6.11: Simplified flow chart for the field decomposition algorithm.
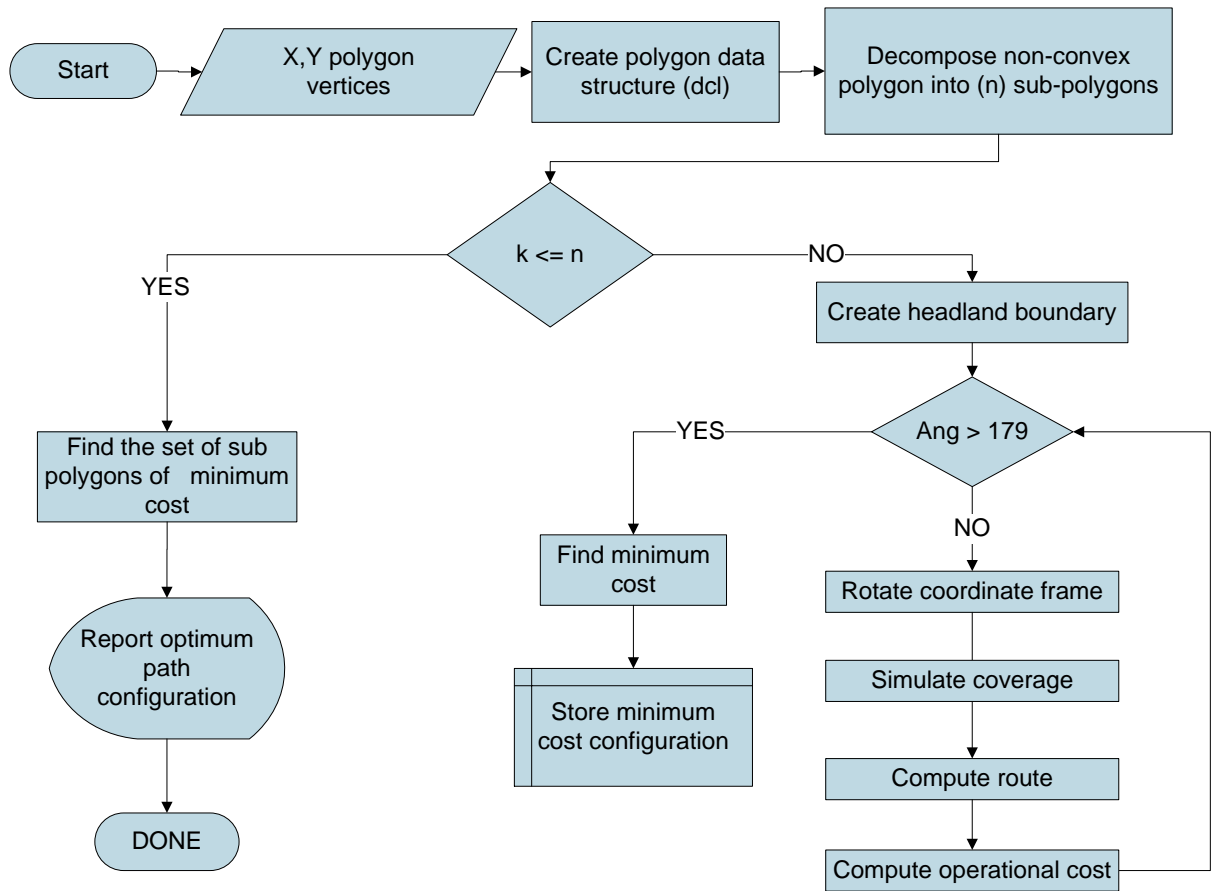
65

Figure 6.12: Simplified flow chart of the field decomposition routing algorithm.

6.3.3   Test procedure

The algorithms were evaluated on six field boundaries, with no more the one non-convex vertex in each, and with areas between 35 ha and 88.2 ha (Figure 6.13). Each field was processed by the single field routing algorithm and the field decomposition routing algorithm for comparison purposes.

The machine configuration used in the simulation was an 18.3 m corn planter (24 row at 30" spacing), capable of developing a speed of 7.2 km/h while planting. A speed of 4 km/h was assumed for the turns and 10 km/h was assumed for non-working straight traveling. The machinery cost was based on a typical custom rate for corn planting. Barry (2012) reported a range of custom rates for conventional corn planting operation from 12.8 to 18.3 $/acre used by Ohio state producers. Therefore, a value of 14 $/acre

66

(34 $/ha), which was also corroborated by a specific Midwestern producer, was used in the simulation. Because the machinery cost needed in the analyses was relative to working time, machinery field efficiency for planting operation was necessary. ASABE (2011) suggests that field efficiency for a planting operation with fertilizer application would be within the range of 50 % and 85 %. Thus, based on the machine effective field capacity (C_{ef}; Equation 6.4) and the assumed field efficiency (E_f) of 70 %, the approximately hourly cost was 315 $/hour. Regarding input cost during planting, Duffy (2012) stated costs varying from 299 up to 358 $/acre (738 to 950 $/ha). Thus, a value of 790 $/ha, which was also corroborated by Midwestern producers, was used in the simulation. More specifically, the total input cost was composed by: seed (296 $/ha), chemical (49 $/ha), and fertilizer (445 $/ha).

One of the issues investigated was related to the tradeoff between minimizing machinery cost and off-target application cost; therefore, the minimum machinery, minimum coverage, and optimum operational cost routes were evaluated in the tested polygons.
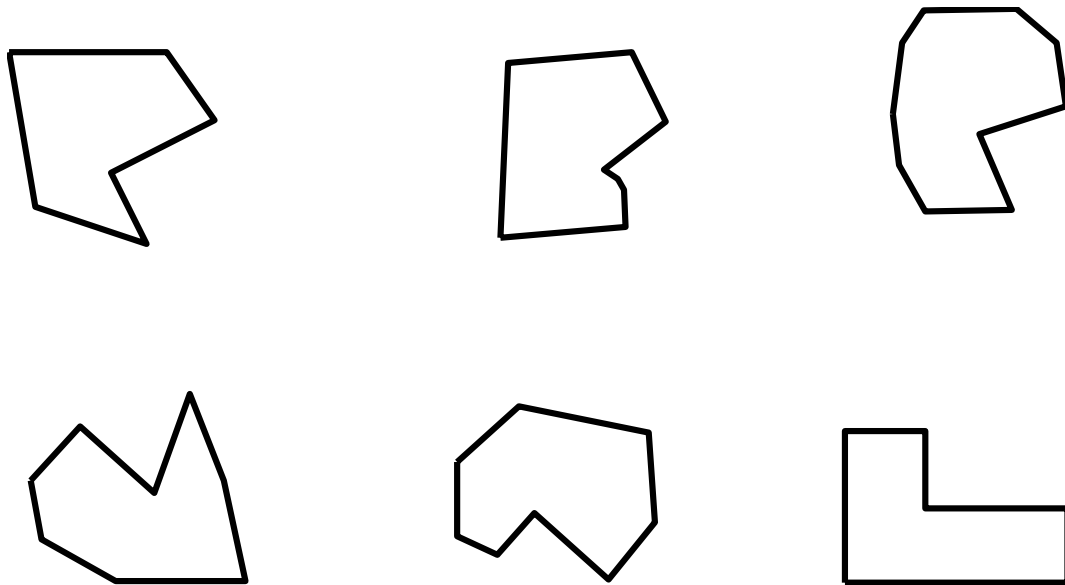
Figure 6.13: Field polygons used to test the routing algorithms.

$$C_m = C_{ef} \cdot E_f \cdot C_{ma} = \frac{V \cdot L}{10} \cdot E_f \cdot C_{ma} \qquad \text{Equation 6.4}$$

Where:

C_{ef}: Machine effective field capacity (ha/h)

E_f: Machine field efficiency (decimal)

V: Machine working rated speed (km/h)

L: Machine working width (m)

C_m: Machine hourly cost ($/h)

C_{ma}: Machine cost per unity of area ($/ha)

6.4   Results and Discussion

6.4.1   Single field routing algorithm

From the six polygons evaluated, only one (Field 5) presented an optimum path configuration that minimized both machinery and coverage costs. In the others, the minimum operational cost path coincided with the path that resulted in a minimum coverage cost. With the exception of Field 5, the operational cost difference between using the optimum path for machinery cost and optimum path for coverage cost varied from 4.3 $/ha up to 15.0 $/ha yielding total cost differences that varied from $31.7 to $1,324.7, depending on the field size (Table 6.1). Note that machinery cost ($/ha) was approximately 20 % lower than the derived base cost (34.6 $/ha). That is due to the fact that machine servicing time was not included in the simulation algorithm causing an overestimation of machinery field efficiency which yielded a lower machinery cost.

A simulated route for optimum operational and machinery cost for field one is presented in Figure 6.14 and the cost profile is presented in Figure 6.15. Note that both simulated routes were parallel to one of the boundary polygon segments. In this case, the optimum route orientation for machinery cost clearly coincided with the longest segment of the polygon, which is a common practice used in a farming operations. However, this was not the case for optimum operational cost route, although the optimum route orientation still coincides with one of the polygon's segment. That behavior tended to be repeated for all the tested polygons (Appendix A). Therefore, this property could be used to restrict the searching orientation to the ones parallel or near parallel to the polygon's segments thereby drastically reducing the required processing time for a given field.

Table 6.1: Results obtained from the single field routing algorithm with the six tested field polygons.

Field	Optimum *	Angle (degrees)	Area (ha)	Time (hours)	Final Cost ($/ha)			Cost Difference**	
					Supplies	Machinery	Total	$/ha	$ total
1	Mac	90.0	37.3	3.2	816.5	26.9	843.4		
1	Cov	165.2	37.3	3.3	807.4	27.6	835.1	8.3	309.5
1	Ope	165.2	37.3	3.3	807.4	27.6	835.1		
2	Mac	86.8	35.7	3.0	805.4	26.2	831.6		
2	Cov	4.6	35.7	3.1	803.3	27.4	830.7	0.9	31.7
2	Ope	4.6	35.7	3.1	803.3	27.4	830.7		
3	Mac	89.4	64.5	5.4	812.9	26.2	839.2		
3	Cov	13.4	64.5	5.6	805.8	27.2	833.0	6.1	396.1
3	Ope	13.4	64.5	5.6	805.8	27.2	833.0		
4	Mac	165.0	46.5	4.0	816.3	27.3	843.6		
4	Cov	24.0	46.5	4.1	811.6	27.6	839.3	4.3	200.9
4	Ope	24.0	46.5	4.1	811.6	27.6	839.3		
5	Mac	99.3	46.0	3.9	809.5	26.9	836.4		
5	Cov	99.3	46.0	3.9	809.5	26.9	836.4	0.0	0.0
5	Ope	99.3	46.0	3.9	809.5	26.9	836.4		
6	Mac	90.0	88.2	7.2	813.7	25.7	839.4		
6	Cov	0.0	88.2	7.3	798.4	26.1	824.4	15.0	1324.7
6	Ope	0.0	88.2	7.3	798.4	26.1	824.4		

* Mac; Cov, and Ope stands for Machinery, Coverage and Operational cost, respectively.
**Cost Difference between optimum route for machine and optimum route for total operational cost.
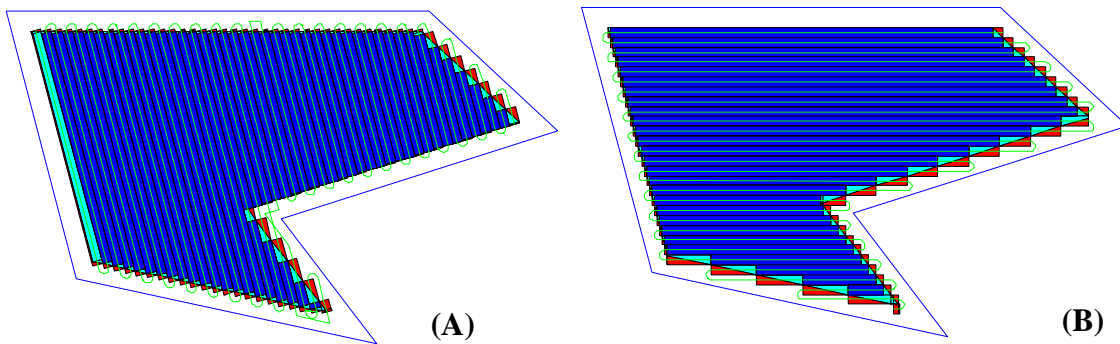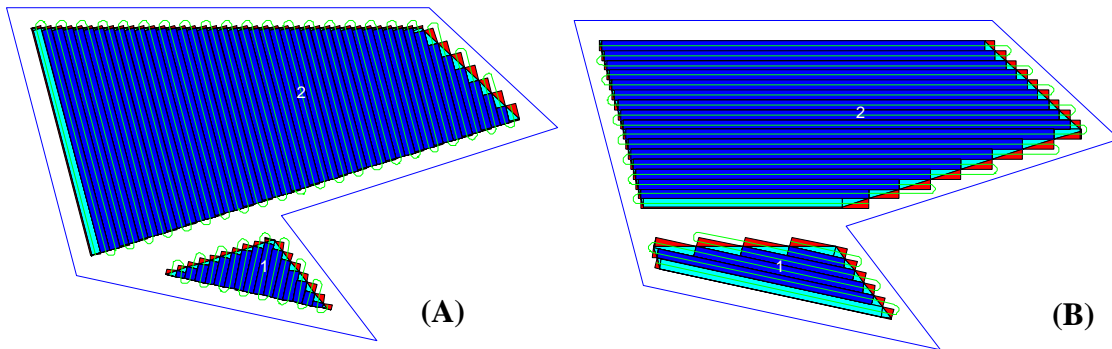

Figure 6.14: Simulated route for optimum operational cost (A), and optimum machinery cost (B).
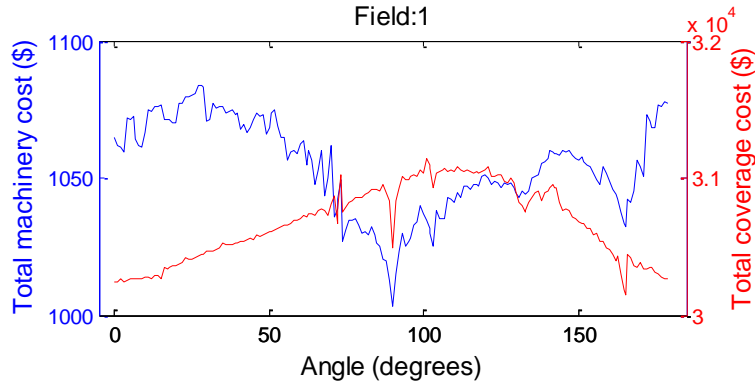
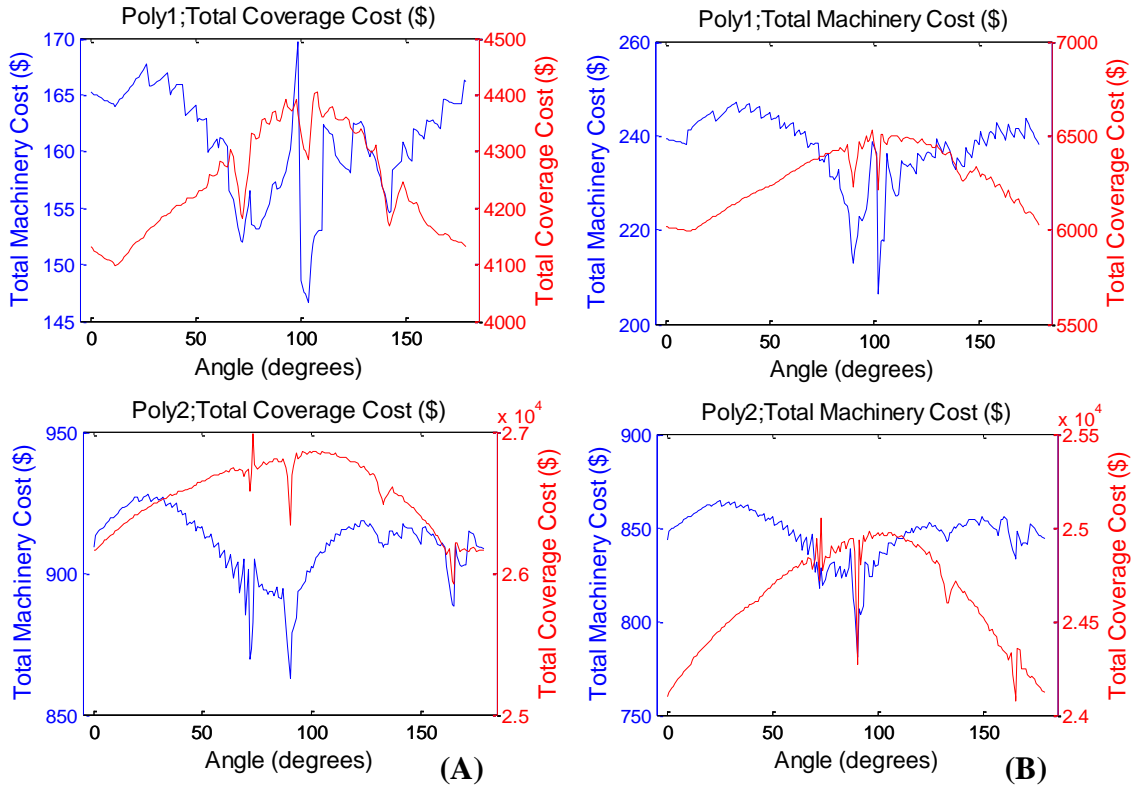Figure 6.15: Cost profile for simulated routes according to the orientation angle.

6.4.2 Field decomposition routing algorithm

From the six polygons evaluated with the F\field decomposition routing algorithm, only one (Field 6) presented an optimum path configuration that coincided with both minimum machinery and coverage costs (Table 6.2). Fields 1, 2, and 4, presented a minimum cost route the same as the minimum coverage cost. Fields 3 and 5 presented distinct routes for minimum cost due to machinery, coverage and total operation. However, the cost difference was negligible and one can say that the minimum operational cost route coincided with the minimum coverage route for this situation.

Table 6.2: Results obtained from the field decomposition routing algorithm with the six tested field polygons.

| Field | Area (ha) | Optimum cost route ($/ha) based on | | | Marginal savings ($/ha) | | Marginal savings ($) |
		Machinery (a)	Supplies (b)	Total Operation (c)	(a) to (b)	(b) to (c)	(a) to (b)
1	37.3	842.6	832.1	832.1	10.5	0.0	391.65
2	35.7	848.8	827.7	827.7	21.1	0.0	753.27
3	64.5	837.4	832.0	831.8	5.4	0.2	348.3
4	46.5	843.1	835.1	835.1	8.0	0.0	372.0
5	46.0	856.5	835.7	835.6	20.8	0.1	956.8
6	88.2	820.6	820.6	820.6	0.0	0.0	0.0

A simulated route for optimum operational and machinery cost for field one is presented in Figure 6.16, and the cost profile is presented Figure 6.17. Due to the fact that the set of sub-polygons was different, two cost profile graphs are presented. One can observe that the characteristic of the optimum route being parallel to one of the polygon's

70

segment fails on the triangular sub-polygon presented in Figure 6.16 (A). This behavior was noted for other triangular polygons (Appendix C) indicating that further investigation is needed before using the orientation of the polygon segments as a rule for defining the orientations for path simulation.

As far as the gain regarding the optimum route when using the field decomposition method proposed in this study, there was some improvement in the minimum operation cost (Table 1.3). The marginal savings ranged from 0.8 $/ha up to 4.2 $/ha for the evaluated polygons. However, the headland area for the decomposed fields is considerably bigger when compared to the single field since a headland area was created around every individual sub-polygon. This situation should receive a penalty regarding the optimization process, considering the fact that headland area is a region of probable lower production due to the machinery traffic during maneuvering. Therefore, further investigation is needed in order to establish the tradeoff of increasing headland area in order to lower the operational cost.

Figure 6.16: Simulated route for optimum operational cost (A), and optimum machinery cost (B).

71

Figure 6.17: Cost profile for simulated routes according to the orientation angle. Route for minimum coverage cost (A) and minimum machinery cost (B).

Table 6.3: Optimum cost routes when using the two proposed routing algorithms.

Field	Area (ha)	Operational cost ($/ha)		Marginal savings	
		Single field	Field decomposition	($/ha)	($)
1	37.3	835.1	832.1	3.0	111.9
2	35.7	830.7	827.7	3.0	107.1
3	64.5	833.0	831.8	1.2	77.4
4	46.5	839.3	835.1	4.2	195.3
5	46.0	836.4	835.6	0.8	36.8
6	88.2	824.4	820.6	3.8	335.2

6.5   Conclusions

The study revealed that the cost due to off-target application area had a greater impact in the final operational cost than machinery operation cost thus confirming the

importance of considering off-target application in the route planning process. Furthermore, the following specific conclusions were drawn from the study:

- Two routing algorithms based on off-target application area and machinery field efficiency were developed and tested. In the first, the field polygon was considered as a whole in the simulation and in the later the field polygon, if non-convex, was decomposed into a set of convex polygons before simulation.

- The machinery cost output in terms of $/ha produced by the algorithm was lower than the derived base price due to the fact that machinery servicing was not contemplated in the proposed algorithm; thus, it should be addressed in future work in order to achieve a more accurate computation.

- In both studied approaches, it was found that cost due to off-target application area had a greater impact in the final operational cost than machinery operation cost for the studied fields.

- The field polygon decomposition method was limited to only one non-convex vertex and needs to be improved in order to allow better evaluation of the proposed routing method.

- Field decomposition technique presented an small improvement in the computation of the minimum cost route; therefore, not an interesting solution for the studied fields given the fact that the headland areas were larger than the single field routing algorithm.

- The base line rotation method for routing simulation used in this study demands great computational processing time; thus, alternative criterion should be evaluated in order to improve computational power demand and processing time.

CHAPTER 7: SUMMARY AND CONCLUSIONS

Methods for improving machine fleet management in agricultural are of great value in agricultural production systems since thy have a direct impact on the producer's profit. Researchers have dedicated effort to many aspects of machinery management and lately have developed methods for improving the route planning for field operation tasks. The majority of the earlier work was related to the machine field efficiency, but with the advent of the automatic section control, the off-target-application area became a common topic among the discussed issues. Questions regarding parameters for the decision-making process about adopting automatic section control for a given machine configuration and set of field geometries as well as how the width of the controlled section (width resolution) would affect the potential results were often raised. Other common question were with regard to how machine width, field size and shape would affect off-target application area, how can off-target application area could be estimated by a simple method, and how optimal route planning could affect all these parameters. Therefore, the work presented in this dissertation addresses the above issues according to the three main objectives of the project.

The goal of the work conducted under objective one, was to develop a software tool (*FieldCAT*) capable of providing a quantitative estimate of off-target application of inputs that would occur because of limited resolution of machine section control width and path orientation for different field shapes. The method was developed and validated with field data confirming the usefulness of the tool for off-target application area estimation beforehand. Results clearly showed the potential savings that could be achieved with the implementation of automatic section control technology. *FieldCAT* was also used to illustrate that path orientation can have a significant impact on input errors due to point rows and headland encroachment.

The development of the *FieldCAT* computational tool facilitated a comprehensive study of the interactions of machine working width, field size and field shape, in terms of off-target application areas (Objective 2). That portion of the work revealed that the relationship between field area and off-target application area for fields of the same complexity can be linearized by applying a natural logarithmic transformation to both axes. The slopes of the linearized curves for fields of different complexity were the same

and the intercepts were a function of the field complexity. It was found in that study that the effects of machine working width on off-target application areas for fields of same size were linear as long as the ratio headland/area (**H/A**) was less than 0.6. As expected, complex field shapes increased the off-target area more rapidly according to the implement width when compared to the simple fields. Regarding the use of field shape descriptors for off-target application area estimation, the percent off-target application exhibited some correlation to several different shape descriptors when fields were all scaled to a common reference area. When field size was taken into account, only perimeter/area (**P/A**) and **H/A** exhibited reasonable trends; however, **P/A** was sensitive to implement width while **H/A** presented more stable across varying machine widths since it was the only descriptor that carried direct information about the machine working widths. Therefore, **H/A** was found to be the best indicator of off-target application area. The linear model was fitted to data after a variance stabilization transformation and was able to estimate percent off-target application area within ±6.7 % error at 2 standard deviations on the validation dataset. Although the **H/A** model turned out to be simple and straight forward to compute, the model was only capable of estimating the average off-target application area. Coverage simulation is still needed if detailed information about the path coverage orientation that yields the absolute minimum off-target application area was desired.

Finally the off-target application area was merged with machine efficiency to determine route planning algorithms that would minimize overall operational cost of a specific field task. The study evaluate the tradeoff between minimum cost route for machine efficiency and minimum cost route for minimum off-target application areas. The algorithms considered machine configuration, machine cost parameters, input cost parameters, and field boundary geometry. Two routing methods were proposed. In the first, the field polygon was considered as a whole in the simulation and in the latter the field polygon, if non-convex, was decomposed into a set of convex polygons before simulation. In both methods, it was found that cost due to off-target application area had a greater impact in the final operational cost for the studied fields.

CHAPTER 8: SUGGESTIONS FOR FUTURE WORK

The work presented herein represents a significant contribution to the area of agricultural machinery fleet management with some limitations that can be addressed on future research. By the time the last portion of this research was accomplished, more efficient computing techniques for certain processes were discovered that could be implemented in *FieldCAT* to decrease computational power demand, allowing faster solution for more complex boundary geometry. For instance, a faster algorithm for presenting the coverage maps was developed in later work as well as more efficient coverage simulation based on the transformed coordinate system created by the coordinate frame rotation. .

Regarding the second objective, the relationships investigated were well defined; however, the developed model based on the shape descriptor *H/A* was only valid for overall average off-target areas. Given that off-target area will vary considerably according to path orientation, it still necessary to run a full simulation to identify the list off-target application coverage patterns. One relationship that could investigated in the future is to develop/identify a shape descriptor that presents a relationship with the off-target area variation for a given field and machinery configuration. Furthermore, relationships between field shape descriptors and orientation of minimum and maximum off-target application areas could be investigated.

With respect to the third objective, several suggestions can be pointed out for future work, starting with the number of non-convex vertices in a non-convex polygon. Both of the presented routing algorithms were limited to non-convex polygons with no more than one non-convex vertex. Such capability is mandatory for solutions regarding more complex field geometry. Considering that the number of non-convex vertices increases computational power requirement, a robust polygon simplification method will be necessary in order to process the field boundary maps obtained from a machine equipped with a GNSS receiver collecting geographical position data at a high sampling rate.

Given the fact that headland areas are most likely less productive areas in the field, the minimization of such would be an interesting resource in a routing algorithm. For instance, one can observe in the maps presented in the appendices that the

assumption of two machine passes around the field (headland region) provided plenty of space for the "U" turn maneuver in many situations. A headland minimization algorithm could be developed such that it would find the maneuver model ("flat" turn; " bulb" turn; "asymmetric bulb turn", and "fishtail' turn) that would require the minimum headland area for a given machine configuration, and of course, the geometric condition of the polygon boundaries.

In the algorithms presented, the optimum route was achieved by an exhaustive search among 179 different paths orientation, which took a considerable amount of time for processing, especially for the algorithm based on the field decomposition approach. It seems that for the majority of the final routes, the route orientation was parallel to one of the polygons segments with exception of the polygons of a triangular format. One could investigate why and what are the conditions in which the triangular polygon present such behavior. From that, a heuristic approach could be implemented in which, for polygon forms other than triangular, a search would be carried at angles close to the ones of the polygon segments. For instance, a simulation would start few degrees before the angle parallel to a certain segment, and would keep changing the angle, as long as the objective function result was going towards a minimum, or else, it would go to an angle similar to a next segment. In this approach, segments of similar angles could be skipped as well as segments with short length. Of course for fields with a high number of vertices, this approach may still not improve computation time very much; thus, there is a need for robust field boundary simplification method.

Another point of investigation is to include in the routing algorithm the capability of handling machine servicing. This is a very important aspect in the realm of machine routing for operations such as planting, fertilizing, and spraying; but even more critical, in the harvesting operation.

APPENDIX

APPENDIX A: FIELD COVERAGE ANALYSIS TOOL TUTORIAL

1. Importing data

Select "New Field" option under the "File" menu. The data can be imported from a shapefile or from a text file. Many field management programs will output field boundaries in shapefile format. There is a field boundary shape file in the sample folder that was extracted from the zip file downloaded from FieldCAT web page. You are then asked for a Field ID. This can be any number to identify the analysis, and it will be tagged onto the filename of the boundary file. You can use different numbers to if you run different scenarios on the same field.

The boundary coordinates will then project from degrees latitude/longitude to Cartesian coordinates if they have not already been projected by another program and stored with the shapefile. You may be asked for the units of the data. This is the unit system (meters or feet) used to store the data, and may be different from what is displayed on the screen. This unit system must match the dataset if it was projected earlier by another software package. If you are not sure, choose one and verify the field areas later. If they are wrong, you may have to reload the field and choose a different coordinate system.

The field boundary points should now be displayed on the screen.
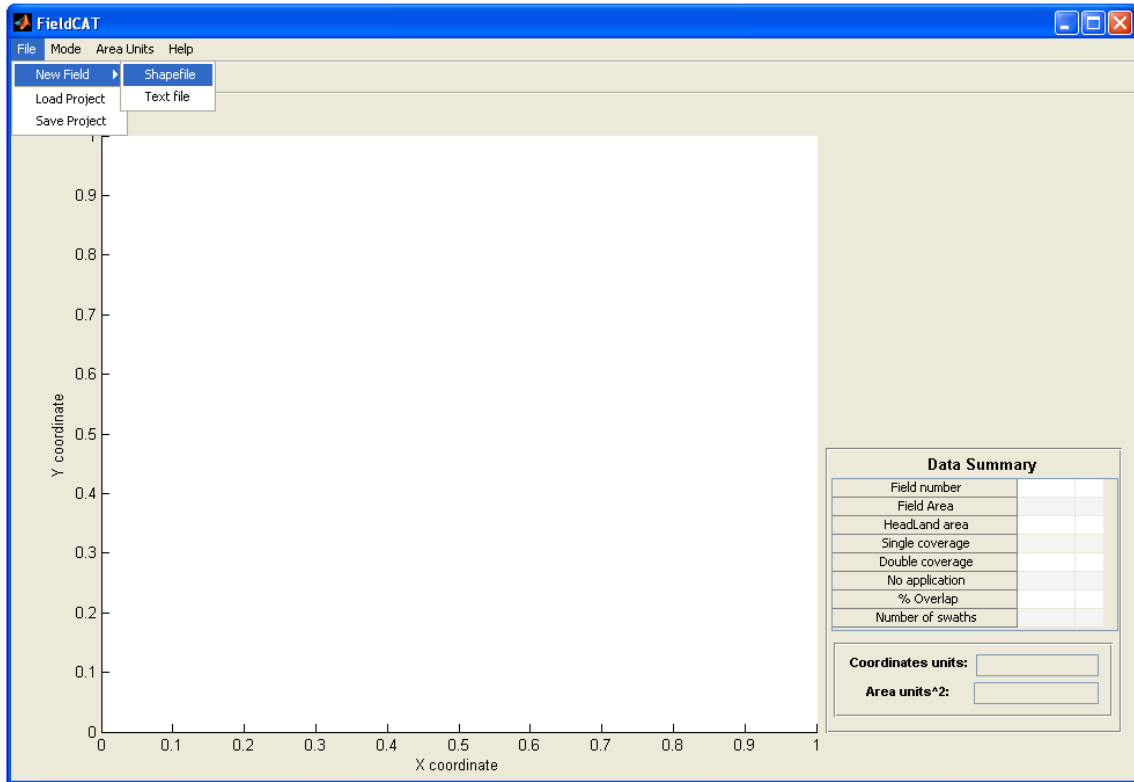
Figure 1: Screen capture of the main program window while selecting a shapefile option for data import.

2.Editing field boundaries

Field boundaries can be designated as navigable or non-navigable areas. All internal non-crop areas that are not connected to the outside field boundary MUST be selected and designated independently.

This task is accomplished by selecting the "Edit Boundary" under the "Mode" menu which makes a group box with the title "Boundary structure edit" appear on the right hand side of the main program window (Figure 2). Check the "Edit boundaries" radio button to enable the boundary regions options. Choose either navigable or non-navigable for the regions you plan to select. Once a boundary region option is selected, click with the mouse inside the map area and the mouse point arrow will change to a cross.

Drag a box to select the region. The selected points will turn blue forming a polygon (Figure 3). You can use several boxes to keep adding points to the region.

81

Once the whole region is selected, save it by clicking on the "Save region" pushbutton. The saved regions will disappear from the map area. Note that an individual region can be selected in several steps, but only one whole region must be saved at a time. If more than one individual region is saved at a time, the coverage pattern algorithm will not work correctly. In the example shown in Figure 2, there are 3 different small independent internal regions that must be selected and saved individually. The waterway could also be designated as navigable to allow machinery patterns to pass through it. The outside boundary does not need to be explicitly designated since the software automatically assumes that it is non-navigable.
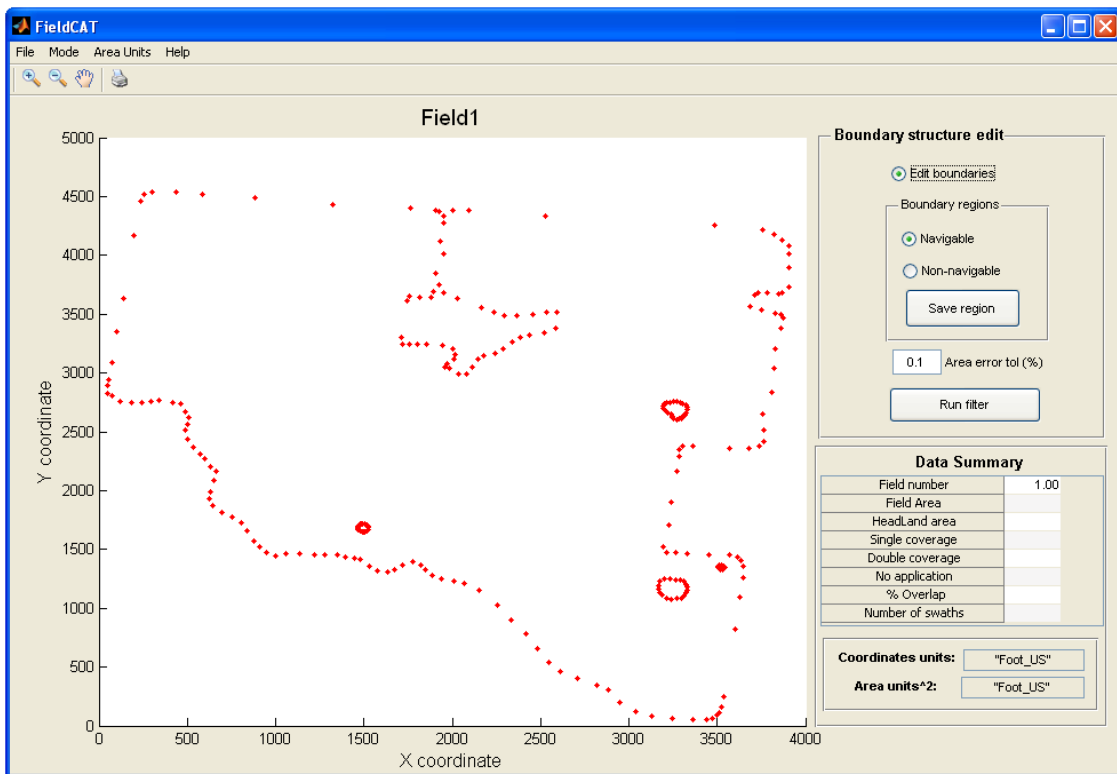
Figure 2: Screen capture of the main program window during the "boundary editing mode"
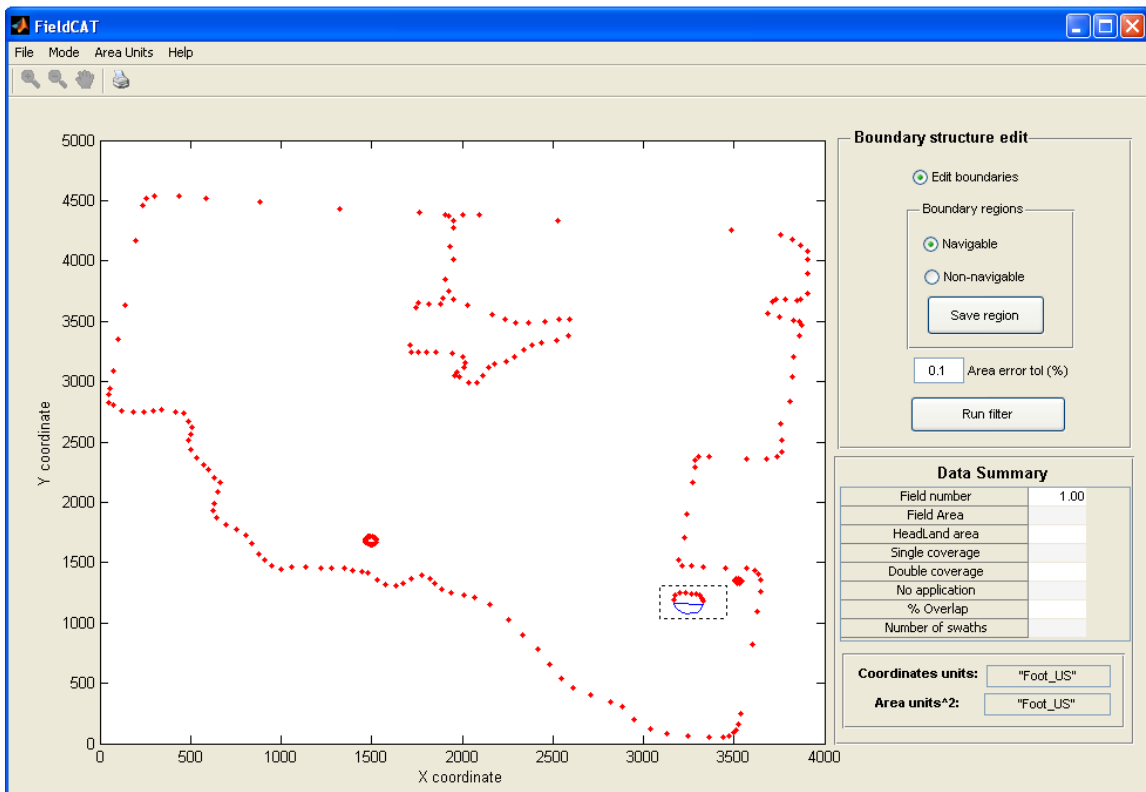
Figure 3: Screen capture while selecting individual navigable regions within field boundary.

OBS: All individual regions within the field boundaries must be selected.
The project can be saved by selecting the "Save project" option under the "File" Menu. A project can be saved any time in the process. Perhaps naming the projects according to the step in which it is saved can be handy to go back and try something different.

3. Filtering polygons

Once all internal areas are designated, you are ready to filter the boundary to eliminate unnecessary points. Change the area error tolerance if you wish and then click the "Run filter" pushbutton. The filter output should look something like Figure 4 where the dots represent the coordinates of the original polygon and the circles represent the filtered polygon. A message box will appear reporting the average percentage area error among the different regions in the polygon. Visually inspect the filtered polygon and make the area tolerance more restrictive if necessary. If the

83

filtered polygon satisfactorily represents the raw field boundary, save the filtered data for later usage. Pay attention to where you are storing the files.
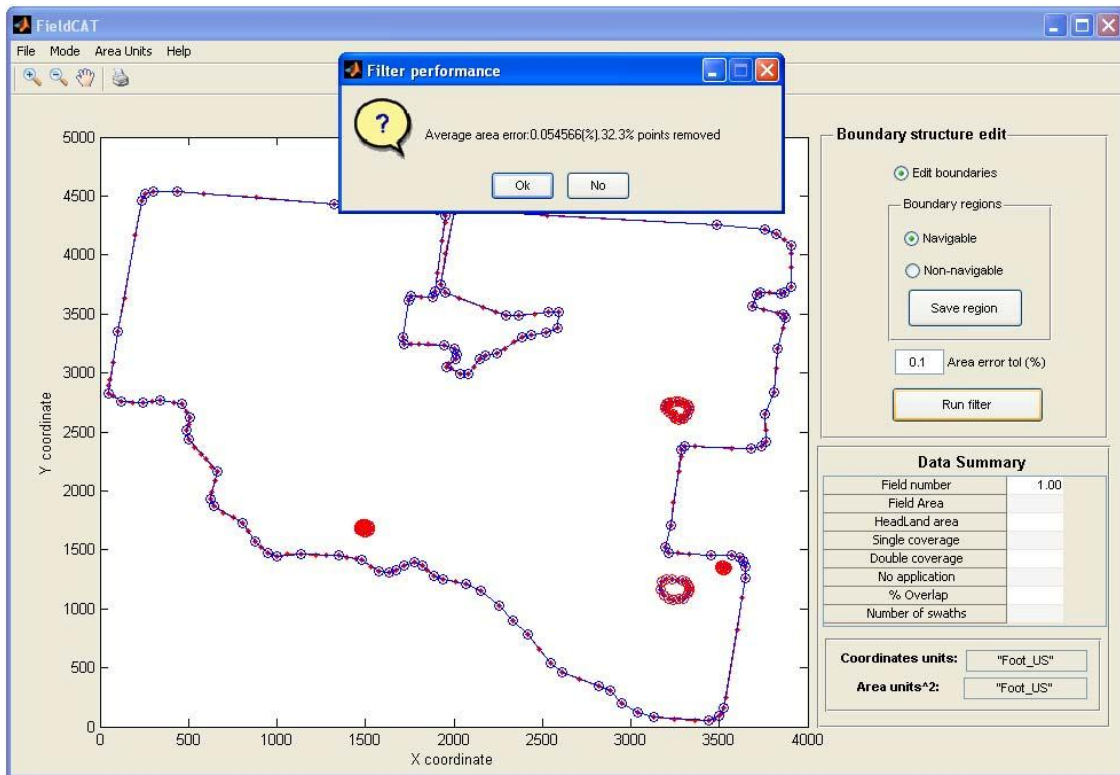
Figure 4: Screen capture presenting the output of the filter polygon process

4. *Coverage analysis*
4.1. *Parameter set-up*

Select the "Generate Coverage" option under the "Mode" Menu. A group box titled "Coverage Analysis" will appear on the right hand side of the main program window taking place of the "Boundary structure edit" group box (Figure 5).

Insert the headland width (usually a multiple of the machine width) and machine making sure that the numbers match the "coordinate units" displayed at the right hand side of the main program window.

Under the boom configuration, there is an option to use a single configuration, or vary the boom section widths in order to evaluate the performance trend for different boom configurations. To analyze a single configuration, enter the individual boom section widths separated by commas in the text box next to the "Single config." radio

button. For example, on a 12 row (30 ft.) planter, you would enter "30" for whole planter control, "15,15" for split planter, "2.5,2.5,2.5,2.5,2.5,2.5,2.5,2.5, 2.5,2.5,2.5,2.5" for individual row control, or some unique configuration such as "2.5,2.5,5,10,5,2.5,2.5". Just make sure all sections add up to the machine width.

For the "Varying config" option, you may insert the minimum and maximum number of boom sections to be analyzed separated by comma, i.e. "1,12" for a 12 row planter would analyze everything from whole planter control to individual row control. You can also load a list of custom boom section configurations by clicking on the "Load Conf" push button and typing each configuration into a dialog box that pops up (Figure 6). Only one configuration should be inserted per line with the sections widths separated by comma.

Next you choose the path orientation options for the analysis. You may choose a single orientation "Angle" in which the coverage is going to be generated or you may choose to rotate the path orientation by selecting the "Rotate" radio button. For the rotate option, insert the starting angle, the angle increment, and the maximum angle of rotation in the textbox next to "Rotate" radio button. The angles are clockwise from North and must be between 0 and 180 degrees. For example, "0,10,170" would analyze path orientations of 0, 10, 20, 30, … 170 degrees. Be aware that generating more paths could cause computation time to increase significantly, especially with older and slower computers!
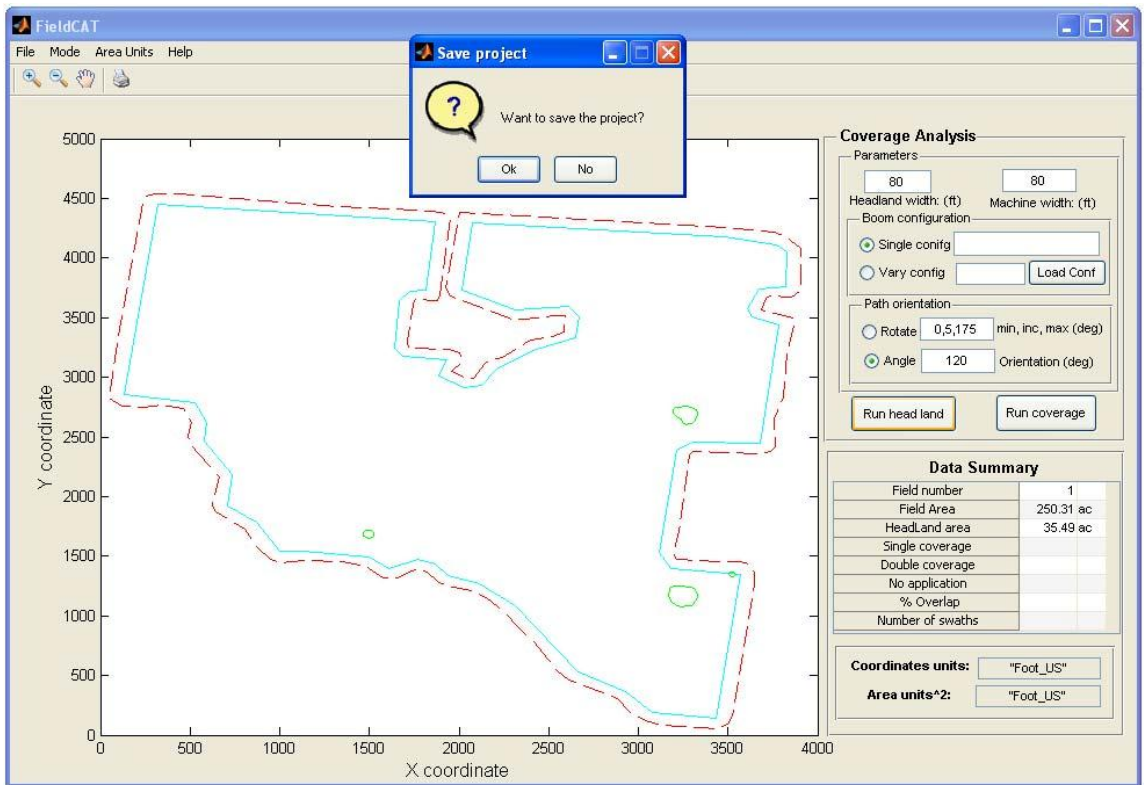
Figure 5: Screen capture off the "coverage analysis" mode. Generated headland
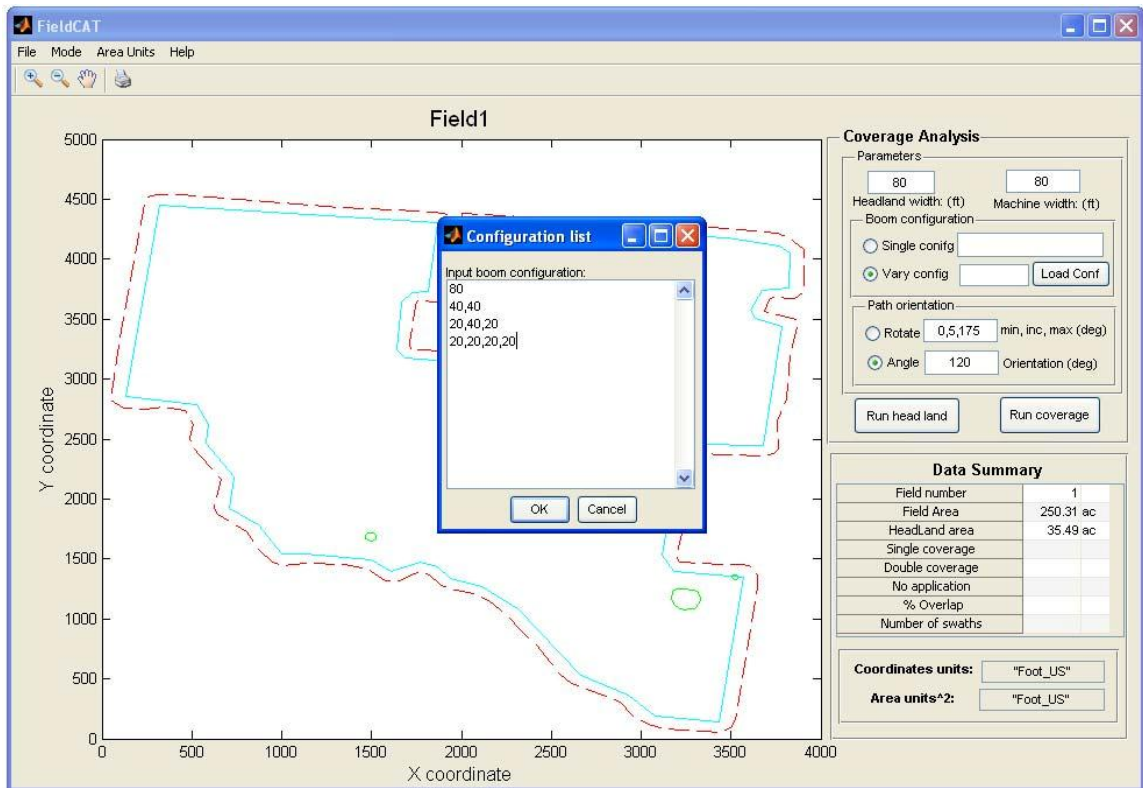
Figure 6: Coverage analysis mode. Loading a list of boom configurations.

4.2. Creating Headland

Once all the data are input, click on "Run Head land" to generate the headlands inside the field boundary. If the headland areas are incorrect, you may need to go back and try a different scheme for selecting navigable and non-navigable areas.

4.3. Coverage generation

Once the parameters are inserted and the headland is generated correctly, click on the "Run coverage" pushbutton for coverage generation. When the folder browser pops up, choose a location for the output files. For each coverage pattern, FieldCAT will create a data structure called "Fieldxx_xxx_xsec.mat", where the first couple x's after the word "Field", refers to the Field ID. The next three x's refers to the path orientation, and the x previous the word "sec", refers to the number of sections used on

that specific analyses. A dataset containing the data related to the path rotation and the boom section variation is also generated. The respective datasets are stored in the same folder as the ".mat" data structure file, but with a different type of file extension. The extension files for the rotation dataset and for the boom section varying dataset are ".rot" and ".sec" respectively which are used later in the Results Presentation module. A plot of the generated coverage should be displayed on your screen (Figure 7). The dark and light blue represent the areas covered ounce, the red color represent the off-target areas, and green areas represents no application. A summary of the results are presented in the "Data Summary" table found in the main program window.
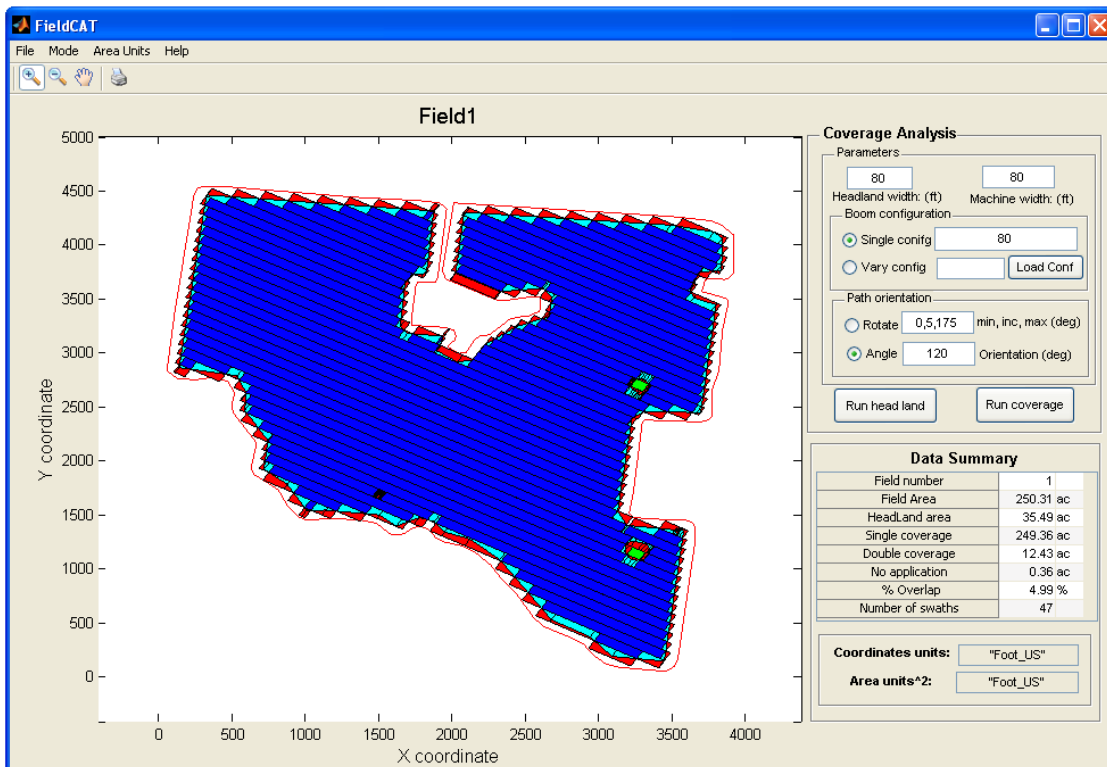
Figure 7: Coverage Analysis mode. Coverage output

5. *Results Presentation*

The Results Analysis window (Figure 8) is loaded by checking the "Result Analysis" option under the "Mode" menu. Data are presented in two regions of the "Results window", the "Rotation Analysis" group box and the "Boom Section Analyses" group box.
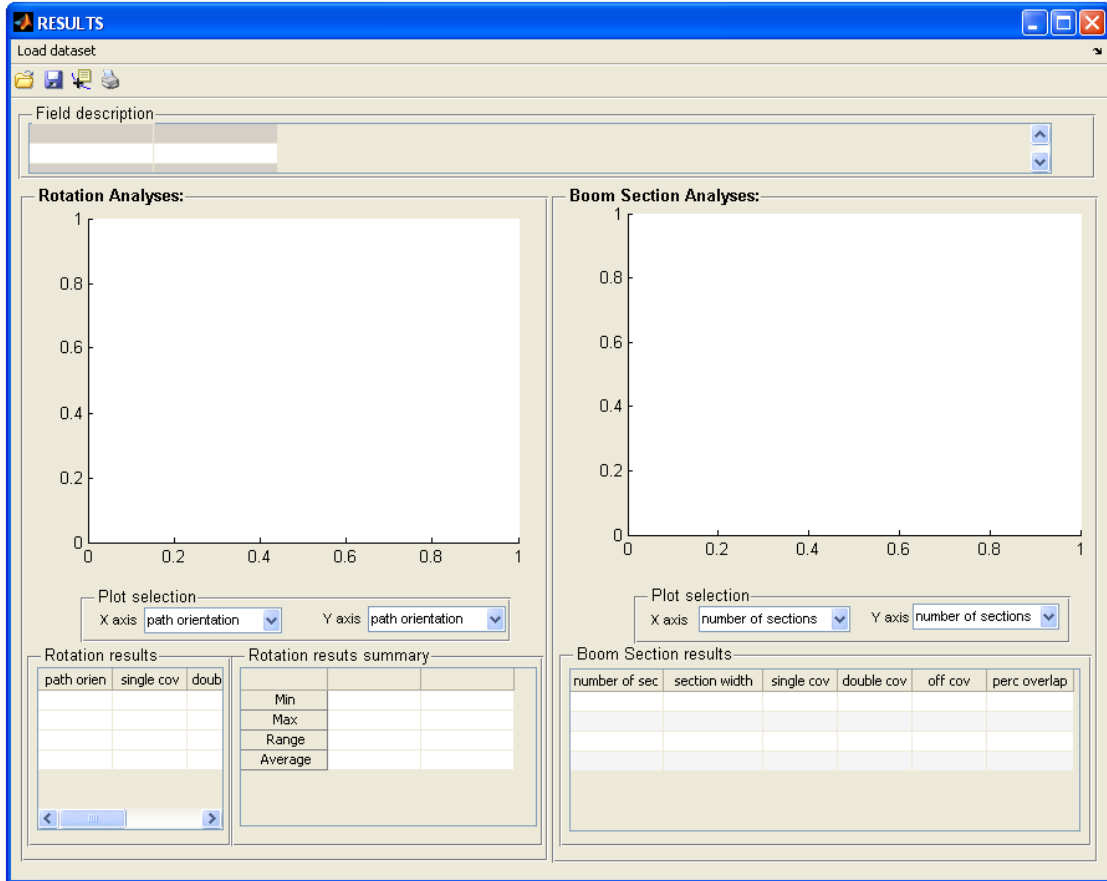
Figure 8: Screen capture of the "RESULTS" window under the "Results Analysis" mode

The "Field description" group box displays some of the basic information related to the Field in question such as ID number, data coordinates and output units, network area, headland coverage and machine width. The results of the rotation analyses are presented on the "Rotation results" table. The data presented on the "Rotation results" table can be presented in the graph above it by selecting the information to be plotted in the x and y axis listboxs in the "Plot selection" group box. The descriptive statistics (minimum, maximum, range, and average value) of the selected data are then presented on the "Rotation results summary" table.

Under the "Boom section Analyses" group box, the results are presented is the "Boom Section results" table. Like the Rotation Analysis, the user can plot the data presented in the table by selecting the data of the x and y axis in the listboxs located at the "Plot selection" group box.

A nice feature about the "Results presentation" module is that the user could

evaluate the percent overlap profile due to path orientation and then run a boom section analysis on the path orientation of minimum overlap in order to evaluate the boom section performance. For instance, the data presented in Figure 8 are from a coverage path orientation varying from 0 to 175 degrees at 5 degrees increments.

Note that the minimum overlap (3.5%) orientation is given at 95 degrees. Then, the boom section analysis was carried out by varying the number of sections from 1 to 30.
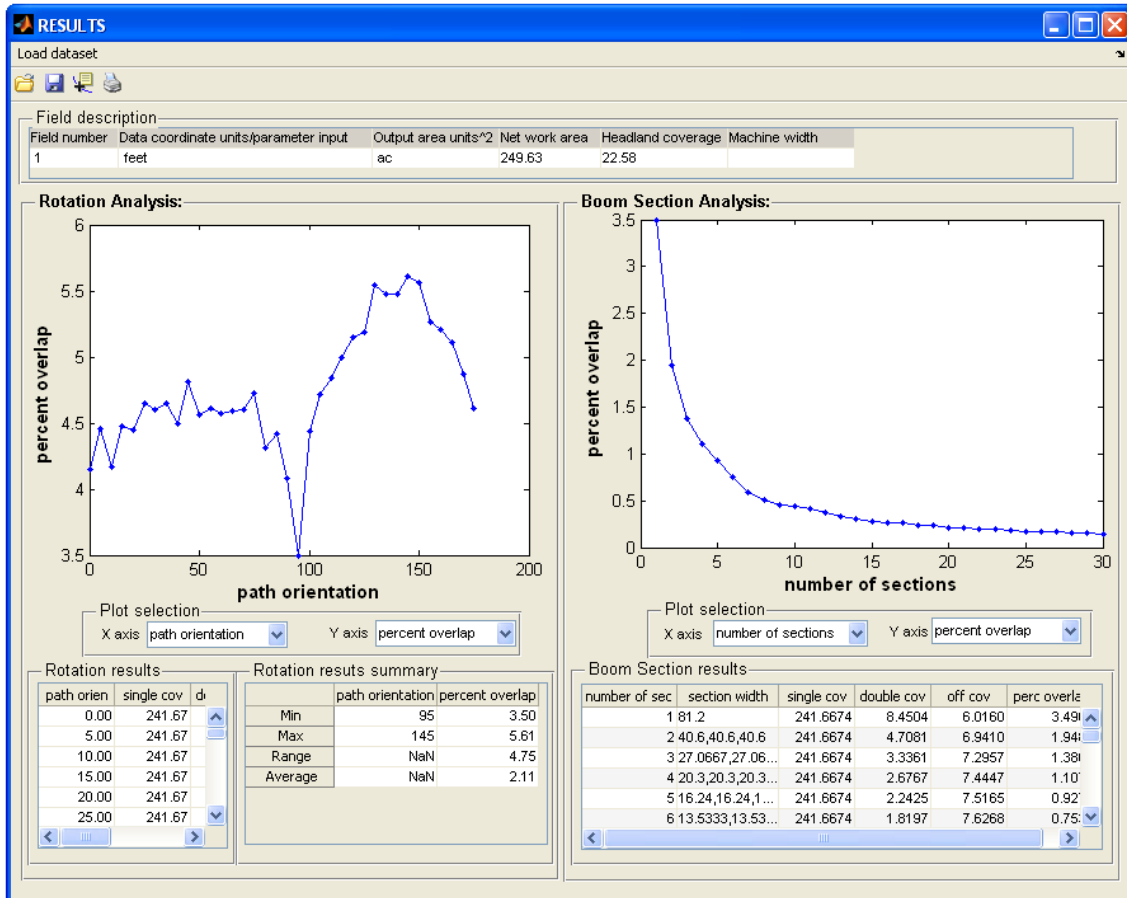
Figure 9: Field analysis output example

Field:2

Field:4

Field:5

Field:7

96
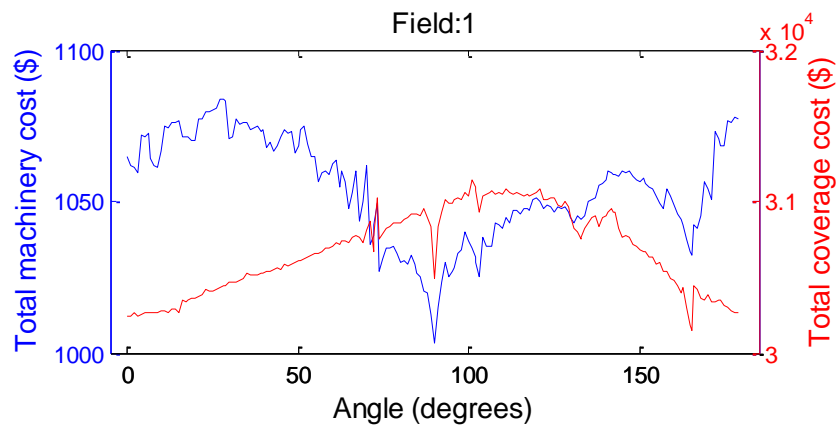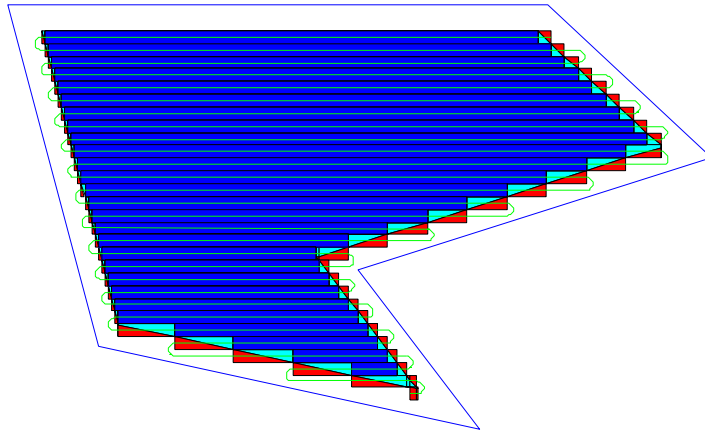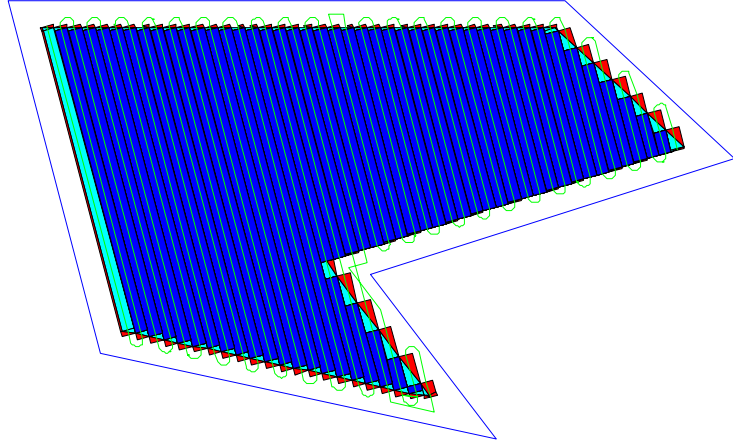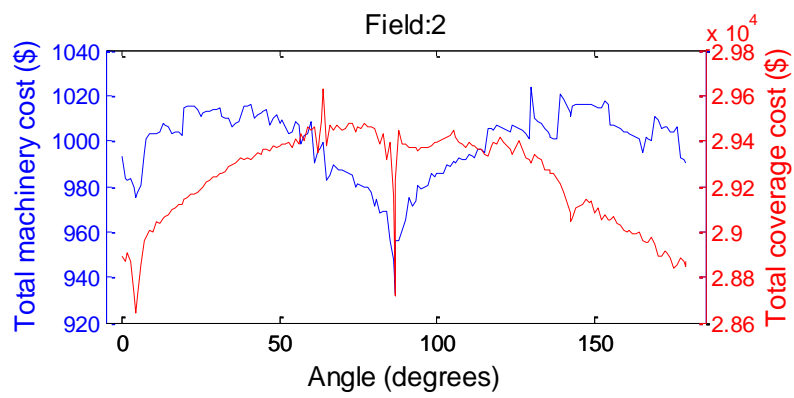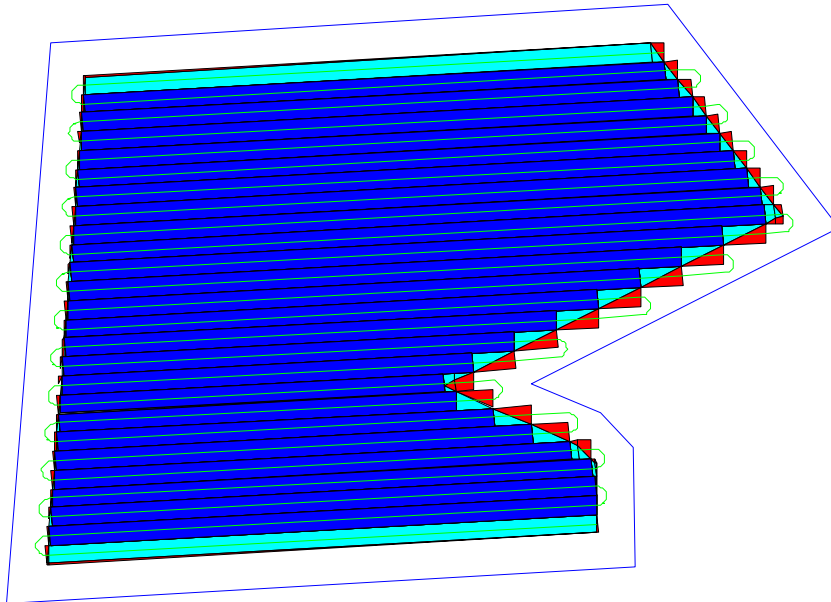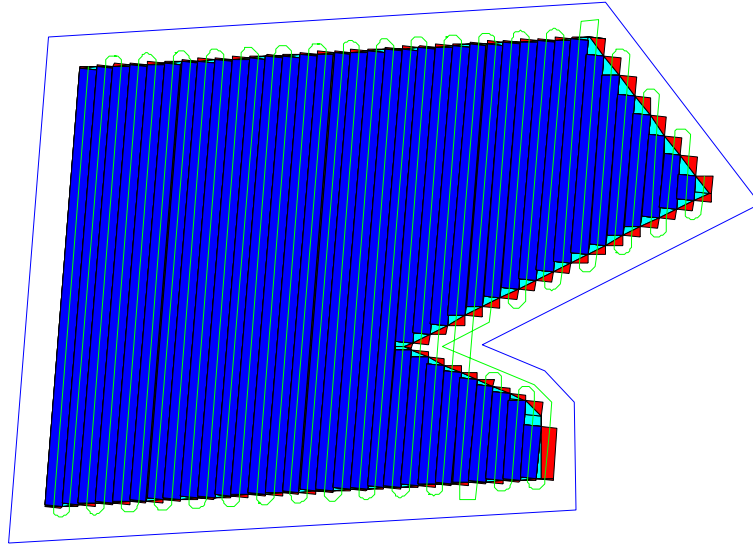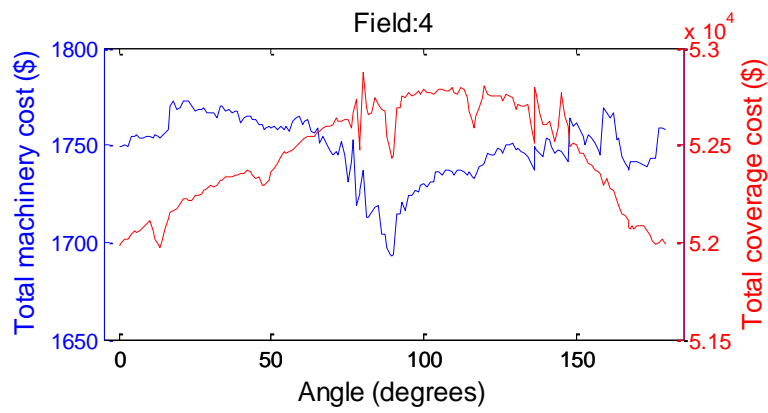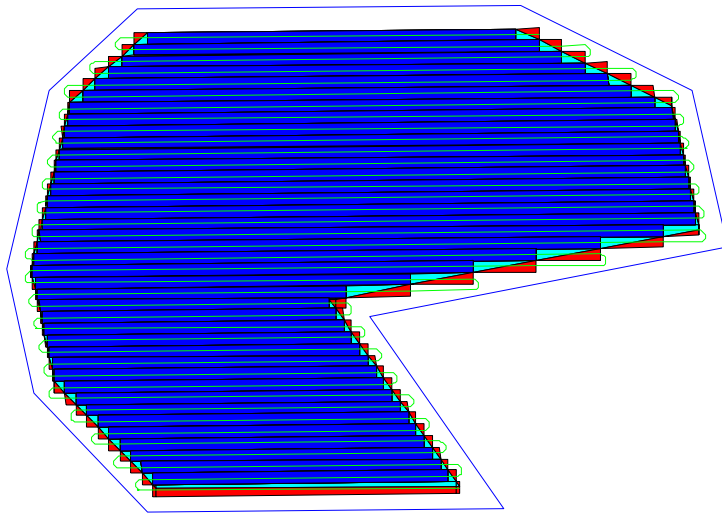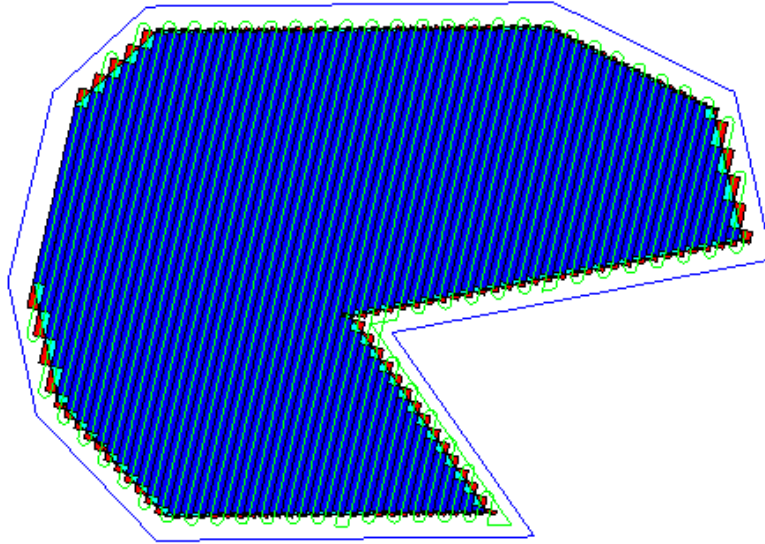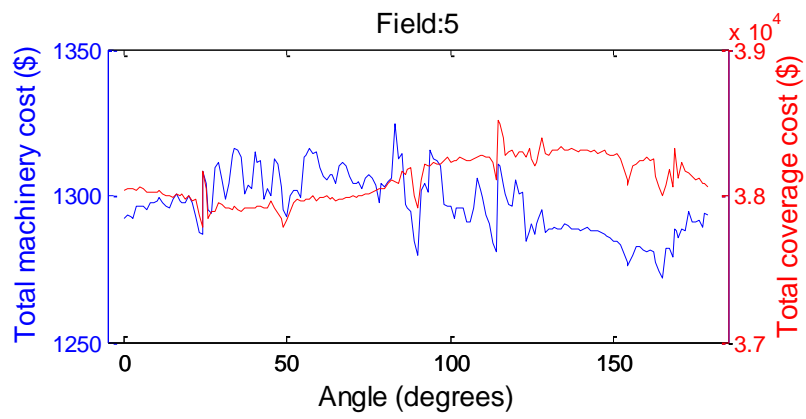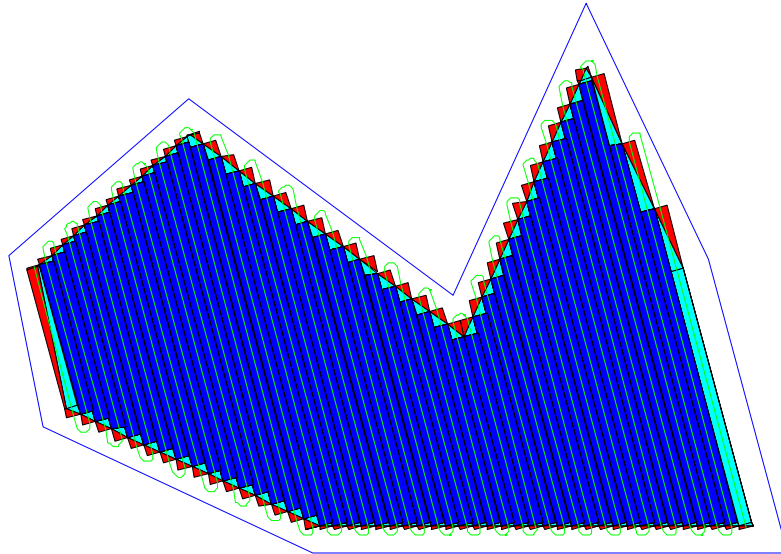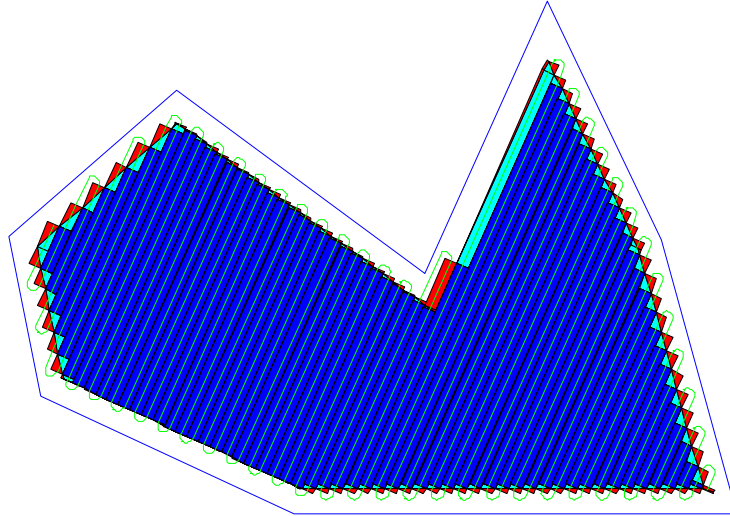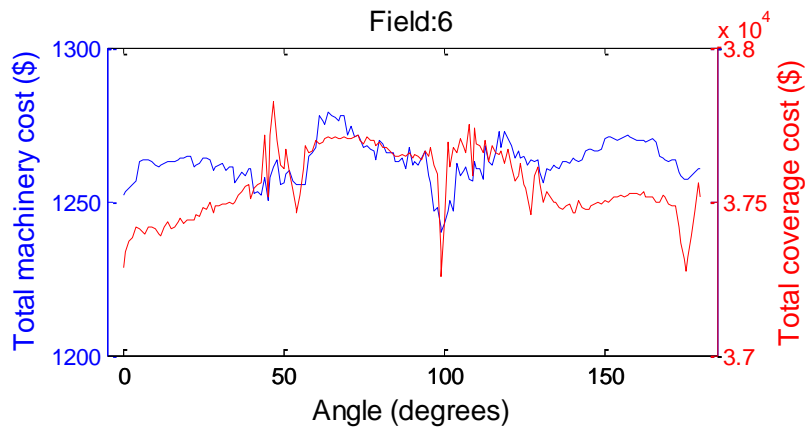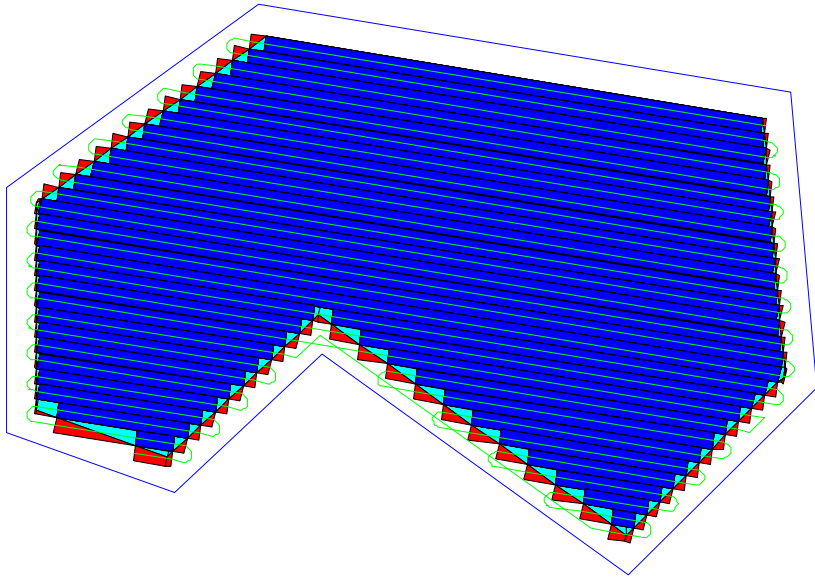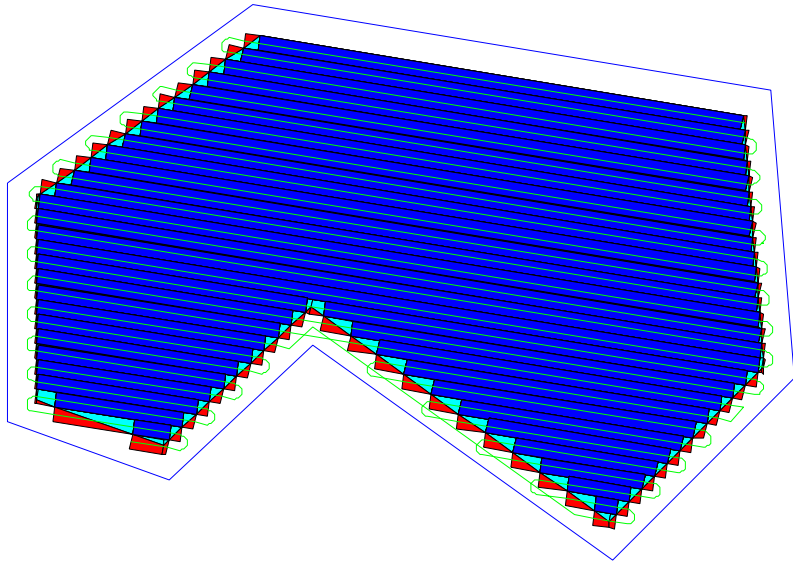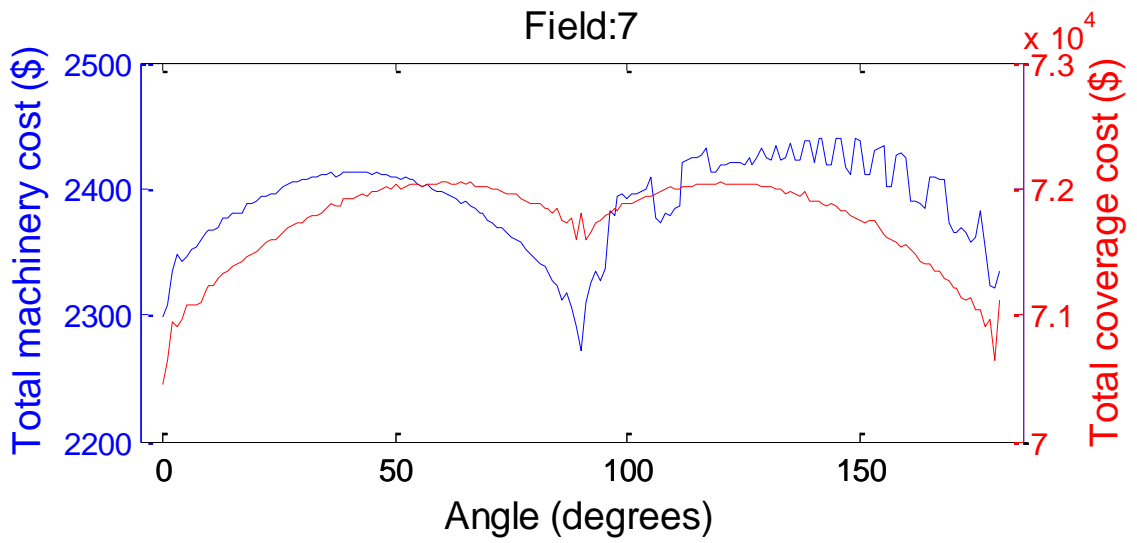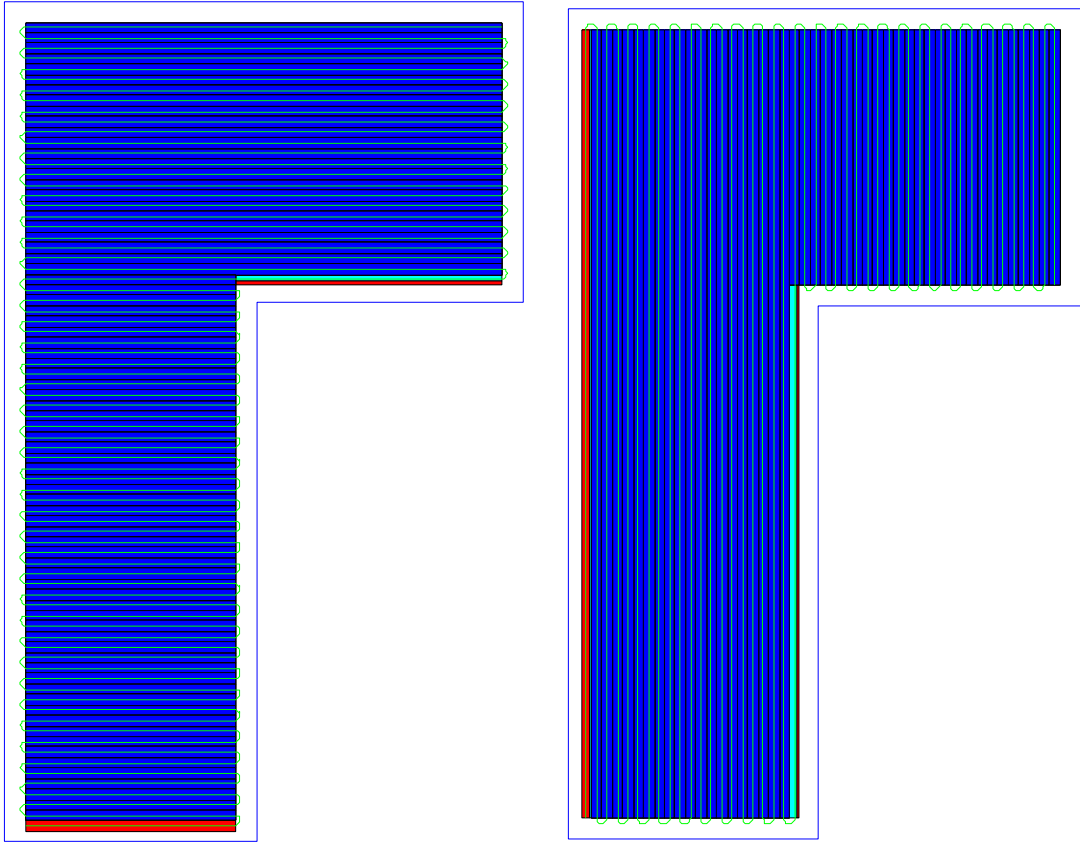
APPENDIX C: FIELD DECOMPOSITION ROUTING ALGORITHM OUTPUT
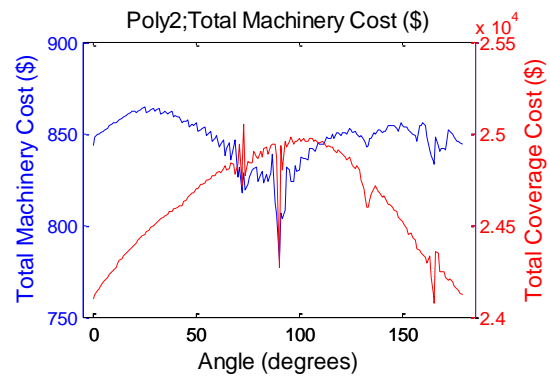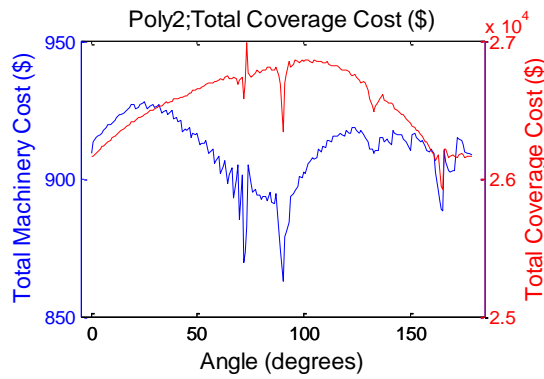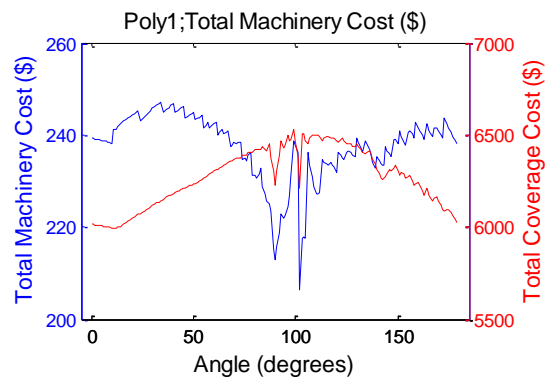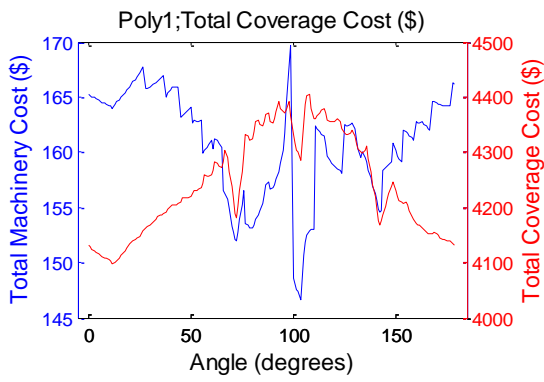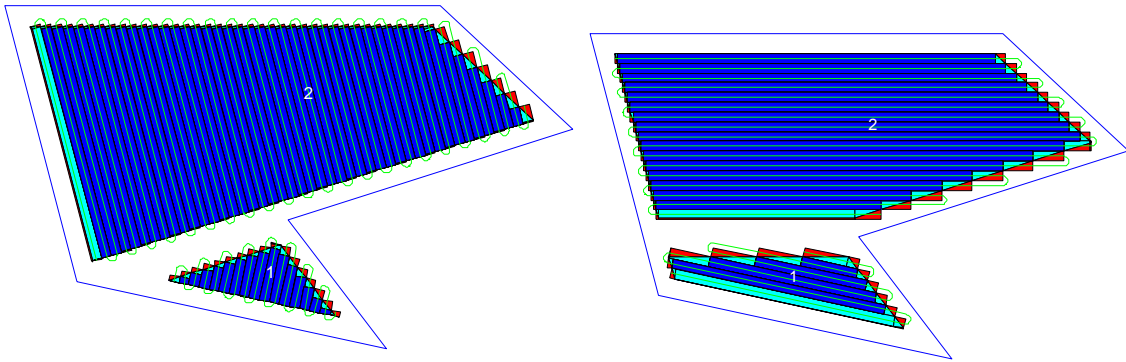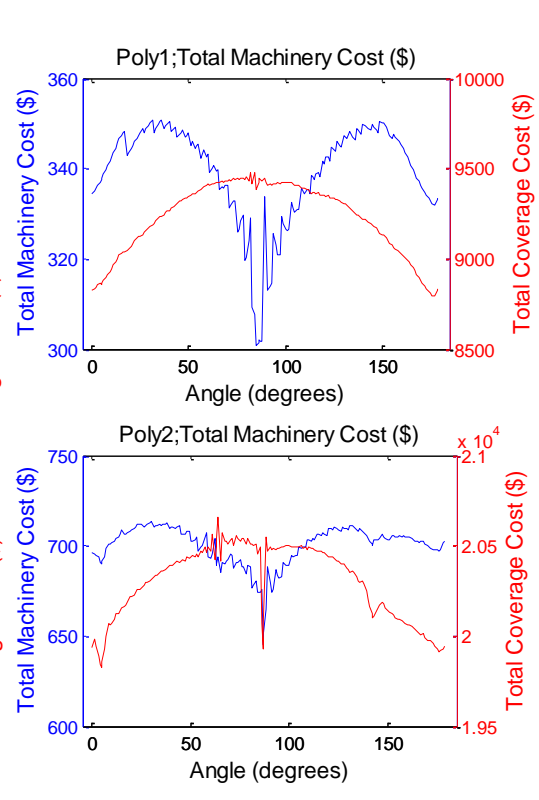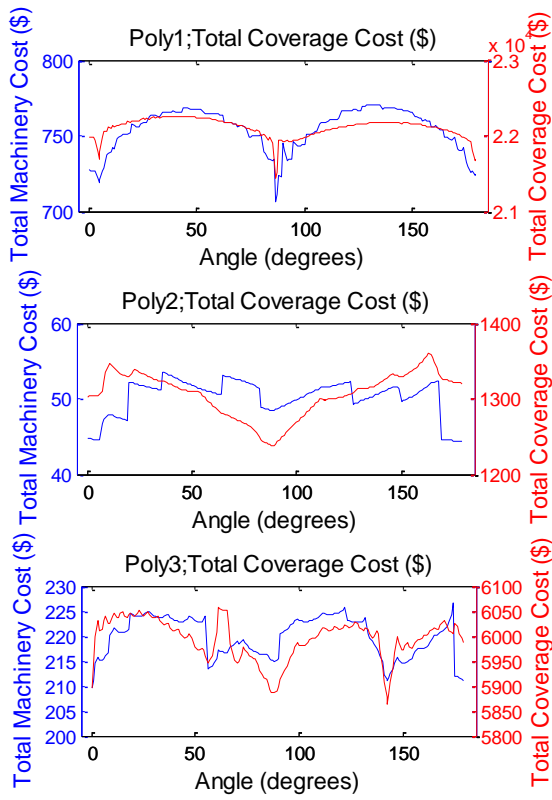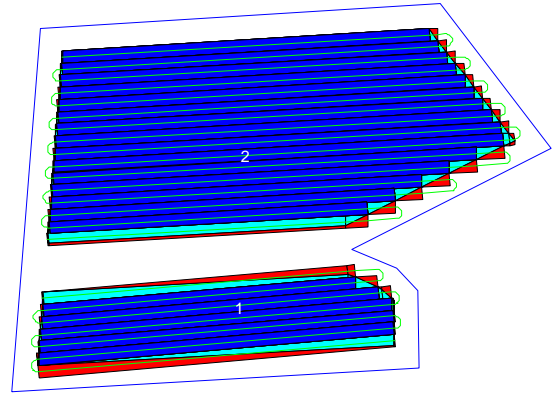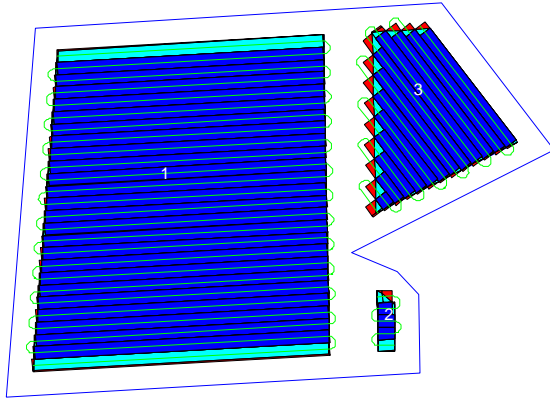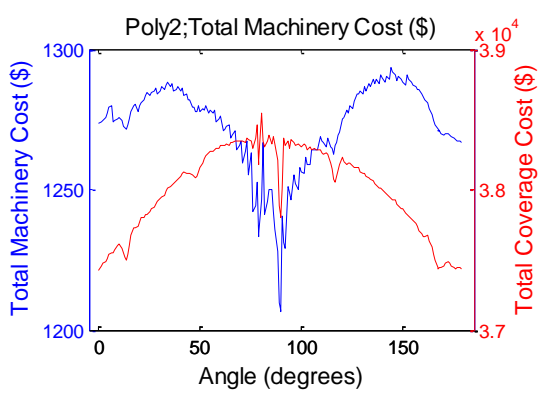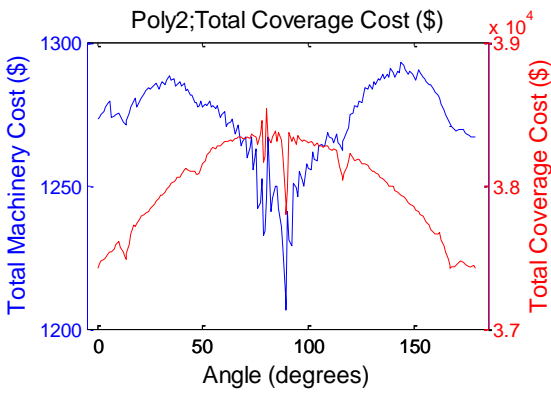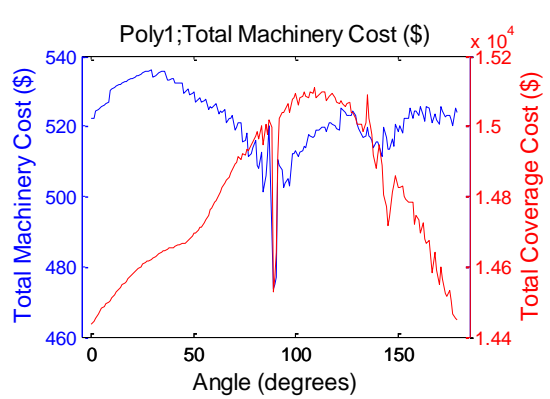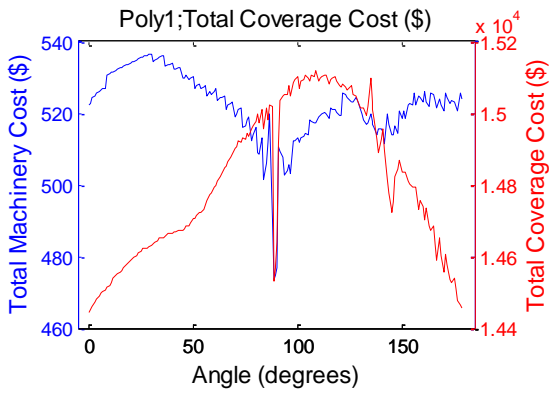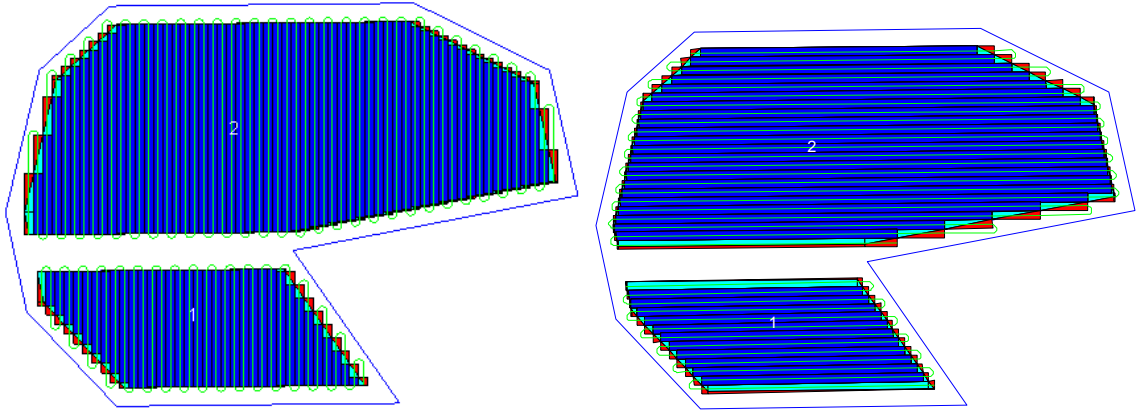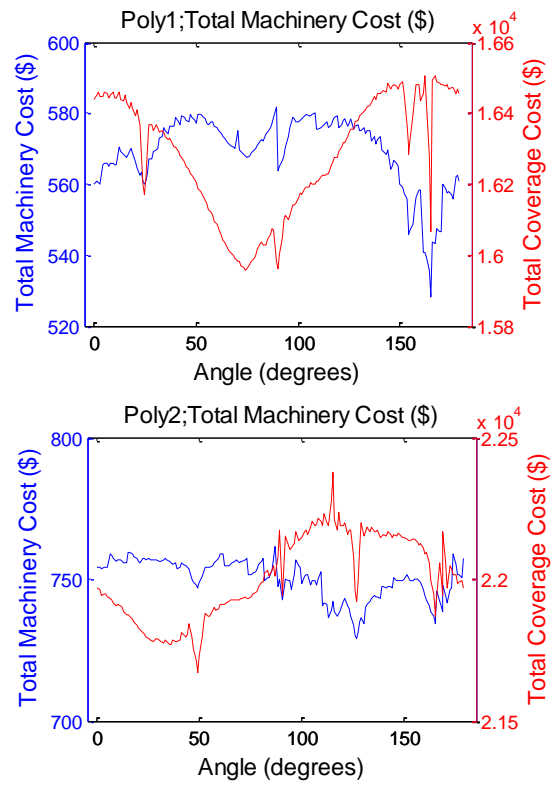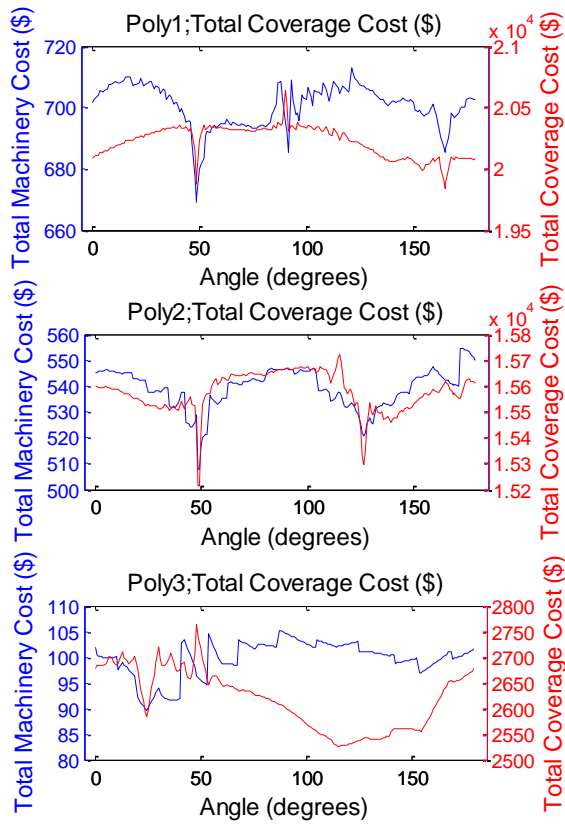
REFERENCES

ASABE. 2011. ASAE D497.7 Agricultural Machinery Management Data. *Standards of ASABE*.

Barry, W. 2012. Ohio Farm Custom Rates 2012. In *The Ohio State University Extension*.

Batte, M. T., and M. R. Ehsani. 2006. The economics of precision guidance with auto-boom control for farmer-owned agricultural sprayers. *Computers and Electronics in Agriculture* 53(1):28-44.

Bochtis, D., S. Vougioukas, Y. Ampatzidis, and C. Tsatsarelis. 2007. Field Operation Planning for Agricultural Vehicles: A Hierarchical Modeling Framework. *the CIGR Ejournal* IX.

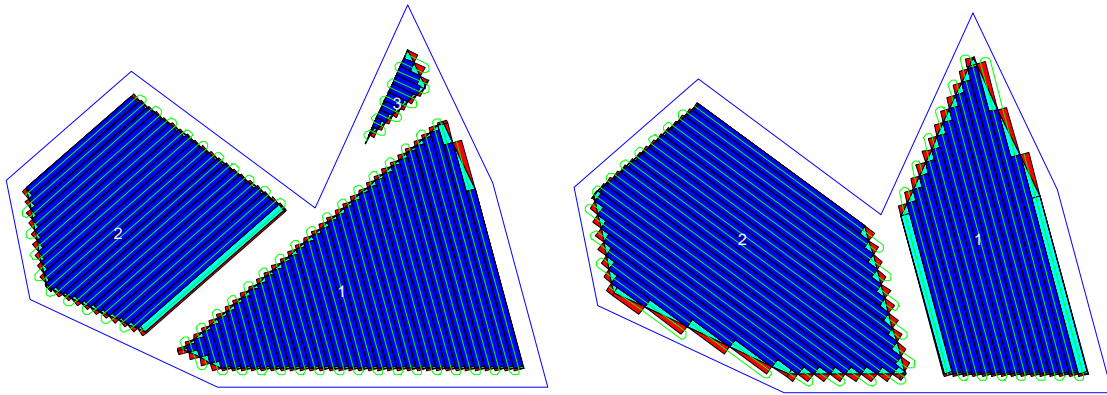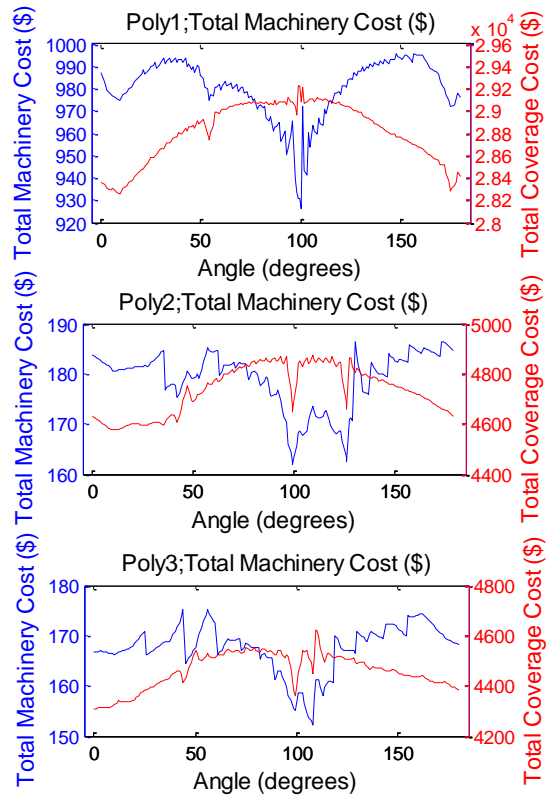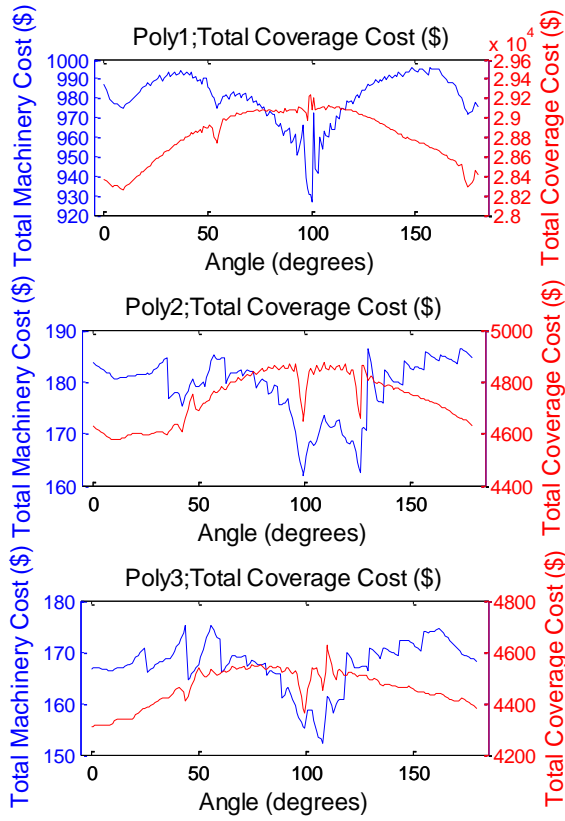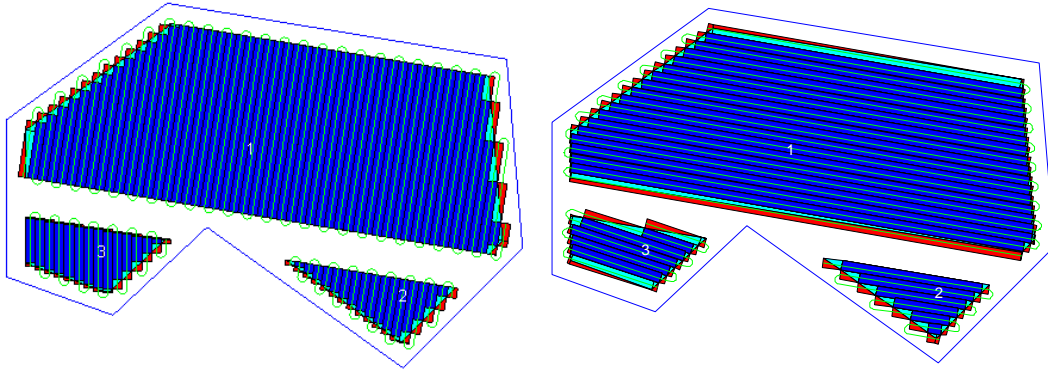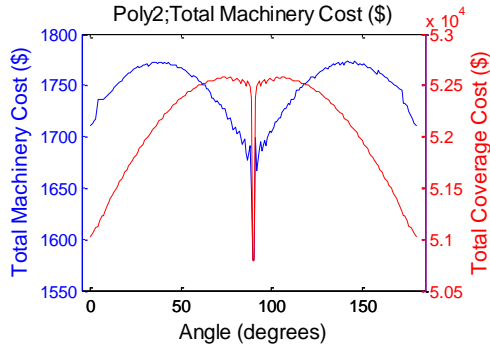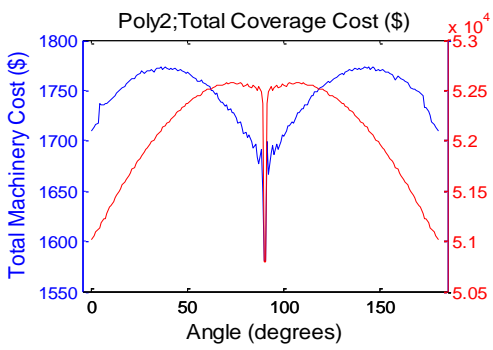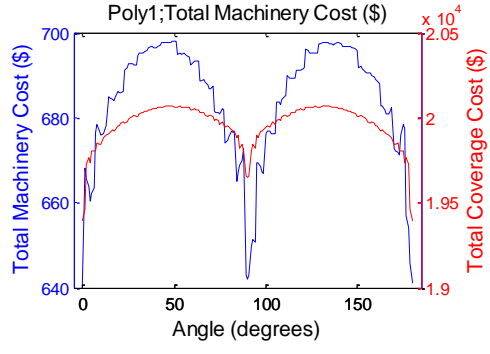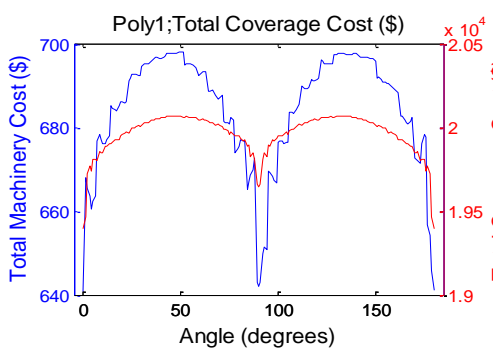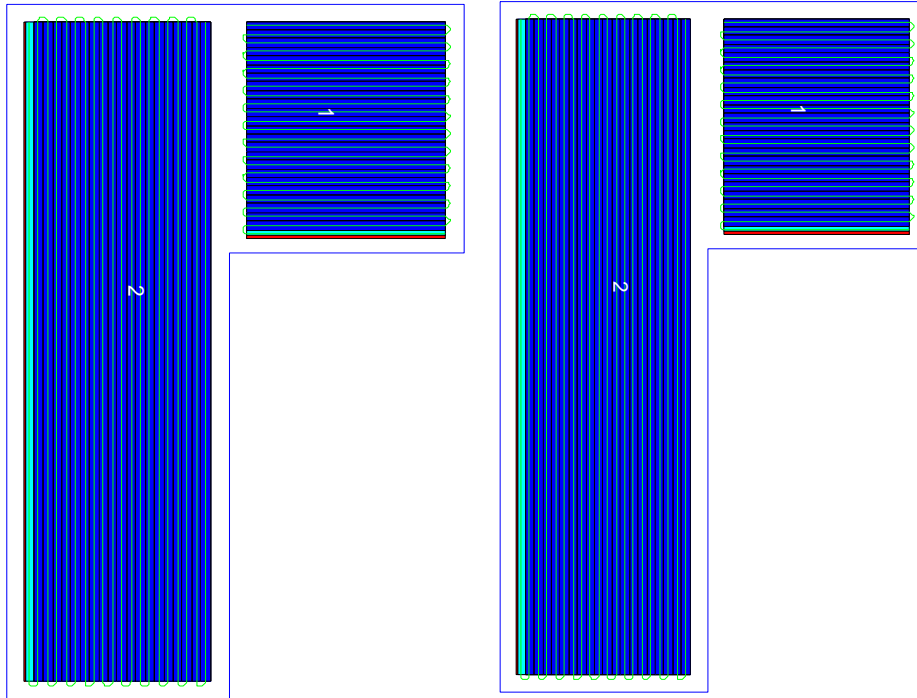Bochtis, D. D., and S. G. Vougioukas. 2008. Minimising the non-working distance travelled by machines operating in a headland field pattern. *Biosystems Engineering* 101(1):1-12.

Brinkhoff, T., H. Kriegel, R. Schneider, and A. Braun. 1995. Measuring the Complexity of Polygonal Objects. In *Proceedings of ACM International Workshop on Advances in Geographic Information Systems*. Baltimore, MD, USA.

Bruin, S., P. Lerink, A. Klompe, T. van der Wal, and S. Heijting. 2009. Spatial optimisation of cropped swaths and field margins using GIS. *Computers and Electronics in Agriculture* 68(2):185-190.

Choset, H. 2000. Coverage of Known Spaces: The Boustrophedon Cellular Decomposition. *Autonomous Robots* 9(3):247-253.

Choset, H., and P. Pignon. 1997. Coverage Path Planning: The Boustrophedon Cellular Decomposition. In *International Conference on Field and Service Robotics*.

Clarke, G., and J. Wright. 1964. Scheduling of vehicles from a central depot to a number of delivery points. *Operations Research* 12(4):568-581.

Dillon, C. R., S. A. Shearer, J. P. Fulton, and M. Kanakask. 2003. Optimal Path Nutrient Application Using Variable Rate Techonology. In *4th European Conference on Precision Agriculture*. Berlin, Germany.

Dillon, C. R., S. A. Shearer, J. P. Fulton, and S. K. Pitla. 2007. Improved Profitability Via Enhanced Resolution of Variable Rate Application Management in Grain Crop Production. In *Precision Agriculture '07, Proceedings at the 6th European Conference in Precision Agriculture*. Skiathos,Greece.

Duffy, M. 2012. Estimated Costos of Crop Production in Iowa-2012. In *Ag Decision Maker*.

Edwards, W. 2009. Estimating Farm Machinery Costs. In *Ag Decision Maker*. Iowa State University.

Gonzalez, X. P., C. J. Alvarez, and R. Crecente. 2004. Evaluation of land distributions with joint regard to plot size and shape. *Agricultural Systems* 82(1):31-43.

Grisso, R. D., P. J. Jassa, and D. E. Rolofson. 2001. Analysis of Traffic Patterns and Yield Monitor Data for Field Efficiency Determination. *Applied Engineering in Agriculture* 18(2):171-178.

Hofstee, J. W., L. E. E. M. Spatjens, and H. IJken. 2009. Optimal Path Planning for Field Operations. In *Precision Agriculture '09, Proceedings at 7th European Conference on Precision Agriculture*. Wageningen, the Netherlands.

Huang, W. H. 2001. Optimal line-sweep-based decompositions for coverage algorithms. In *Robotics and Automation, 2001. Proceedings 2001 ICRA. IEEE International Conference on*.

Hunt, D. 2001. *Farm Power and Machinery Managment*. Iowa State University Press, Ames, Iowa.

Jin, J., and L. Tang. 2006. Optimal Path Planning for Arable Farming.

Jin, J., and L. Tang. 2010. Optimal Coverage Path Planning for Arable Farming on 2D Surfaces. *Transactions of the ASABE* 53(1):283-295.

KDGI. 2006. Digital ortho photo imagery for Kentucky. Frankfort, Ky.: Kentucky Division of Geographic Information.

Kise, M., N. Noguchi, K. Ishii, and H. Terao. 2002. Enhancement of Turning Accuracy by Path Planning for Robot Tractor. In *Pp. 398-404 in Automation Technology for Off-Road Equipment, Proceedings of the July 26-27, 2002 Conference (Chicago, Illinois, USA)*. St. Joseph, Mich.: ASAE.

Luck, J. D., S. K. Pitla, S. A. Shearer, T. G. Mueller, C. R. Dillon, J. P. Fulton, and S. F. Higgins. 2010a. Potential for pesticide and nutrient savings via map-based automatic boom section control of spray nozzles. *Computers and Electronics in Agriculture* 70(1):19-26.

Luck, J. D., R. S. Zandonadi, B. D. Luck, and S. A. Shearer. 2010b. Reducing Pesticide Over-Application with Map-Based Automatic Boom Section Control on Agricultural Sprayers. *Transactions of the ASABE* 53(3):685-690.

Luck, J. D., R. S. Zandonadi, and S. A. Shearer. 2011. A Case Study to Evaluate Field Shape Factors for Estimating Overlap Errors with Manual and Automatic Section Control. 54(4):1237-1243.

MathWorks. 2009. *MatLab, version 7.7*. Natick, MA. The Mathworks.

Mickelaker, J., and S. A. Svensson. 2009. Auto-boom Control to Avoid Spraying pre-defined Areas. In *Precision Agriculture '09, Preceedings at the 7th European Conference in Precision Agriculture*. Wageningen, Netherlands.

Molin, J. P., R. F. Reynaldo, F. P. Povh, and J. V. Salvi. 2009. Performance of auto-boom control for agricultural sprayers. In *Proceedings at the 7th European Conference in Precision Agriculture*. Wageningen, Netherlands.

Noguchi, N., J. F. Reid, Q. Zhang, and J. D. Will. 2001. Turning Function for Robot Tractor Based on Spline Function.

Oksanen, T. 2007. Path Planning Algortithms for Agricultural Field Machines. PhD dissertation. Helsinki University, Department of Automation and Systems Technology, Helsinki, Finland

Oksanen, T., and A. Visala. 2004. OPTIMAL CONTROL OF TRACTOR-TRAILER SYSTEM IN HEADLANDS. In *Automation Technology for Off-Road Equipment,Proceedings of the 7-8 October 2004 Conference (Kyoto, Japan)Publication Date 7 October 2004*.

Oksanen, T., and A. Visala. 2007. Path Planning Algorithms for Agricultural Machines. *the CIGR Ejournal* IX.

Oksanen, T., and A. Visala. 2009. Coverage Path Planning Algorithms for Agricultural Field Machines. *Journal of Field Robotics* 26(8):18.

Peura, M., and J. Iivarinen. 1997. Efficiency of Simple Shape Descriptors. In *In 3rd International Workshop on Visual Form*. Capri,Italy.

Reid, J. F. 2004. MOBILE INTELLIGENT EQUIPMENT FOR OFF-ROAD ENVIRONMENTS. In *Automation Technology for Off-Road Equipment,Proceedings of the 7-8 October 2004 Conference (Kyoto, Japan)Publication Date 7 October 2004*.

Shockley, J., C. Dillon, T. Stombaugh, and S. Shearer. 2012. Whole farm analysis of automatic section control for agricultural machinery. *Precision Agriculture* 13(4):411-420.

Sisk, J. L. 2005. A fuzzy logic approach for determing optimal cropping patterns based on field boundary geometry. University of Kentucky, Biosystems and Agricultural Engineering, Lexington, KY

Souza, L. B. L., and D. Guliato. 2008. A Feature Extractor Based on Complexity Applied to Classification of Breast Tumors. In *XII Seminario de Iniciacao Cientifica*. Uberlandia, MG.

Spekken, M. 2010. Optimizing Routes on Agricultural Fields Minimizing Maneurvering and Servicing Time. Master's Thesis. Wageningen University and Research Centre, Laboratory of Geo-Information Science and Remote Sensing, Wageningen, The Netherlands

Stoll, A. 2003. Automatic Operation Planning for GPS-guided Machinery. In *Precision Agriculture*. Wageningen.

Stombaugh, T. S., R. S. Zandonadi, J. D. Luck, and S. A. Shearer. 2010. Toos for Evaluating the Potential of Automatic Section Control. In *10th International Conference on Precision Agriculture*. Denver, Colorado, USA.

Taïx, M., P. Souères, H. Frayssinet, and L. Cordesses. 2006. Path Planning for Complete Coverage with Agricultural Machines. In *Field and Service Robotics*, 549-558. S. i. Yuta, H. Asama, E. Prassler, T. Tsubouchi, and S. Thrun, eds: Springer Berlin / Heidelberg.

Zandonadi, R. S., J. D. Luck, T. S. Stombaugh, M. P. Sama, and S. A. Shearer. 2011. A Computational Tool for Estimating Off-Target Application Areas in Agricultural Fields. *Transactions of the ASABE* 54(1):41-49.

Zandonadi, R. S., T. S. Stombaugh, J. D. Luck, and S. A. Shearer. 2009. Software Tool for Estimating Overlapped Areas in Agricultural Field Operations. In *ASABE Paper No. 096957*. Reno, Nevada: St. Joseph, Mich.: ASABE.

Zhang, D., and G. Lu. 2004. Review of shape representation and description techniques. *Pattern Recognition* 37(1):1-19.

RODRIGO SINAIDI ZANDONADI

DATE AND PLACE OF BIRTH

November 27, 1978, Goioerê, Paraná, Brasil

EDUCATION

M.S., Biosystems and Agricultural Engineering, University of Kentucky, Lexington, Kentucky. 2008.

B.S., Agricultural and Environmental Engineering, Universidade Federal de Viçosa, Viçosa, Minas Gerais, Brasil. 2005.

PROFESSIONAL EXPERIENCE

Assistant Professor, Institute of Agricultural and Environmental Sciences. Universidade Federal de Mato Grosso, Sinop, Mato Grosso, Brasil. February, 2011 to present.

Engineer Associate, Department of Biosystems and Agricultural Engineering, University of Kentucky, Lexington, Kentucky; August, 2008 to January 2011.

Graduate Research Assistant, Department of Biosystems and Agricultural Engineering, University of Kentucky, Lexington, Kentucky; August, 2005 to July, 2008.

REFEREED JOURNAL ARTICLES

Luck, J. D., Zandonadi, R. S., Shearer, S. A. A case study to evaluate field shape factors for estimating overlap errors with manual and automatic section control. Transactions of the ASABE, v.54, 2011.

Zandonadi, R. S., Luck, L. D., Stombaugh, T. S., Sama, M. P., Shearer, S. A. Computational Tool for Estimating Off-Target Application Areas in Agricultural Fields. Transactions of the ASABE, v.54, 2011.

Luck, Joe D., Pitla, Santosh K., Zandonadi, R. S., Sama, Michael P., Shearer, Scott A. Estimating off-rate pesticide application errors resulting from agricultural sprayer turning movements. Precision Agriculture (Print), 2010.

Zandonadi, R. S., Stombaugh, T. S., Shearer, S. A., Queiroz, D. M., Sama, M. P. Laboratory Performance of a Mass Flow Sensor for Dry Edible Bean harvesters. Applied Engineering in Agriculture. , v.26, 2010.

Luck, J. D., Zandonadi, R. S., B. D. Luck, Shearer, S. A. Reducing Pesticide Over-Application with Map-Based Automatic Boom Section Control on Agricultural Sprayers. Transactions of the ASABE. v.53, 2010.

Rodrígues, A. M, Queiroz, D. M., Espinosa, G. B., Zandonadi, R. S. Determinación de Propriedades Físicomecánicas de los Frutos de Café (Coffea Arábica Varidedad Catuai) Relacionas con la Cosecha Mecanizada. Revista Ciencias Técnicas Agropecuarias. v.15, 2006.

Zandonadi, R. S., Pinto, F. A. C., Sena Jr., D.G., Queiroz, D. M., Viana, P. A., Montovani, E. C. Identification of lesser cornstalk borer attacked maize plants using infrared images. Biosystems Engineering. v.91, 2005.

Sena Jr., D.G., Santos, N. T., Pinto, F. A. C., Queiroz, A. C., Zandonadi, R. S. Efeito da iluminação na segmentação de imagens de plantas de milho atacadas pela lagarta do cartucho. Engenharia na Agricultura. v.12, 2004.

BOOK CHAPTER

Pinto, F. A. C., Queiroz, D. M., Zandonadi, R. S., Emerich, I. N., Sena Jr., D.G. Uso de Técnicas de Agricultura de Precisão para a Cafeicultura de Montanha In: Efeitos da Irrigação Sobre a Qualidade e Produtividade do Café, 2003, v.1.

CONFERENCE PROCEEDINGS

Zandonadi, R. S., Stombaugh, T. S., Queiroz, D. M. Algoritmo para planejamento de rotas para máquinas agrícolas utilizando como critério sobreposição de áreas e eficiência de campo In: XL Congresso Brasileiro de Engenharia Agrícola, 2011, Cuiabá.

Luck, J. D., Zandonadi, R. S., B. D. Luck, Shearer, S. A. Effects of Field Shape and Size on Application Errors Using Manual and Automatic Boom Section Control on a Self-Propelled Agricultural Sprayer In: ASABE international metting, Pittsburgh, Pennsylvania. ASABE international metting. , 2010.

Stombaugh, T. S., Zandonadi, R. S., Luck, J. D., Shearer, S. A. Tools for evaluating teh potential of automatic secton control In: 10th International Conference on Precision Agriculture, 2010, Denver,CO.

Stombaugh, T. S., Zandonadi, R. S., Dillon C. R. Assessing the Potential of Automatic Section Control In: 7th European Conference on Precision Agriculture, 2009, Wageningen, Netherlands.

Luck, J. D., Pitla, S. K., Zandonadi, R. S., Shearer, S. A. Development of GIS-Based Chemical Distribution Maps from Sprayer Performance Data In: 2009 ASABE Annual International Meeting, 2009, Reno, Nevada.

Sama, M. P., Stombaugh, T. S., Zandonadi, R. S., Shearer, S. A.Dynamic GNSS testing and Applications In: 2009 ASABE Annual International Meeting, 2009, Reno, Nevada.

Zandonadi, R. S., Stombaugh, T. S., Queiroz, D. M., Shearer, S. A. Mass Flow Sensor for Combines with Bucket Conveyors In: 7th European Conference on Precision Agriculture, 2009, Wageningen, Netherlands.

Zandonadi, R. S., Stombaugh, T. S., Luck, J. D., Shearer, S. A. Software Tool for Estimating Overlapped Areas in Agricultural Field Operations In: 2009 ASABE Annual International Meeting, 2009, Reno, Nevada.

Zandonadi, R. S., Stombaugh, T. S., Shearer, S. A., Sama, M. Laboratory Performance of a Low Cost Mass Flow Sensor for Combines In: 2009 ASABE Annual Internation Meeting, 2008, Providence, Rhode Island.

Zandonadi, R. S., Queiroz, D. M., Pinto, F. A. C., Sena Jr., D.G., Alves, E. A. Variabilidade Espacial da Produção, Maturação dos Frutos e Qualidade do Café de Montanha In: ConBAP-Congresso Brasileiro de Agricultura de Precisão, 2004, Piracicaba-SP.

Zandonadi, R. S. Análise do Efeito da Variação da Iluminação em Imagens Digitais de Baixo Custo In: XIV-Simpósio de Iniciação Científica, 2004, Viçosa.

Zandonadi, R. S., Pinto, F. A. C., Sena Jr., D.G., Botellho, A. E. Avaliação de Redes Neurais Artificiais para Determinação da Coberturado Solo. In: XIV-Simpósio de Iniciação Científica, 2004, Viçosa.

Zandonadi, R. S., Queiroz, D. M., Pinto, F. A. C. Determinação de Parâmetros de Lavouras Cafeeiras de Montanha Utilizando Imagens Orbitais In: XIV-Simpósio de Iniciação Científica, 2004, Viçosa.

Zandonadi, R. S., Queiroz, D. M., Sena Jr., D.G., Pinto, F. A. C. Avaliação da cobertura do Solo Utilizando Imagens Digitais Infravermelho Próximo In: XIII Simpósio de Iniciação Científica, 2003, Viçosa.

Zandonadi, R. S., Queiroz, D. M., Sena Jr., D.G., Pinto, F. A. C. Avaliação da Variabilidade Espacial da Produção do Café de Montanha In: XIII Simpósio de Iniciação Científica, 2003, Viçosa.

Zandonadi, R. S. Avaliação de Índices para Identificação de Plantas de Milho Atacadas pela Lagarta Elasmo em imagens Digitais In: XI Simpósio de Iniciação Científica, 2002, Viçosa.

Zandonadi, R. S., Stombaugh, T. S., Shearer, S. A., Queiroz, D. M. Low Cost Device for Grain Flow Sensing on a Bucket Elevator In: IV Simposio Internacional de Agricultura de Precisao-SIAP 2007, 2007, Vicosa-MG.

Alves, E. A., Pinto, F. A. C., Queiroz, D. M., Santos, N. T., Zandonadi, R. S. Analise da variabilidade da qualidade de bebida do cafe dereja em relacao a face de exposicao ao sol

das plantas In: 3o Simposio Internacional de Agricultura de Precisao, 2005, Sete Lagoas.

Zandonadi, R. S., Queiroz, D. M., Pinto, F. A. C., Alves, E. A., Cerqueira, E. S. A. Análise de correlação entre índices espectrais e parâmetros de lavouras de café de montanha utilizando imagens de satélites. In: 3o Simposio Internacaional de Agricultura de Precisao, 2005, Sete Lagoas.

Pinto, F. A. C., Alves, E. A., Queiroz, D. M., Sena Jr., D.G., Zandonadi, R. S. Mapeamento da qualidade do café cereja em uma fazenda da região das matas de Minas Gerais. In: 3o Simpósio Internacional de Agricultura de Precisão. 3o Simpósio Internacional de Agricultura de Precisão. , 2005. v.1. p.1 - 4

Zandonadi, R. S., Campos, J. M. S., Pinto, F. A. C., Queiroz, D. M., Sena Jr., D.G. Identificação de Plantas Atacadas pela Lagarta Elasmo feita por Algoritmo Classificador e por Especialistas Humanos In: III SINTAG - Simpósio Internacional de Tecnologia de Aplicação, 2004, Botucatu.

Zandonadi, R. S., Pinto, F. A. C., Sena Jr., D.G., Queiroz, D. M. Efeito do Tamanho de Blocos de Imagens Digiais na Classificação Automática de Plantas de MIlho Atacas por Elasmopalpus Lignosellus In: II SIAP - Simpósio Internacional de Agricultura de Precisão, 2002, Viçosa.

 Zandonadi, R. S. Identificação de Plantas Atacadas pela Lagarta Elasmo (Elasmopalpus Lignosellus) em Imagens Digitais de Plantas de MIlho In: XXXVI CONBEA - Congresso Brasileiro de Engenharia Agrícola, 2002, Salvador-BA.